# Underground Injection Control
# Carbon Sequestration
# Class VI Permit Application

## APPLICATION NARRATIVE
## 40 CFR 146.82(a)

## Tallgrass High Plains Carbon Storage, LLC
## Western Nebraska Sequestration Hub

January 2025

Prepared by:

Jessica Gregg (Director, Geoscience Compliance)
Tallgrass High Plains Carbon Storage, LLC
370 Van Gordon St
Lakewood, CO 80228

## TABLE OF CONTENTS

## LIST OF FIGURES

## LIST OF TABLES



## LIST OF EQUATIONS

## LIST OF ATTACHMENTS

| File Name | Description |
|---|---|
| 2.2.1a_HighPlains_Conestoga_1_AoR_Map_Arch_D_1-20k _land-topo.pdf | A map of the AoR with all required information per 14 CFR §146.82 at a scale of 1 in. to 1,667 ft (1:20,000). |
| 2.2.1b_HighPlains_Conestoga_1_AoR_Map_ArchE_1-16k _SatImage.pdf | An AoR basemap version at 1:16,000 scale with a recent satellite imagery basemap. |
| 2.2.2_Goose_Egg_Structure_Map_TVDSS_1-48k_ArchE.pdf | Large-scale structure contour map on the top of the upper confining zone, the Goose Egg Formation. |
| 2.2.2_Lyons_Structure_Map_TVDSS_1-48k_ArchE.pdf | Large-scale structure contour map on the top of the proposed injection zone, the Lyons Formation. |
| [redacted] | [redacted] |
| 3.4.1b_AoR Oil and Gas Well List_(S&P Enerdeq)-dist.xlsx | Spreadsheet with a list of all oil and gas wellbores within the AoR and pertinent information (depths, formation at TD, well type, status, etc.) from S&P Enerdeq and cross-checked with Nebraska Oil and Gas Commission. |
| 3.4.1b_AoR Water Well List_NE_DNR-dist.xlsx | Spreadsheet with all water wells within the AoR from the Nebraska Department of Natural Resources groundwater wells database. |
| 3.4.1c_Oil and Gas Well Files_AoR_NOGCC.zip | Well files and logs for all oil and gas wells within the AoR. |
| 3.4.1d_Water Well Files_NE_DNR.zip | Well files for all water wells within the AoR. |
| Figures_WNSHub_Conestoga.zip | Zip file containing full-resolution PDFs for all of High Plains' generated figures included in the text of the application documents. |
| List of Cited References_WNSHub_Conestoga.xlsx | A spreadsheet containing a list of all references cited with links to where they can be downloaded, acquired, or purchased. |
| NE_Final_GDB.gdb | An ESRI file geodatabase containing project-specific data (proposed well locations, AoR boundary, etc.) and other pertinent spatial data referenced in the application narrative. |
| Tallgrass_Juniper M1 QGEO UBI Interpretation 8280-9500ft MD 240.pdf | Full-resolution interpreted image log acquired from the Juniper M-1 well (API: 49-021-29548). |

## ACRONYMS AND ABBREVIATIONS

Note: All terms are written as used in the text.

| | |
|---|---|
| ° | degrees |
| % | percent |
| 2D | two dimensional |
| 3DHP | 3D Hydrography Program |
| **A** | |
| AoR | Area of Review |
| API | American Petroleum Institute |
| ATSM | American Society for Testing and Materials |
| **B** | |
| bbl | barrel(s) |
| Bcf | billion cubic feet |
| bgs | below ground surface |
| BHP | bottomhole pressure |
| BHT | bottomhole temperature |
| BOP | blowout preventer |
| **C** | |
| CBL | cement bond log |
| CCS | carbon capture and storage |
| CCUS | carbon capture, utilization, and storage |
| CFR | Code of Federal Regulations |
| $CO_2$ | carbon dioxide |
| CRA | crushed rock analysis |
| **D** | |
| DIC | dissolved inorganic carbon |
| DJ | Denver-Julesburg |
| DOC | dissolved organic carbon |
| DOE | Department of Energy |
| **E** | |
| EF | efficiency factor |
| EHS | environmental, health, and safety |
| EJ | environmental justice |
| ELAN | elemental analysis |
| EOS | equation of state |
| EPA | Environmental Protection Agency |
| ERP | emergency response plan |
| ERRP | emergency and remedial response plan |
| ESHIA | Environmental, Social and Health Impact Assessment |

| | |
|---|---|
| **F** | |
| F | Fahrenheit |
| FMI | formation microimager |
| High Plains | Tallgrass High Plains Carbon Storage, LLC |
| ft | feet/foot |
| ft/D | feet per day |
| ft/mile | feet per mile |
| $ft^2/D$ | square feet per day |
| $ft^3/sec$ | cubic feet per second |
| **G** | |
| $g/cm^3$ | grams per cubic centimeter |
| gpm | gallons per minute |
| GR | gamma ray |
| GSDT | Geologic Sequestration Data Tool |
| **H** | |
| HHRA | human health risk assessment |
| HPMI | high-pressure mercury injection |
| **I** | |
| IPAC | Information for Planning and Consultation |
| IEA | International Energy Agency |
| in. | Inch |
| **L** | |
| lbm | pound mass |
| lbf | pound force |
| LCZ | lower confining zone |
| **M** | |
| M | thousand; earthquake Moment Magnitude (when preceding a number) |
| Ma | million years ago |
| Mcf | thousand cubic feet |
| Mpsi | thousand pounds per square inch |
| $\mu$D | microdarcy |
| mD | millidarcy |
| MD | measured depth |
| MDT | Modular Formation Dynamics Tester |
| mg/L | milligrams per litter |
| MICP | mercury injection capillary pressure |
| MMcf | million cubic feet |
| Mt | megatonne/million metric tons |
| Mta | megatonne per annum/million metric tons per year |
| **N** | |
| NCS | net confining stress |

| | |
|---|---|
| NDEE | Nebraska Department of Environment and Energy |
| NHD | National Hydrography Dataset |
| NMR | Nuclear Magnetic Resonance |
| NOGCC | Nebraska Oil and Gas Conservation Commission |
| NPDES | National Pollutant Discharge Elimination System |
| NSHM | National Seismic Hazard Model |
| **O** | |
| OD | outside diameter |
| ohm·m / Ω·m | ohm meters – unit of resistivity |
| **P** | |
| P&A | plug and abandon |
| PISC | post-injection site care |
| PLSS | Public Land Survey System |
| $P_p$ | pore pressure |
| ppm | parts per million |
| psi | pounds per square inch |
| psi/ft | pounds per square inch per foot |
| psig | pounds per square inch gauge |
| **Q** | |
| Quanti.Elan™ | SLB's mineralogical inversion application that provides quantitative formation evaluation of openhole logs level by level |
| **R** | |
| RCA | routine core analysis |
| RCRA | Resource Conservation and Recovery Act |
| Reference Wells | [redacted] |
| RHOB | bulk density log |
| Rw | resistivity of connate water |
| **S** | |
| SCADA | supervisory control and data acquisition |
| sec | Second |
| SHmax | maximum horizontal stress |
| SHmin | minimum horizontal stress |
| SP | spontaneous potential |
| SRT | step-rate test |
| SS | subsea |
| $S_v$ | vertical stress |
| SWD | saltwater disposal |
| **T** | |
| Tallgrass | Tallgrass Energy, L.P. |
| TD | total depth |

| | |
|---|---|
| TDS | total dissolved solids |
| TVD | true vertical depth |
| TVDSS | true vertical depth subsea |
| **U** | |
| UCZ | upper confining zone |
| UIC | Underground Injection Control |
| U.S. | United States |
| USDW | Underground Source of Drinking Water |
| USFWS | U.S. Fish & Wildlife Service |
| USGS | U.S. Geological Survey |
| UST | underground storage tanks |
| **W** | |
| WHP | wellhead pressure |
| WNS Hub | Western Nebraska Sequestration Hub |
| wt% | weight percent |
| **X** | |
| XRD | X-ray diffraction |
| XRF | X-ray fluorescence |

## 1.0 PROJECT BACKGROUND AND CONTACT INFORMATION

According to the International Energy Agency (IEA), 40 million metric tons (Mt) of carbon dioxide ($CO_2$) are captured worldwide annually.[1] By 2070, the world's population will need to capture and store more than 10,000 Mt of $CO_2$ to meet the IEA's Sustainable Development Scenario plan—making new projects and investment paramount to achieving these goals.[2] As of the 2015 Paris Agreement, North America planned to create a carbon emission-free power sector by 2035. This goal would require eliminating approximately five billion Mt of $CO_2$ per year by 2035.[3]

Tallgrass Energy, L.P. (Tallgrass), headquartered in Leawood, Kansas, is a committed leader at the forefront of the United States' decarbonization efforts. Tallgrass is a pipeline and gas storage company that enables a high quality of life by delivering energy and services that fuel homes and businesses. Tallgrass' subsidiary, Tallgrass High Plains Carbon Storage, LLC (High Plains), was formed to focus on Tallgrass' carbon sequestration efforts.

Tallgrass and predecessor companies have operated natural gas storage fields for more than 70 years. Tallgrass operates 90 wells, 74 billion cubic feet (Bcf) of underground natural gas storage capacity, and 20,470 compression horsepower across Huntsman and East Cheyenne, Wyoming underground gas storage fields. These gas storage operations provide Tallgrass with critical subsurface working knowledge and skillsets that transfer directly to the sequestration of $CO_2$, specifically the injection, monitoring, and storage of gaseous fluids in porous reservoirs.

High Plains proposes drilling and completing a carbon sequestration injection well and one monitoring well in southeastern Kimball County, Nebraska, to safely sequester carbon dioxide (the "Project"). **Table 1.1** provides the Project information, including the well names, well utilizations, and coordinates. A nearby stratigraphic characterization well, the Juniper M-1 (API No. 49-021-29548), located in southeastern Wyoming, was used to support the site characterization for this project. Two field offices, each located approximately 30 miles from the Conestoga I-1 injection well, will have the capabilities to support maintenance operations and emergency response (**Table 1.2**).

Table 1.1—Information and location of proposed Project wells.

| Well Name | Use | Latitude* | Longitude* | PLSS |
|---|---|---|---|---|
| Conestoga I-1 | Injection | [redacted] | [redacted] | [redacted] |
| Conestoga M-2 | Monitoring | [redacted] | [redacted] | [redacted] |

* NAD83

Table 1.2—Field office locations for maintenance and emergency response deployments.

| Field Office Name | Address | Approximate Distance to Conestoga I-1 (miles) |
|---|---|---|
| Huntsman Gas Storage Field | 2835 CR 111, Sidney, NE 69162 | 27 |
| Pine Bluffs Sequestration Hub | 90 CR 161, Pine Bluffs, WY 82082 | 33 |

1 https://www.iea.org/reports/about-ccus
2 https://www.whitehouse.gov/briefing-room/statements-releases/2021/04/22/fact-sheet-president-biden-sets-2030-greenhouse-gas-pollution-reduction-target-aimed-at-creating-good-paying-union-jobs-and-securing-u-s-leadership-on-clean-energy-technologies/
3 https://www.usgs.gov/faqs/how-much-carbon-dioxide-does-united-states-and-world-emit-each-year-energy-sources

This application will:

- Characterize the geology and reservoir characteristics of the proposed injection well location to verify that the proposed injection reservoir and seal are suitable for long-term $CO_2$ storage.
- Describe the methodology for determining the Area of Review (AoR) and review any potential requirements for corrective-active measures.
- Describe the engineering design of the injection well and monitoring wells.
- Provide an overview of the Project-related operational plans including:
    - Pre-Operational Logging and Testing
    - Testing and Monitoring
    - Emergency Response
    - Financial Assurance assessment informed by a risk assessment approach
- Review the plugging of the injection and monitoring wells, post-injection site care, and site closure. In accordance with all federal regulations for Class VI wells; the permit will be updated every five years.
- Evaluate the AoR for environmental justice (EJ) related impacts during Project operation and post-injection monitoring.

## 1.1 Project Goals

Drill a $CO_2$ injection and sequestration well into the Lyons Formation to sequester 2.26 million tons per annum (Mta) of $CO_2$ for approximately 12 years for a cumulative injected mass of 27.1 Mt. This project will not be on native lands, with the injection well positioned on private lands and the overall sequestration project occupying private lands.

The Standard Industrial Classification (SIC) code for this project is 4953 – Refuse Systems (nonhazardous waste disposal sites).

## 1.2 Project Partners and Collaborators

A list of all groups responsible for funding and/or contributing technical material to the Project is provided in **Table 1.3**.

Table 1.3—Applicant, project partners, and collaborators.

| Category | Company Name | Role |
|---|---|---|
| Applicant | Tallgrass High Plains Carbon Storage LLC | UIC Permit Operator, UIC Applicant and authorship, technical feasibility, technical modeling |

UIC – Underground Injection Control

## 1.3 Project Timeframe

The planned Project timeframe including key components of the pre-injection, injection, and post-injection phases are summarized in **Figure 1.1**.

Figure 1.1—Anticipated Project timeframe for High Plains' proposed $CO_2$ sequestration project as part of the Western Nebraska Sequestration Hub.

## 1.4 Proposed Injection Mass/Volume and $CO_2$ Source

The proposed injection volume is 2.26 Mta for 12 years, which would amount to a total injected volume of 27.1 Mt. The injectate stream's chemistry will consist of approximately 95% $CO_2$ and less than 150 parts per million (ppm) $H_2O$. *Section 7.0* discusses the injectate composition in detail.

## 1.5 Injection Depth Waver and/or Aquifer Exemption

### *1.5.1 Injection Depth Waiver*

No injection depth waiver is requested or required for the proposed Project. All injection and storage are proposed to occur below the area's lowermost underground source of drinking water (USDW).

### *1.5.2 Aquifer Exemption*

No new or expanded aquifer exemption is requested or required for the proposed Project as all injection and storage will occur in zone(s) that are currently non-USDWs.

## 1.6 Contact Information

**Craig Spreadbury | Vice President, Carbon Capture & Sequestration**
Tallgrass High Plains Carbon Storage, LLC
370 Van Gordon St
Lakewood, CO 80228
craig.spreadbury@tallgrass.com

**Jessica Gregg | Director, Geoscience Compliance**
Tallgrass High Plains Carbon Storage, LLC
370 Van Gordon St
Lakewood, CO 80228
jessica.gregg@tallgrass.com

## 1.7 List of Permits or Construction Approvals [40 CFR 144.31I(6)]

No permits or construction approvals have been applied for or received at the time of this initial Class VI application submission. Federal, state, and local permitting and notifications will commence upon submission of this Class VI application. **Table 1.4** identifies the potential environmental permits that High Plains may need to obtain pursuant to 40 CFR §144.31(e)(6).

Table 1.4—Permit approvals and submissions.

| Agency/Permit Type | Permit No. | Status |
|---|---|---|
| RCRA - Hazardous Waste Management | Will provide when received | Not filed |
| UIC - Underground Injection of Fluids | R07-NE-0003 | Under EPA Review |
| NPDES Discharge of Surface Water | Will provide when received | Not filed |
| PSD - Air Emissions from Proposed Sources | Will provide when received | Not filed |
| Non-attainment Program Under the Clean Air Act | Will provide when received | Not filed |
| National Emissions Standards for Hazardous Air Pollutants Pre-Construction Approval Under the Clean Air Act | Will provide when received | Not filed |
| Dredge and Fill Permitting Program Under Section 404 of the Clean Water Act | Will provide when received | Not filed |
| State and Local Permits | Will provide when received | Not filed |

RCRA - Resource Conservation and Recovery Act
NPDES - National Pollutant Discharge Elimination
PSD - Prevention of Significant Deterioration

High Plains intends to file a Storage Facility Permit Application with the Nebraska Oil and Gas Conservation Commission (NOGCC) per Title 267, Chapter 7, prior to the construction of this project.

## 1.8 List of State, Tribe, and Territory Contacts [40 CFR 146.82(a)(20)]

State and territory contact information is listed in **Table 1.5**, including private oil and gas exploration and production operators within the AoR. The storage facility and associated AoR are not located on tribal lands and thus no contact information is provided.

Table 1.5—State, tribe, and territory contacts.

| Agency | Phone Number |
|---|---|
| Kimball County Nebraska Sheriff's Office | 308-235-3615 |
| Kimball County Volunteer Fire Department | 308-235-2141 |
| Nebraska State Patrol | 402-471-4545 |
| Kimball County Emergency Manager | 308-254-7003 |
| Underground Injection Control (UIC) Program Director | 913-551-7992 |
| U.S. Environmental Protection Agency National Response Center (24 hours) | 800-424-8802 |
| U.S. Environmental Protection Agency, Region 7 | 913-551-7003 |
| Nebraska Department of Natural Resources | 402-471-2363 |
| Nebraska Department of Environment & Energy | 402-471-2186 |
| Nebraska Oil and Gas Conservation Commission | 308-254-6919 |
| Bureau of Land Management (Cheyenne, WY) | 307-775-6256 |
| [redacted] | [redacted] |

## 2.0 SITE CHARACTERIZATION

This application will demonstrate that the Conestoga I-1 location is ideally situated for the permanent storage of captured $CO_2$ for several reasons, including but not limited to:

- The Lyons Formation is an excellent injection interval of continuous, thick [redacted] high-porosity [redacted]), and high-permeability ([redacted]) sandstone at the Conestoga sequestration site. Conestoga I-1 is expected to sequester 2.26 million tonnes per year (Mta) for a total of 27.1 million tonnes (Mt) over 12 years.
- The Lyons Formation is bounded by contiguous upper (Goose Egg Formation) and lower (Satanka Formation) confining layers comprised of impermeable shales, siltstones, and anhydrite.
- The Lyons Formation and confining seal units are *not* structurally complex. The formations have a gentle local and regional structural dip with no identified faults, open fractures, or geologic hazards within the modeled plume/pressure front extent (Area of Review).
- One injection zone penetration currently exists within the Area of Review (AoR). The injection well will be designed to prevent fluids from migrating to underground sources of drinking water (USDWs).
- The operator, Tallgrass High Plains Carbon Storage, LLC (High Plains), will control the pore space occupied by the modeled plume.
- Saturations indicate that the zone is saline, with no economically recoverable hydrocarbon resources within the gross injection interval within the AoR.

The proposed injection well has been designed to preserve seal integrity beyond the Project's life. Wellbores will be constructed with metallurgies and acid-resistant cement to prevent out-of-zone migration of injection or formation fluids and protect groundwater resources.

The site characterization provides text, tables, and figures to fulfill the site characterization requirements listed in 40 CFR §146.82(a)(2), (3), (5), and (6). References are appropriately cited, and a list of all citations with links to where the source can be downloaded or acquired is provided in **List of Cited References_WNSHub_Conestoga.xlsx**. A guide of detailed site characterization discussions is provided in **Table 2.1.**

The subject sequestration Project is proposed for the Permian-aged Lyons Formation within the Denver-Julesburg (DJ) Basin in western Nebraska. The Lyons Formation is an eolian sandstone found approximately [redacted] below the ground surface at the proposed well location.

Data, information, and interpretations described in this section are summarized in the following text, demonstrating the location of Conestoga I-1 and the AoR to be geologically and hydrologically favorable for the permanent storage of $CO_2$:

- The extent and structure of the DJ Basin, along with its tectonic setting, are an ideal location for $CO_2$ storage. Much of the basin consists of relatively simple structures with shallow dips (less than one degree within AoR). Recent faulting is absent from the injection and upper/lower confining zones. No significant seismic hazards are present in the AoR (*Sections 2.1, 2.3*).
- The regional geologic setting is well constrained due to thousands of wellbore penetrations from petroleum exploration and production that began in the 1880s within the DJ Basin (*Section 2.2*).

- Within the AoR, the Lyons Sandstone is an excellent reservoir for injection with high porosity (average [redacted]) and permeability (average [redacted]). (*Sections 2.4.1, 2.5).*
- Within the AoR, the Lyons Sandstone is highly saline with no economic quantities of hydrocarbons (*Sections 2.1.3.6, 2.8.1*).
- The Lyons Sandstone is encountered at ideal depths for pressures and temperatures favorable for storing supercritical $CO_2$, thousands of feet below currently exploited groundwater aquifers and the lowermost USDW (*Sections 2.4.1, 2.7*).
- The Lyons Sandstone is laterally extensive with no known structural or stratigraphic traps within the AoR. No faulting within the Lyons Sandstone was identified in the AoR or the surrounding area (*Section 2.2*).
- The Lyons Sandstone has the pore volume to store many times more $CO_2$ than proposed by this Project (*Section 2.10.2.1*).
- The Lyons Sandstone is vertically bound by the laterally continuous Goose Egg Formation upper confining layer consisting of approximately [redacted] ft of low permeability siltstone, shale, and anhydrite (*Sections 2.4.2, 2.10.2*).
- As the Lyons Sandstone is an open saline aquifer, $CO_2$ would be confined vertically by the overlying Goose Egg Formation while lateral confinement would initially occur via residual and solubility trapping and then ultimately via mineral trapping (Xu et al., 2001; Bachu and Adams, 2003; Bachu, 2006; Saadatpoor et al., 2010; Kampman et al., 2014; Ajayi et al., 2019) (*Sections 2.2.2, 2.10.2*).
- No detrimental geochemical interactions are expected between the injectate and the formations or formation fluids. This expectation will be confirmed via future core and fluid analyses along with geochemical modeling (*Section 2.8*).
- One existing well penetrates the injection and upper confining zones within the AoR. The injection well will be engineered to prevent fluids from migrating from the approved injection zone (*Sections 3.4.1, 5.0*).

Table 2.1—Site characterization summary.

| CFR | Section Title | Section No. | Sub-Section Title | Sub-Section No. |
|---|---|---|---|---|
| 40 CFR 146.82(a)(3)(iii) | Regional Geology, Hydrology, and Local Structural Geology | 2.1 | Tectonic and Structural History | 2.1.1 |
| | | | Stratigraphy | 2.1.2 |
| | | | General Hydrogeology | 2.1.3 |
| 40 CFR 146.82(a)(2), 146.82(a)(3)(i) | Maps and Cross Sections of the Area of Review | 2.2 | Map of Area of Review | 2.2.1 |
| | | | Structure Maps of the Injection and Confining Zones | 2.2.2 |
| | | | Cross Sections Through the AoR | 2.2.3 |
| 40 CFR 146.82(a)(3)(ii) | Faults and Fractures | 2.3 | Literature Review | 2.3.1 |
| | | | Seismic Data | 2.3.2 |
| | | | Well Data | 2.3.3 |
| 40 CFR 146.82(a)(3)(iii) | Injection and Confining Zone Details | 2.4 | Data on the Injection Zone | 2.4.1 |
| | | | Data on the Confining Zone(s) | 2.4.2 |
| 40 CFR 146.82(a)(3)(iv) | Geomechanical and Petrophysical Information | 2.5 | Fractures | 2.5.1 |
| | | | Pore Pressure | 2.5.2 |
| | | | Stress | 2.5.3 |
| | | | Ductility | 2.5.4 |
| | | | Rock Strength | 2.5.5 |
| | | | In-Situ Fluid Properties | 2.5.6 |
| | | | Geothermal Gradient | 2.5.7 |
| 40 CFR 146.82(a)(3)(v) | Seismic History | 2.6 | Summary of Seismic History and Available Data | 2.6.1 |
| | | | Seismic Risk | 2.6.2 |
| 40 CFR 146.82(a)(3)(vi), 146.82(a)(5) | Hydrologic and Hydrogeologic Information | 2.7 | Hydrostratigraphy and Underground Sources of Drinking Water | 2.7.1 |
| | | | Springs | 2.7.2 |
| | | | Water Wells Within the AoR | 2.7.3 |
| 40 CFR 146.82(a)(6) | Geochemistry | 2.8 | Fluid Chemistry | 2.8.1 |
| | | | Solid Phase Geochemistry | 2.8.2 |
| | | | Geochemical Modeling | 2.8.3 |
| - | Other Information | 2.9 | Not Applicable | - |
| 40 CFR 146.83 | Site Suitability | 2.10 | Structural and Tectonic Suitability | 2.10.1 |
| | | | Storage Reservoir Suitability (Injection Zone) | 2.10.2 |
| | | | Confining Zone Suitability | 2.10.3 |

## 2.1 Regional Geology, Hydrogeology, and Local Structural Geology [40 CFR 146.82(a)(3)(vi)]

### *2.1.1 Tectonic and Structural History*

The proposed Western Nebraska Sequestration Hub (WNS Hub) is located in Kimball County, 14 miles southeast of the town of Kimball in western Nebraska, in Section 26, Township 13N, and Range 54W. The site is situated in the Denver Basin, also referred to as the Denver-Julesburg Basin or "DJ Basin" (**Figure 2.2**).

Figure 2.1—Regional topographic map of the northern DJ Basin showing the location of the proposed injection well (blue pin) and AoR (red circle). The outline of the DJ is shown in dashed purple.

The DJ Basin is an elongated, asymmetrical syncline structural depression covering approximately 70,000 square miles in southeast Wyoming, southwest Nebraska, and northeast Colorado (**Figure 2.2).** The DJ Basin was formed during the Laramide Orogeny, which occurred approximately 75 million to 35 million years ago. Strata in the basin reaches a maximum thickness of 13,000 ft and consist primarily of Mesozoic and Paleozoic sedimentary rocks overlying a Precambrian metamorphic basement that is approximately 1.6 billion years old (Weimer and Sonnenberg, 1996).

The Front Range of the Rocky Mountains bounds the basin to the west, with the north-south basin axis running roughly parallel to the mountain front **(Figure 2.3**). The deepest portion of the basin is found along the axis, with a steeply dipping western flank that can exceed ten degrees and a gently dipping eastern flank (**Figure 2.3**). The DJ Basin is bound in the northwest by the Hartville Uplift, the northeast by the Chadron Arch, and the southwest by the Apishapa Uplift (Sonnenberg and Weimer, 1981; Hovorka et al., 2003; Bartos et al., 2021; Lee and Bethke, 1994; Higley and Cox, 2007). The basin extends 150 miles east into Kansas and Nebraska, with strata dipping gently west toward the basin axis. The AoR is located east of the basin axis in a region with gently dipping strata and no major faulting.

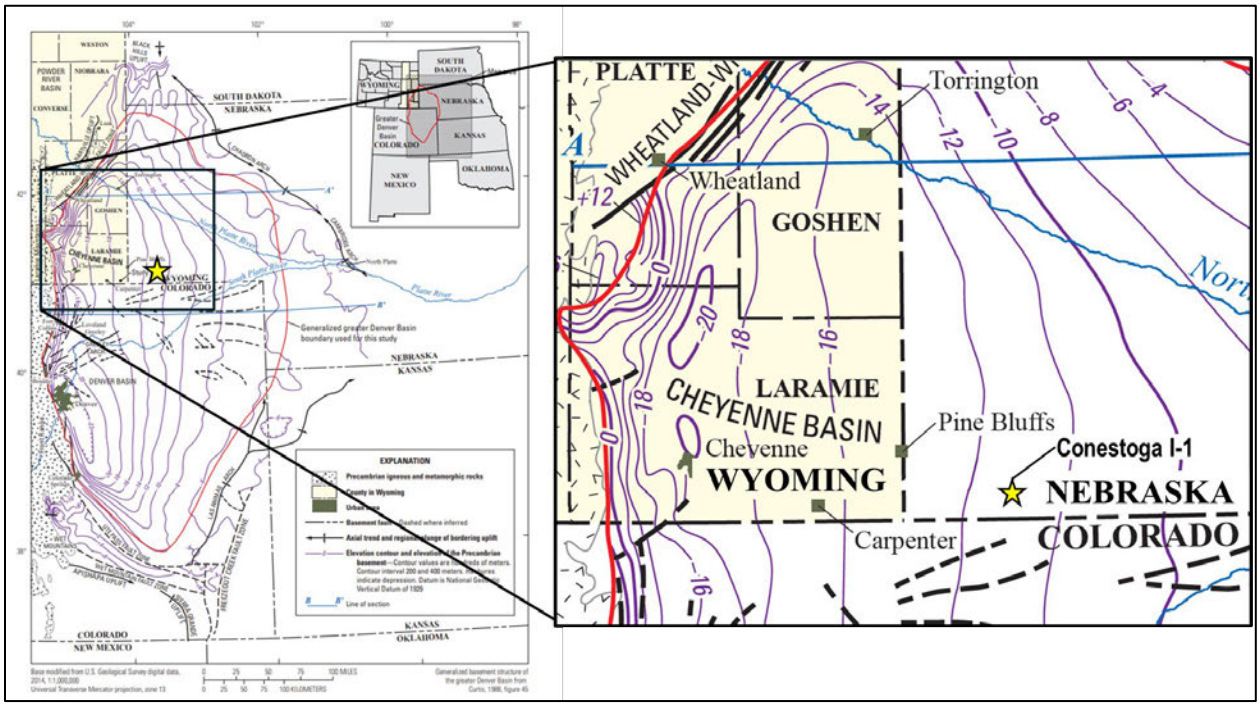

Figure 2.2—Generalized basement structure of the greater DJ Basin in Wyoming, Nebraska, Colorado, and Kansas (after Bartos et al., 2021). The yellow star is the approximate location of Conestoga I-1. Note there is no interpreted faulting within the AoR.

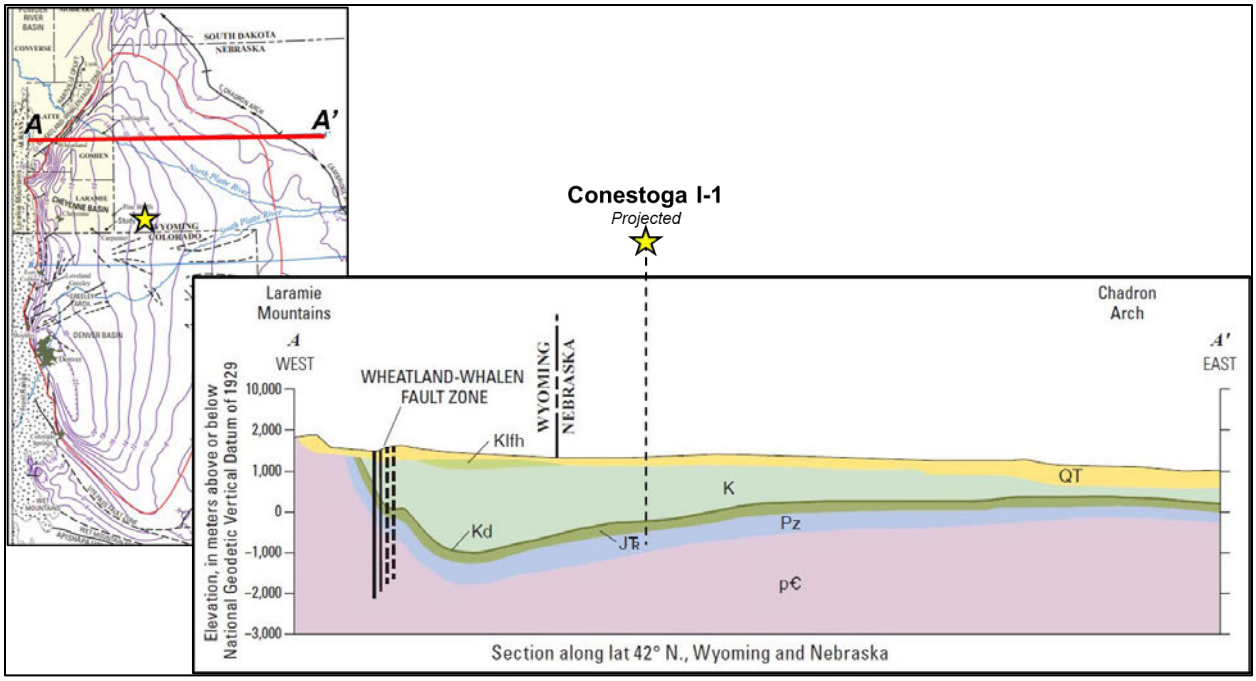


Figure 2.3—Schematic cross-section along latitude 42°N through Wyoming and Nebraska (after Bartos et al., 2021). The inset map indicates the cross-section location and the yellow star shows the general location of Conestoga I-1.

The beginning of the tectonic evolution of the DJ Basin began as early as 1.6 to 1.8 billion years ago with the formation of the Transcontinental Arch (TCA), a northeast-trending basement uplift that formed from the accumulation of accretionary arcs (**Figure 2.4**). Each ancient accretion location resulted in a zone of weakness in the basement, affecting Phanerozoic (500 million years ago [Ma] to recent) location and trends of both tectonics and sedimentation (Carlson, 2003).

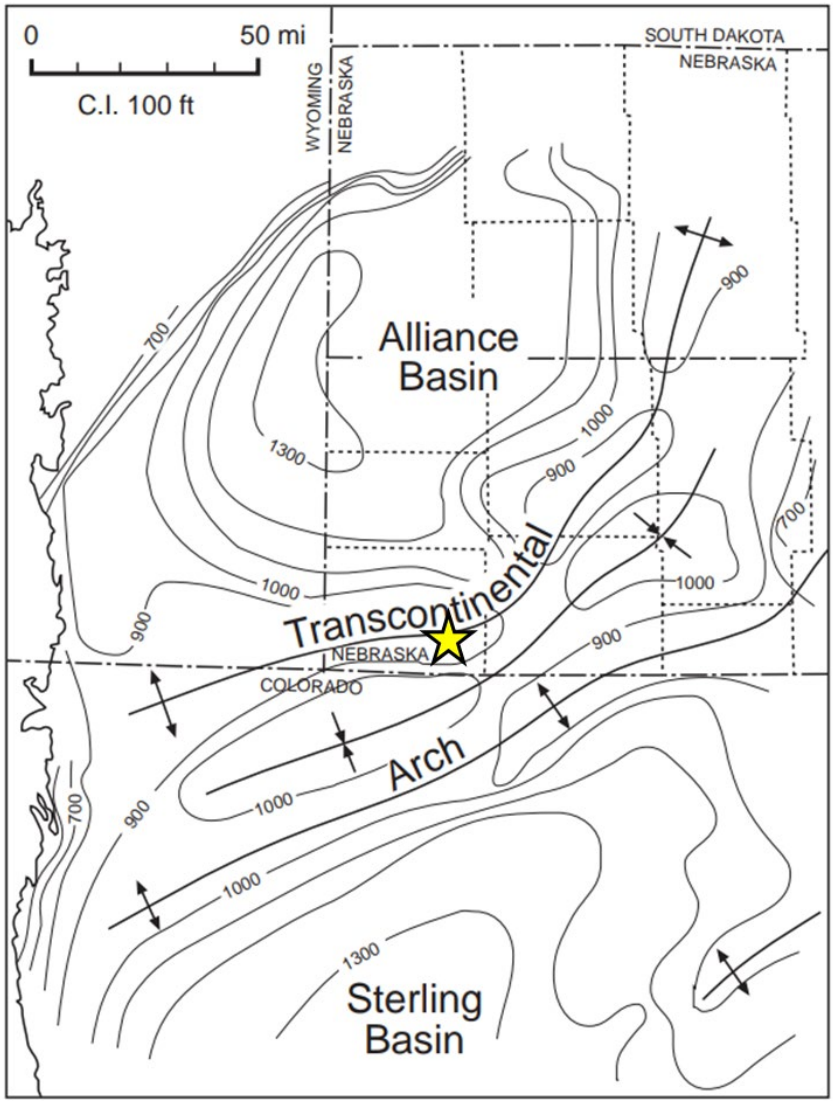


Figure 2.4—Isopach map of the Permian section, northern Denver-Julesburg Basin with paleotectonic events (after Montgomery et al., 1998).

The orientation of the TCA correlates with wrench fault zones along the Colorado Front Range to the west, major lineament trends, and strike-slip faults to the east (Montgomery et al., 1998). During the late Paleozoic (Pennsylvanian-Permian), the region was uplifted due to the ancestral Rocky Mountain orogeny. This deformation is roughly associated with the formation of the front ranges to the west and the Hartville Uplift to the northwest of the DJ Basin (**Figure 2.2**). The Alliance and Sterling basins, divided by the TCA, formed because of subsidence to the east (**Figure 2.4**). According to Garfield et al. (1988), the depositional systems vary from offshore marine deposits to the south (Sterling Basin) to higher energy grainstone and shoal deposits on the TCA to mixed peritidal, evaporitic, and eolian deposits to the north. Many of the hydrocarbon plays in the DJ Basin, specifically the Cretaceous reservoirs, are associated with the TCA. The Laramide Orogeny, which occurred in the Cretaceous between 67.5 Ma until about 50 Ma, was significant in forming the present-day structure of the DJ Basin (Montgomery et al., 1998; Higley and Cox, 2007).

A locator map (**Figure 2.5**) and regional cross-sections (**Figure 2.6**, **Figure 2.7**, **Figure 2.8,** and **Figure 2.9**) were constructed by High Plains using relevant well logs to help convey the regional geologic interpretation of the structure and stratigraphy at the Conestoga I-1 location. The cross sections represent geologic stratigraphic and structural elements from surface to Paleozoic, providing a regional context to the Project. *Section 2.2.3* contains cross-sections specific to the AoR to clarify the regional interpretation by limiting geologic sections to confining and injection intervals. Both cross-sections demonstrate a consistent structural interpretation with laterally extensive confining and injection intervals. A map of the DJ Basin and mapping domain, plus well log control points, is shown in **Figure 2.10**.

Figure 2.5—Regional cross-sectional location map with Lyons structural contours. The yellow star is the approximate location of the Conestoga I-1 injection well.

Figure 2.6—Regional north-to-south cross-section A-A′ showing the entire stratigraphic section from the ground surface to below the base of the storage complex The yellow star indicates the approximate Conestoga I-1 location. The digital log tracks represent gamma ray and deep resistivity logs. The section is approximately parallel to structural strike.

Figure 2.7—Regional north-to-south cross-section A-A′ zoomed in on the injection/confining zone and flattened on the base confining zone surface of the Satanka Formation.

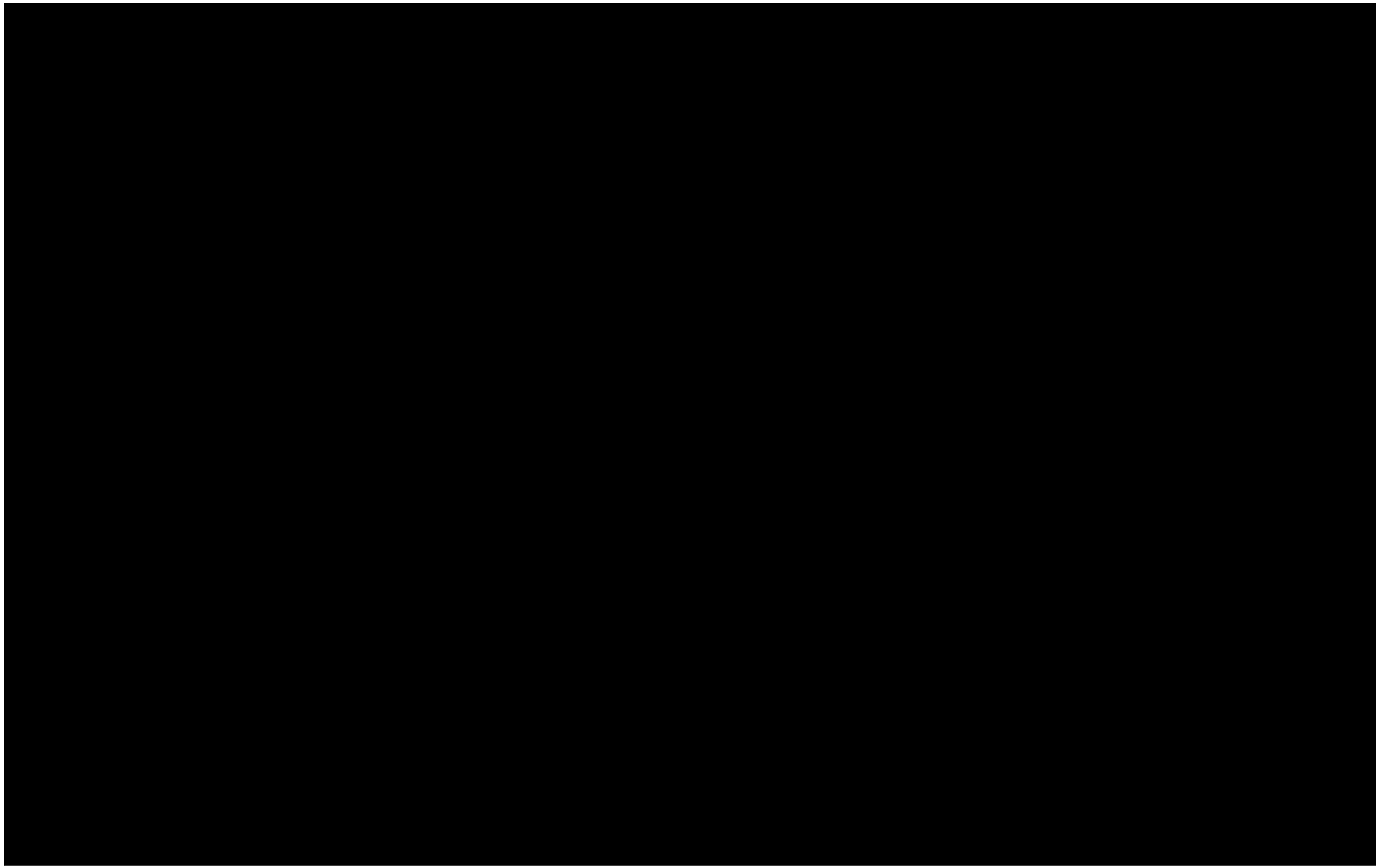

Figure 2.8—Regional west-to-east cross-section B-B′ showing the entire stratigraphic section from the ground surface to below the base of the storage complex. The yellow star indicates the approximate Conestoga I-1 location. The digital log tracks represent gamma ray and deep resistivity wireline logs. The section is approximately parallel to the structural dip.

Figure 2.9—Regional west-to-east cross-section B-B′ zoomed in on the injection/confining zone and flattened on the base confining zone surface of the Satanka Formation.

Figure 2.10—DJ Basin outline and WNS Hub mapping area. Red dots represent the top Lyons Formation surface picks used to map the Lyons' structure.

### *2.1.2 Stratigraphy*

The DJ Basin contains a thick sequence of sedimentary rocks ranging from Cenozoic to Paleozoic in age (**Figure 2.11, Figure 2.12**). Nearly 70 percent of these sedimentary rocks are Cretaceous in age (Higley and Cox, 2007). The maximum thickness of the DJ Basin sedimentary sequence is approximately 13,000 ft along the synclinal basin axis and comprises shallow marine and continental deposits consisting primarily of sandstones, shales, and evaporites that overlie a Precambrian metamorphic basement.

This region was a shallow marine shelf during the early Paleozoic, followed by uplift and erosion during the middle Paleozoic. Mississippian and Pennsylvanian sedimentary units above this unconformity include marine limestones and shales. The Permian interval above this consists of detrital, carbonate, and evaporite deposits (Clayton and Swetland, 1980). Within the AoR, these early Permian carbonates are part of the Chase Group and consist of the Admire, Council Grove, Amazon, and Wolfcamp formations. The middle Permian-age Lyons Formation, the proposed injection zone, includes a basal calcareous silty sandstone with horizontal, convolute, and flaser-

like bedding with burrows overlain by small-scale cross-beds overlain by large-scale cross-beds at the top of the section. The Lyons Formation is eolian and fluvial, deposited in a desert or sabkha environment (Adams and Patton, 1979). The Triassic and Jurassic rocks of the Goose Egg, Chugwater, Sundance, and Morrison Formations include fluvial sandstones, shales, marine mudstones, evaporites, and limestones. Upper Jurassic rocks include coastal, flood, and alluvial deposits. The overlying Cretaceous rocks, with a maximum thickness of 10,000 ft, consist of deltaic and marine sedimentary rocks (Clayton and Swetland, 1980).

The Lyons Formation was identified as a strong candidate for carbon sequestration by the Bureau of Economic Geology in the 2003 Technical Summary: *Optimal Geological Environments for Carbon Dioxide Disposal in Brine Formations (Saline Aquifers) in the United States* (Hovorka et al., 2003). Containment is provided by the underlying Satanka Formation and overlying Goose Egg (Lykins) Formation confining zones. The thick Cretaceous shale section overlies the lower Cretaceous and provides additional low permeability confining strata between the injection zone and shallow USDWs. The low-porosity mudstones and anhydrites of the Wolfcamp, underlying the Satanka, provide additional low permeability strata below.

General lithologic descriptions of the injection interval and upper and lower confining units are included in *Section 2.4* and can be referenced to the stratigraphic column depicted in **Figure 2.12**.

The Nebraska Geological Survey at the University of Nebraska in Lincoln Divine and Sibray (2017), Sibray et al. (2020), and Bartos et al. (2021) have identified multiple aquifers from Pennsylvanian to Quaternary in age and one USDW within the AoR, referred to as the High Plains Aquifer (HPA) (**Figure 2.12**). The HPA includes Oligocene to Holocene Formations. The lithologic descriptions of major aquifers, minor aquifers, marginal aquifers, and aquitards identified by the Conservation and Survey Division of the University of Nebraska are covered briefly in *Section 2.1.3.4—Regional Aquifers and Confining Units/Aquitards* and in more detail in *Section 2.7.1—Hydrostratigraphy and Underground Sources of Drinking Water*.

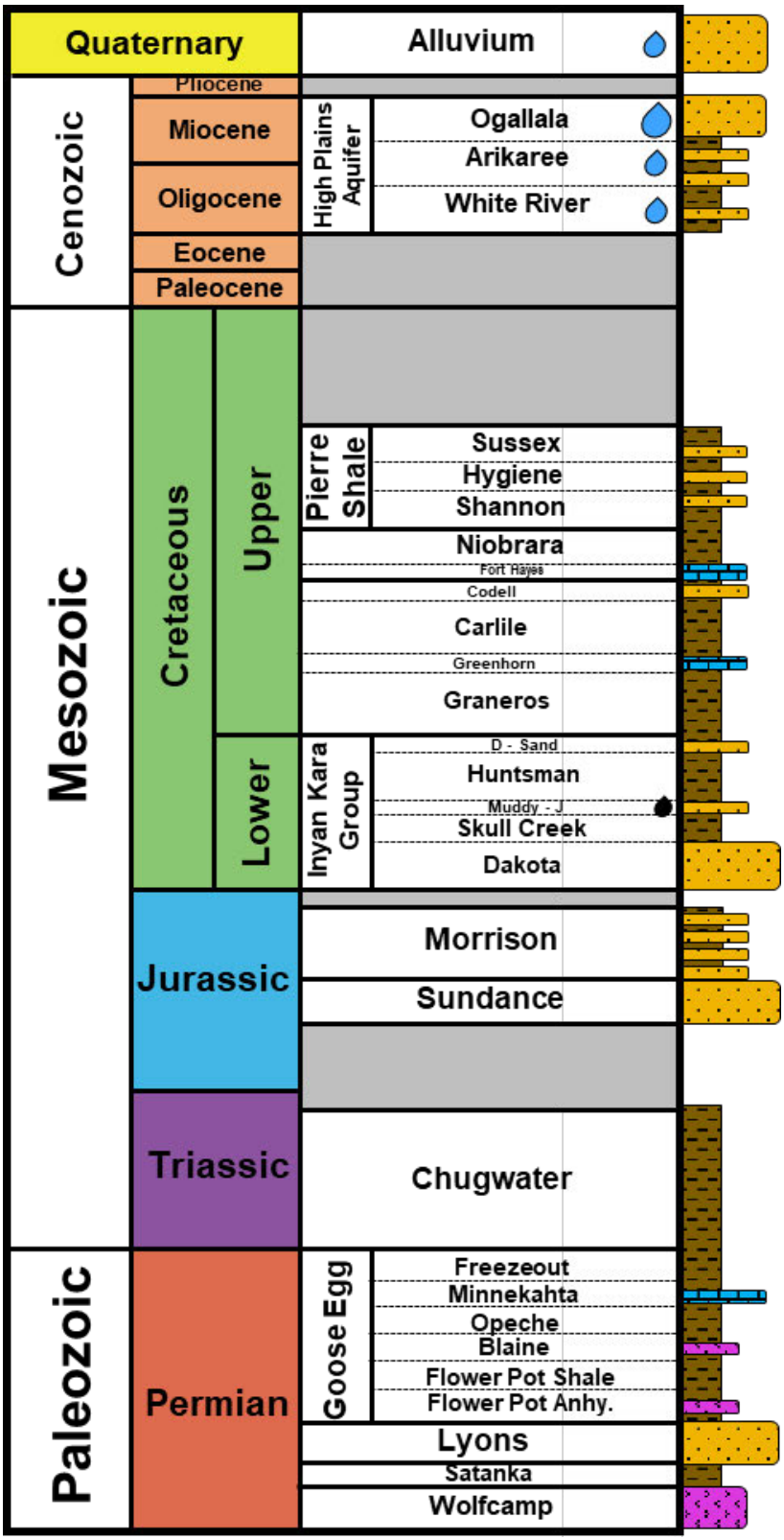


Figure 2.11—AoR-specific stratigraphic column with generalized lithologies. Brown represents shale/silt-rich intervals, yellow represents sandstone-dominant intervals, blue represents carbonate-rich intervals, and pink represents evaporite-rich intervals. USDWs are noted by a blue water droplet, and oil-bearing producing zones (Muddy-J) are indicated by a black droplet.

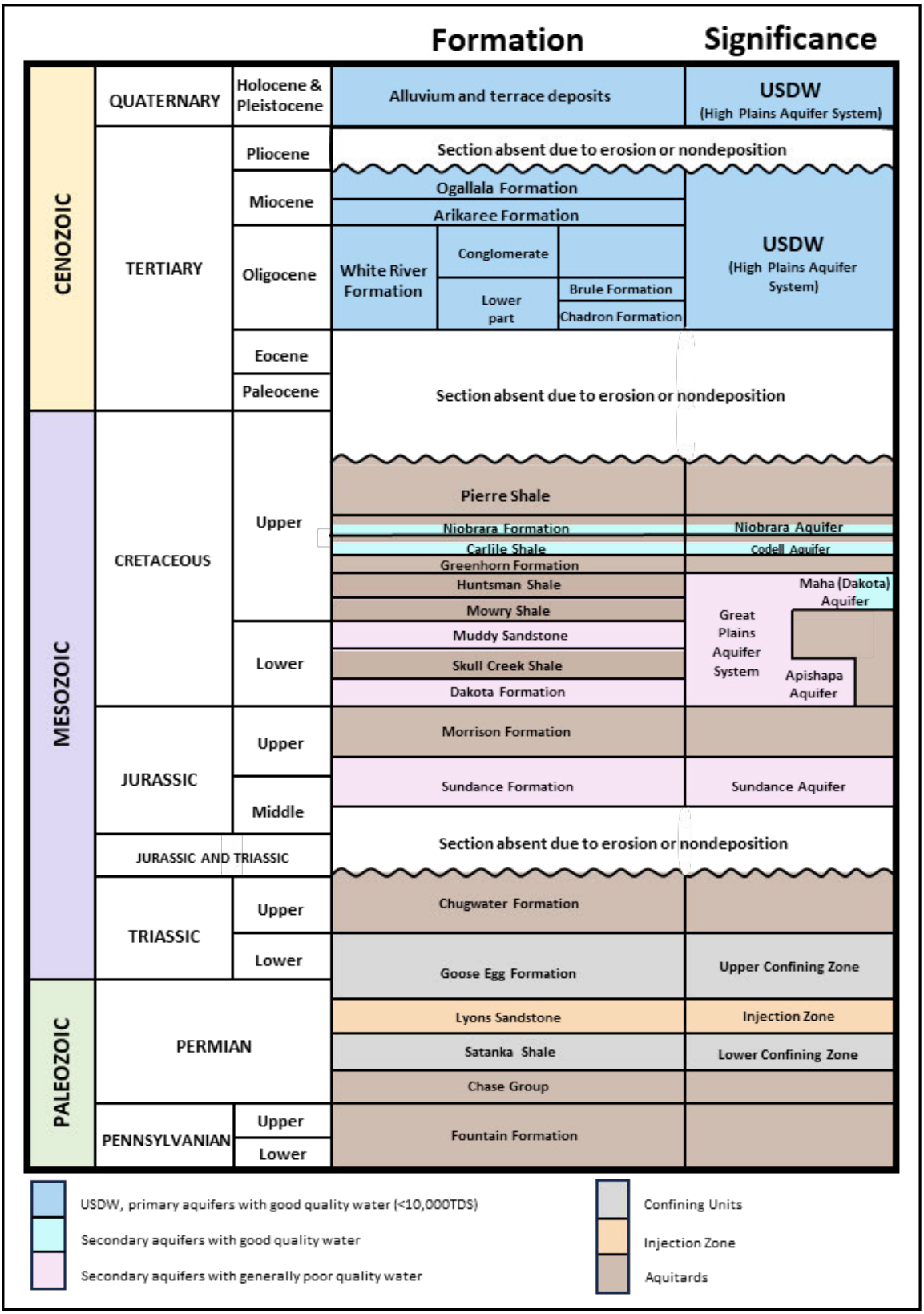


Figure 2.12—Stratigraphic column of the DJ Basin. The shading indicates confirmed USDWs in blue, the proposed injection interval in red, primary confining layers in dark gray, and additional confining layers in light gray (modified from Taucher et al., 2013).

#### *2.1.2.1 Relevant Stratigraphic Formations*

Permian Satanka Formation (Lower Confining Zone)

The Satanka Formation contains interbedded red and gray fine-grained sandstones, gray siltstone, red mudstone, occasional anhydrite beds, and red anhydritic siltstones, exhibiting low porosities and permeabilities in log characteristic and core data. This formation has been interpreted as a mixture of arid fluvial, floodplain, mud flat, and desert lake deposits (Sonnenberg and Weimer 1981). The Satanka provides an impermeable cap, eliminating vertical migration (Clayton and Swetland, 1980). Based on offset correlations, the Satanka has an approximate thickness of [redacted] ft at the proposed Conestoga I-1 site.

Permian Lyons Formation (Injection Zone)

The Lyons Formation is described as a well-sorted, fine-grained, eolian quartzose sandstone in outcrops near Lyons, Colorado (Sonnenberg and Weimer, 1981). However, lithofacies vary due to complex depositional environments and diagenetic cementation, ranging from sandstone to evaporites, carbonate, red shale, and conglomerate (Hovorka et al., 2003; Lee and Bethke, 1994). The Lyons sandstone commonly contains quartz overgrowths, calcite cements, and iron oxide coating. Towards the basin axis, diagenetic alteration removed iron oxide and calcite cement, which resulted in grey diagenetic facies associated with anhydrite and dolomite-filled porosity and petroleum accumulation in the Lyons Formation in western Weld County, Colorado (Lee and Bethke, 1994). The Lyons is generally less than 400 ft thick across the DJ Basin, though it increases to over 500 ft in the southernmost portion of the basin (**Figure 2.13**). Based on offset correlations, the Lyons Formation has an approximate thickness of [redacted] ft at the proposed Conestoga I-1 site.

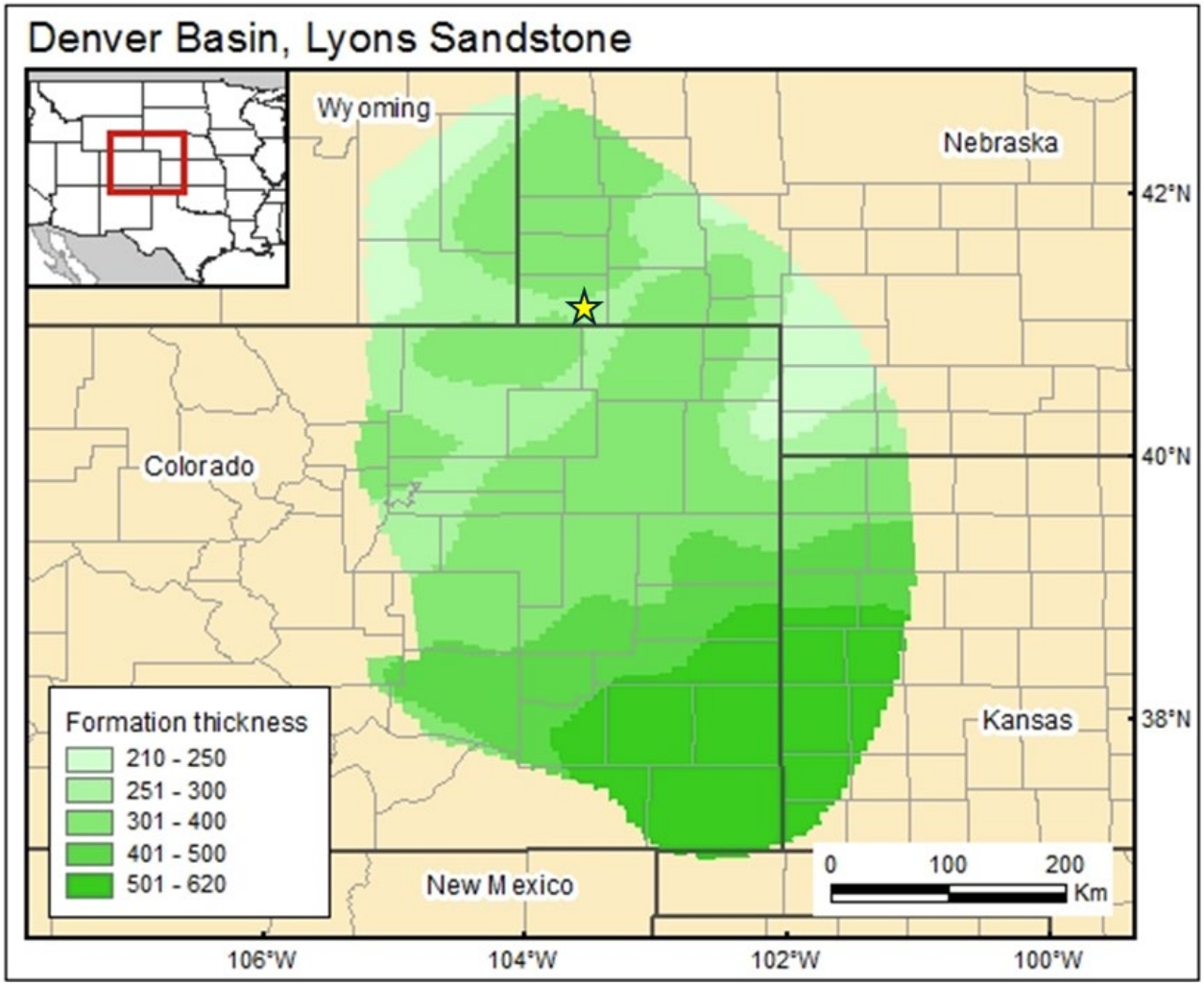


Figure 2.13—Regional mapping of the formation thickness of the Lyons Formation, modified by the BEG (Sonnenberg, 1981; Levandowski et al., 1973; Garbarini and Veal, 1968). The yellow star indicates the proposed injection location.

Regional movement of groundwater allowed diagenetic alteration to remove iron oxide and calcite cement from red beds within the Lyons sandstones, resulting in two mineralogically and diagenetically distinct facies: grey facies and red facies. Grey facies are proximal to the basin axis and indicative of oil presence. They are distinguished by pore-filling dolomite and anhydrite cement and a lack of iron oxide. This is caused by the mixing of water from the Fountain Formation through post-Laramide fractures in the basin axis (Lee and Bethke, 1994; Kendigelen et al., 2023). This distinct grey facies is only present across oil fields in western Weld County and eastern Larimer County, Colorado, far from the AoR. The presence of "red facies" indicates the absence of hydrocarbons and the lack of mixing with Fountain Formation waters. This is due to the absence of cementation associated with interactions closer to basin axis fractures. The Juniper M-1 characterization well acquired core across the entirety of the Lyons Formation, all of which contained red iron-oxide facies associated with high-quality reservoir quality and an absence of hydrocarbons.

The proposed injection formation, the Lyons Formation, is bound to the north by the Alliance Basin and south by the Sterling Basin, where the Lyons Formation changes facies into the time-equivalent Stone Corral Formation, also referred to as the Salt Plain Formation (Oldham, 1997), becoming rich in anhydrite, red silts, dolomite, and sometimes halite (**Figure 2.14** and **Figure 2.15**). The Lyons Formation eolian sandstone and the local facies transition to Stone Corral sabkha facies is well understood across the DJ Basin (**Figure 2.16**). Within the Lyons eolian trend, well log data and subsequent mapping confirm the regional continuity of the Lyons Formation and the confining zones, the Goose Egg Formation (upper) and Satanka Formation (lower).

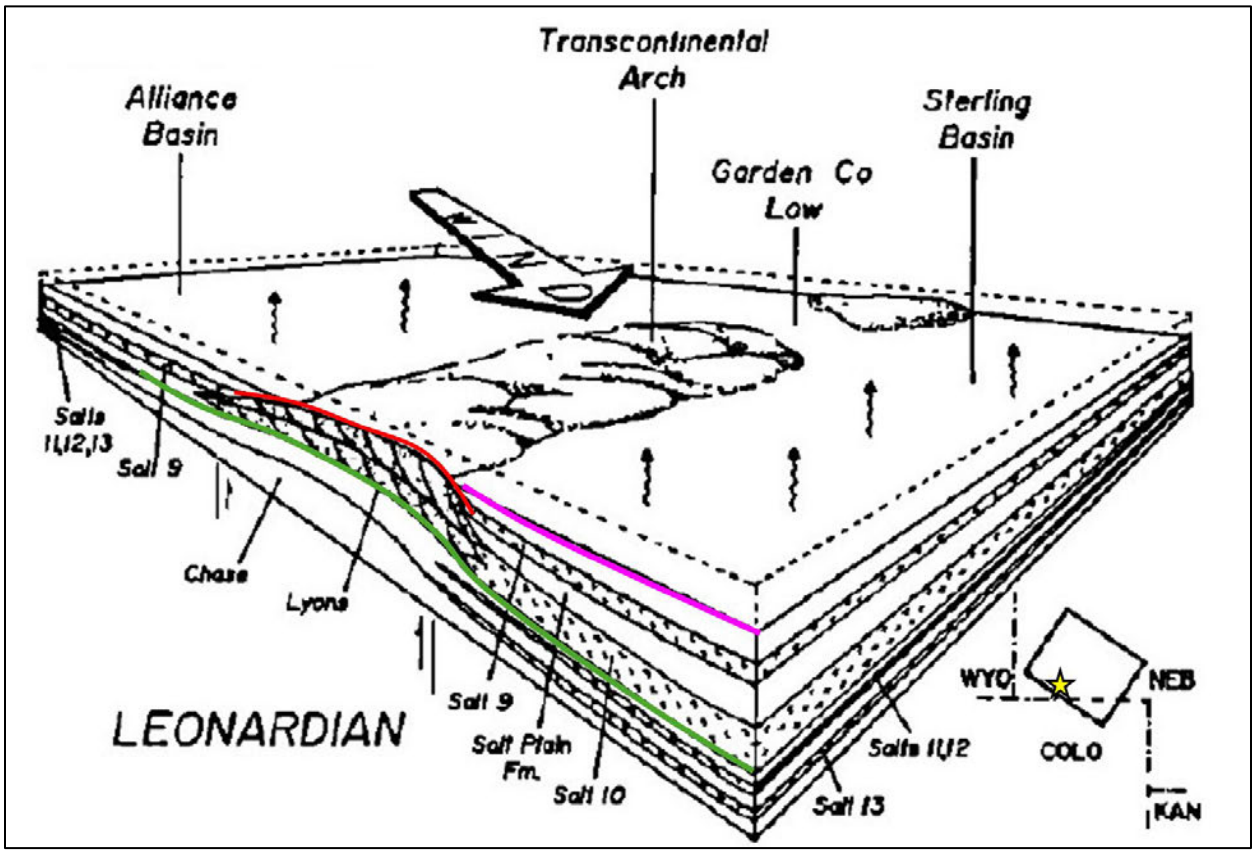


Figure 2.14—Block diagram depicting the facies changes within the Lyons Formation (after Oldham, 1997). The green surface represents the Satanka Formation, as shown in the generalized stratigraphic column. The red surface indicates the Lyons eolian sandstone surface, and the pink surface represents the Stone Corral (or "Salt Plain Formation"), which is a lateral facies change from the Lyons eolian Sandstone. to the

sabkha facies of the Alliance and Sterling basins.

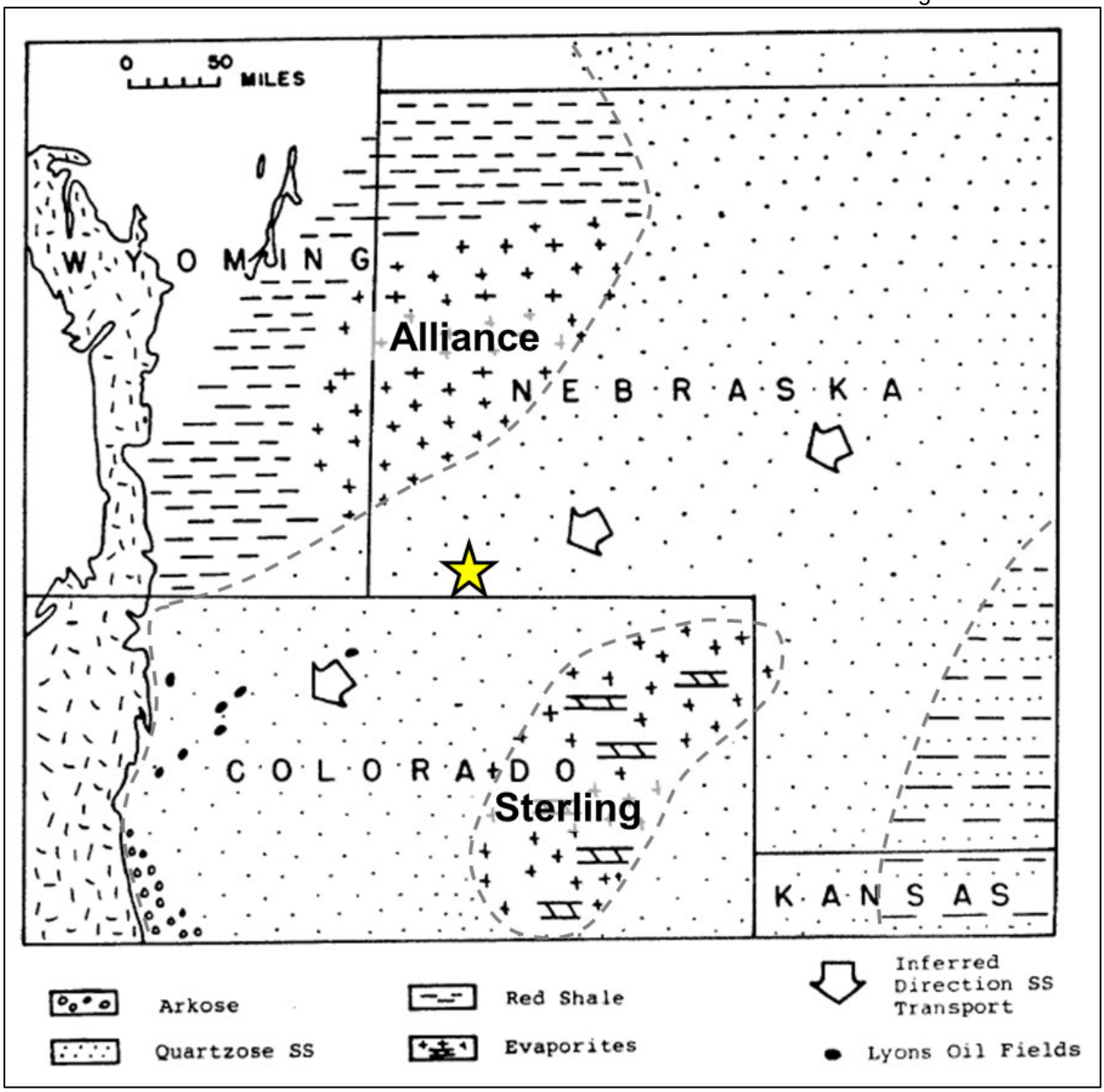


Figure 2.15—Regional lithofacies map of the Lyons Formation (after Sonnenberg, 1981).

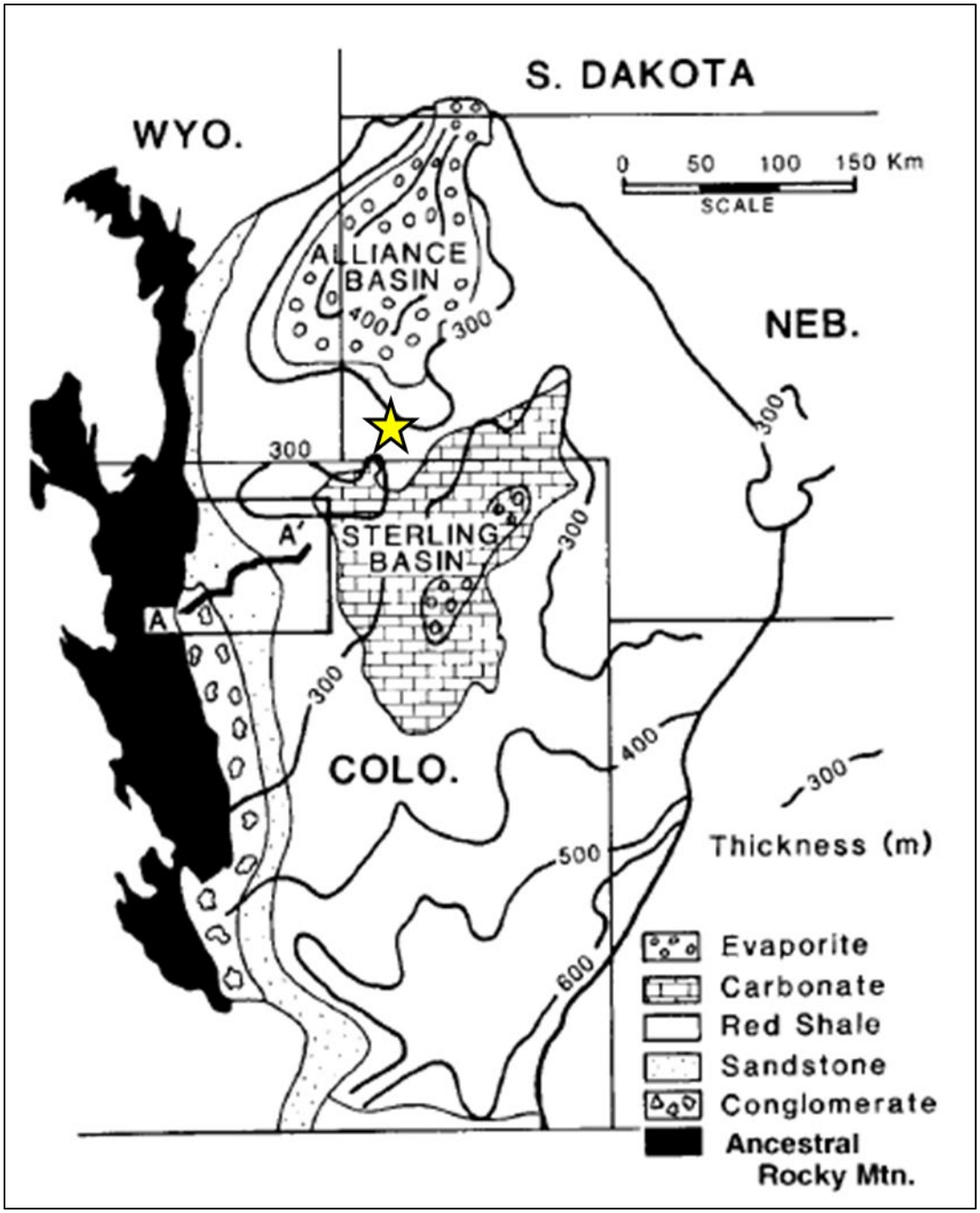


Figure 2.16—A regional isopach and lithofacies map of the Permian sediments, identifying the Alliance and Sterling Basins (after Lee and Bethke, 1994).

Late Permian-Early Triassic Goose Egg Formation (Upper Confining Zone)

This geologic section is typically referred to as the "Goose Egg Group" in Wyoming and the "Lykins Formation" in Northern Colorado (Campbell, 1963). Hereafter, this geologic section will be referred to as the "Goose Egg Formation."

At the proposed Conestoga I-1 location, the Goose Egg is approximately [redacted] ft thick. The Goose Egg Formation is present across the region as thinly-bedded red siltstone, massive anhydrite,

dolostone, and halite, likely deposited in a sabkha landscape with a fluvial sediment influx from the ancestral Rockies into a shallow evaporite basin. Stromatolites, ostracods, foraminifera, sponge spicules, gastropods, and bivalves further indicate a shallow marine deposition (Hagadorn et al., 2019).

A disconformity at the base of the Goose Egg was described by Burk and Thomas (1956). More recent investigations (Oldham, 1996) suggest, and High Plains' interpretation supports, that continual deposition through a sea level transgression occurred where an eolian environment was drowned to form a sabkha/tidal flat environment (**Figure 2.17**). This transgression resulted in a sharp contact between the Lyons Sandstone and overlying Goose Egg anhydrite, with anhydrite cement sometimes found in the uppermost sections of the Lyons Sandstone, as described in the Juniper M-1 core.

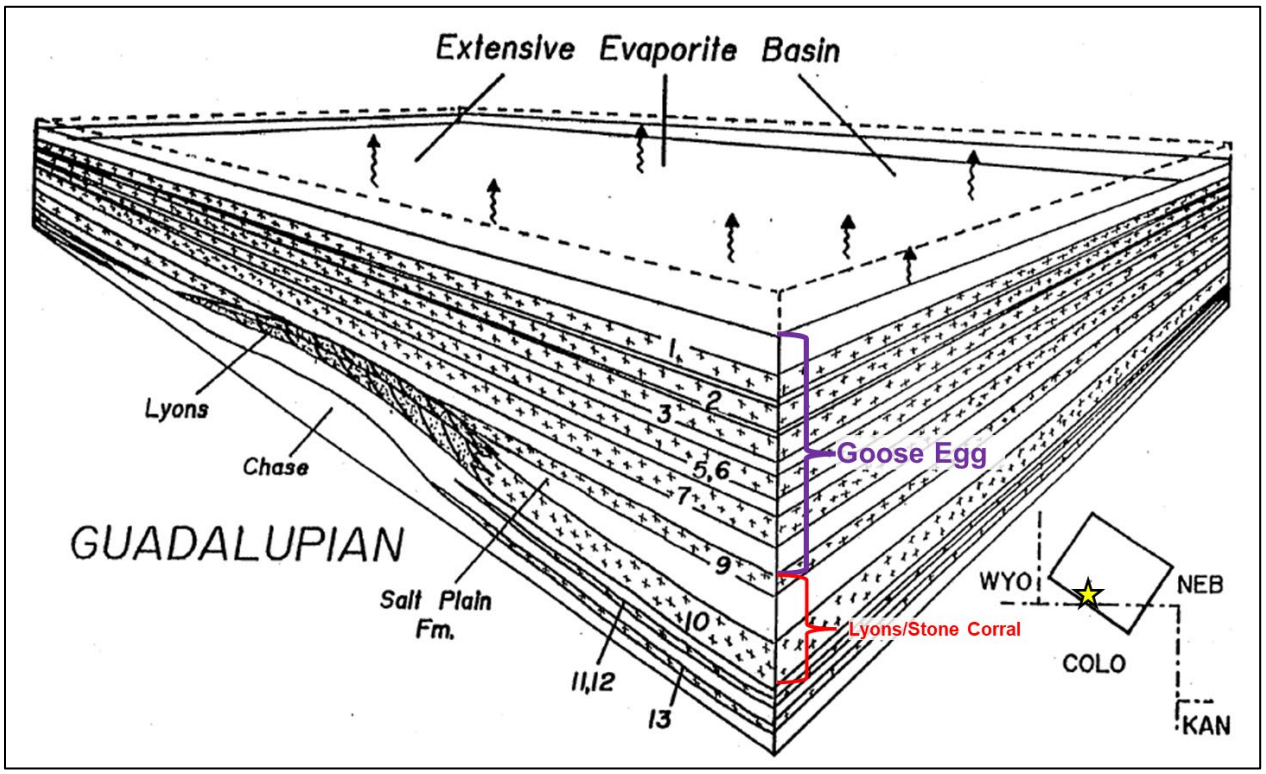


Figure 2.17—Block diagram depiction of Goose Egg Formation deposition over the Lyons/Stone Corral Formation as evaporite basins drown out the eolian system and begin the Goose Egg sequence of thick siltstone, evaporite, and dolostones beds (after Oldham, 1997).

Triassic Chugwater Formation

The Chugwater Formation conformably overlies the Goose Egg Formation and unconformably underlies the Sundance Formation. It is comprised of reddish-orange shale and siltstone with thin gypsum partings near the base. The Chugwater was deposited in an eolian, dry environment with intermittent streams. Literature estimates a thickness of approximately 500 ft regionally (Lowry and Crist, 1967; Love and Christiansen, 1985). At the proposed Conestoga I-1 location, the Chugwater has a thickness of approximately [redacted] ft, as the Triassic-Jurassic sections thin unconformably to the east-southeast of the sequestration location.

Middle/Upper Jurassic Sundance Formation

The Jurassic Sundance Formation sediments in the DJ Basin overlie an unconformity. The Sundance Formation, of the middle to the late Jurassic age, is a greenish-gray glauconitic sand-to-sandy shale underlain by red-to-gray non-glauconitic sandy shale. It was deposited in a shallow inland sea known as the Sundance Sea or the Logan Seaway that covered large parts of western North America during the middle to late Jurassic. The Sundance varies from eolian to marine sandstone in Kimball County. The Sundance Formation has a thickness of approximately [redacted] at the proposed injection site as the formation thins unconformably to the southeast atop the paleo-TCA.

Upper Jurassic Morrison Formation

The Jurassic Morrison Formation is a widespread regional deposit that ranges in depositional environment from restricted marine to fluvial-deltaic to alluvial. The Morrison is characterized by lithologies ranging from sandstone, conglomerate, and varicolored non-marine shales, with localized occurrences of limestone (Mallory, 1972). Site-specific lithology is primarily interbedded shale with thin sandstone and limestone stringers.

The Morrison top marks an unconformity and is reported absent in part of northwestern Nebraska along the trend of the Chadron Arch. This is consistent with early-Cretaceous truncation and non-deposition along the paleo-basin edges. The Morrison Formation has a thickness of approximately [redacted] at the proposed injection site.

Lower Cretaceous Inyan Kara Group

The Cretaceous Inyan Kara, or "Dakota" Group, includes the Dakota/Lakota Sandstone, Skull Creek Shale, Muddy-J Sand, and Huntsman Shale. In literature, the Inyan Kara Group is often referred to as the "Dakota Group." However, for this application, this description will utilize the "Inyan Kara Group" nomenclature to represent this group of formations. The combined Inyan Kara Group is approximately [redacted] thick at the sequestration location and consists of very fine to medium-grained, quartz-rich, siliciclastic sandstone and conglomerate interbedded with mudstone. The Skull Creek Shale overlies the Dakota/Lakota Sandstone. It is a potential hydrocarbon source rock for the overlying sandstone units and is a confining layer for the lowermost Dakota Sandstone. The Skull Creek Shale is regionally extensive across the DJ Basin and was likely deposited in a marginal marine setting or a marine setting. In the Wattenberg field, the porosity of the Inyan Kara Group ranges from 1 to 13 percent and permeability of 0.001 to 100 millidarcy (mD). The water quality ranges from fresh to saline (greater than 10,000 mg/L TDS) (Drake et al., 2014).

The Muddy-J Sandstone, "J-Sand," or "Muddy-J," is about 80 ft thick at the sequestration site and consists of fine- to medium-grained siliciclastic sandstone interbedded with mudstone and is regionally extensive across the DJ Basin. The Muddy-J Sandstone was likely deposited in a deltaic and incised-valley environment that formed due to the shoreline regression of the Cretaceous Western Interior Seaway. The Muddy-J Sandstone has a regional average porosity of 18% and a 0.01 to 2,000 mD permeability. The water quality indicates that the groundwater ranges from fresh to saline (greater than 10,000 mg/L TDS; Drake et al., 2014).

Petrophysical modeling of the three closest penetrations into the Lyons (as discussed in *Section 2.4*) reveals similar characteristics. Sand packages display porosities ranging from [redacted] while mudstone packages have porosities [redacted] The mudstones exhibit extremely low

permeability in the microdarcy [$\mu$D] range, and the sands are estimated to have permeabilities between [redacted] mD. Estimating salinity based on resistivity measurements (Rw) was not feasible due to the likely presence of residual hydrocarbons (see *Section 2.8.1.4.2* for further details).

The Huntsman, or "Belle Fourche" Shale, is considered source rocks in the DJ Basin and sealing units for the Muddy Sandstone. These shales were deposited in a marine environment during shoreline transgression of the Cretaceous Western Interior Seaway.

Upper Cretaceous Shales

The Upper Cretaceous is comprised of the Greenhorn Limestone, Carlile Shale, Niobrara Shale, and Pierre Shale.

The Greenhorn Formation is a widespread unit that extends north from New Mexico to Canada and east from New Mexico to South Dakota and Minnesota. It is about [redacted] ft thick at the sequestration site and is composed of thin limestones, dark gray to black organic-rich shales, and thin bentonite beds. The Greenhorn Formation has an average porosity of [redacted] and permeability of [redacted] mD.

The Carlile Shale, which includes the Codell Sandstone Member, was deposited in a shallow marine or brackish near-shore environment or on the shelf of the Cretaceous Western Interior Seaway.

The Niobrara Formation, which includes the Fort Hayes Limestone and Smoky Hill Shale Members, was deposited during a sea level rise and consists of interbedded limestone and shale units. The average porosity of the porous units within the Niobrara is [redacted], with a permeability of [redacted] mD. The Niobrara Formation is approximately [redacted] ft thick at the sequestration site.

The Pierre Formation is a gray to black shale deposited in a deep marine environment that confines underlying sandstone beds. The Pierre Shale includes thin linear sand units called the Terry and Hygiene Sandstone. The Pierre Shale is 6,000 to 8,000 ft thick in the DJ Basin. The Hygiene/Larimer member is laterally continuous and was deposited either in an offshore shelf during a regressive shoreline event or nearshore (Drake et al., 2014). The sand units within the Pierre Shale have an average porosity of [redacted] and a permeability of [redacted] mD.

Upper Cretaceous Fox Hills Sandstone and Lance Formation

The youngest Cretaceous deposits in Nebraska are the Fox Hills and Lance formations, which conformably overly the Pierre Shale. The Fox Hills Sandstone is a fine to medium-grained sandstone and shale unit primarily used as a domestic water resource to the west of the AoR (Brendecke and Hinckley, 2014). The Lance Formation is a tan sandstone deposited by streams on a coastal plain along the western edge of the Western Interior Seaway (Pierce, 1997). These sandstone formations pinch out west of the AoR and are not expected to be present at the WNS Hub location.

Oligocene White River Formation (Lowermost USDW)

The White River Formation (WRF) is up to [redacted] ft thick and consists of volcaniclastic, fluvial, eolian, and lacustrine strata. It unconformably overlies Cretaceous rocks and is disconformably overlain by either the Miocene Arikaree or Ogallala formations or Quaternary alluvium (Lowry,

1966). The WRF includes the Brule Formation (above) and Chadron Formations (below). The White River Group makes up the lowermost section of the HPA, and strata within the White River Group are thus considered to be part of the lowermost USDW (**Figure 2.12**).

The Chadron Formation is about [redacted] thick and consists of smectite-rich, bluish-green and gray hummocky mudstone underlying a silty claystone with occasional sandstone channel deposits (Terry, 1998; Babcock et al., 1952). The Chadron Formation was deposited on an erosional surface, resulting in variable thicknesses. The channel deposits are narrow and dispersed. The Chadron is the oldest Tertiary unit in this region and represents the oldest deposition following the retreat of the Western Interior Seaway (Condon, 2005). The upper part of the Chadron serves as a confining unit to the basal, [redacted] ft-thick water-bearing sandstone, which has poor water quality (Brendecke and Hinckley, 2014).

The Brule Formation is a brown to pink-colored sandy siltstone that contains vertical fractures ranging in thickness from inches to several feet that formed as a result of the weight of overlying sediments. Small sand lenses with freshwater presence can be found within the Brule from paleo-channel incisions and infill, but the majority of the Brule's lithology is silt and siltstone. The silt grains are composed primarily of volcanic glass and crystals from active volcanoes during Brule deposition (Diffendal, 2005). The Brule Formation provides water for domestic and stock use in locations where channel sandstone incisions are found or where the formation is highly fractured (Babcock et al., 1952).

Miocene Arikaree and Ogallala Formations (USDW)

The Arikaree Formation includes volcaniclastic sandstones, conglomerates, and siltstone that are up to 400 ft thick in outcrop and pinch out to the southeast. It was deposited in a fluvial and eolian environment. It is topographically high, with only the lower part becoming saturated with water. It can generally yield only moderate amounts of water (Brendecke and Hinckley, 2014).

The Ogallala Formation, with a regional thickness of up to 600 ft, consists of sand, gravel, and poorly to moderately calcium-carbonate cemented sandstone and unconformably overlies the Arikaree Formation or Brule formations. The Ogallala Formation was deposited in a fluvial environment that included eolian and lacustrine settings. The Ogallala Formation is the principal geologic unit in the High Plains aquifer that provides water to domestic and stock wells, with yields to wells dependent on local geology (Babcock et al., 1952). Water levels vary from land surface to greater than 250 ft (Brendecke and Hinckley, 2014).

Lodgepole Creek Quaternary Alluvium (USDW)

The Lodgepole Creek alluvium in this region consists of highly permeable, uncemented, well-sorted sand, silt, and gravel stream deposits, primarily from the Ogallala Formation. The alluvium varies in thickness from 60 to 200 ft (Babcock et al., 1952). This unit is not considered a major water source for high-capacity wells as it is generally thin throughout this region. The alluvium provides the important function of capturing water to recharge the underlying Brule Formation (Brendecke and Hinckley, 2014).

### *2.1.3 General Hydrogeology*

#### *2.1.3.1 Precipitation*

The climate of the Nebraska panhandle is classified as semi-arid. Temperatures vary from an average of 25.1°F in January to 74.4°F in July. The annual average precipitation (data from 1991 to 2020) for Kimball County, Nebraska, is 15.83 in. per year, with a high of 2.82 in. per month (May) and a low of 0.28 in. per month (January).[4] Nebraska has experienced several extreme precipitation events since 2005 with over two inches of rainfall occurring in singular events. Nebraska also experiences periodic intense droughts that can last for several years. Extreme precipitation and periods of droughts are expected to increase in the future (NOAA, 2022).

#### *2.1.3.2 Surface Water Resources*

The significant surface water resources within the AoR are Lodgepole Creek and its tributaries, which include the [redacted] (**Figure 2.18**). Irrigation in this region utilizes groundwater primarily with some surface water usage in Deuel County (two counties east of Kimball County). The AoR is located within the Upper Platte River Basin (**Figure 2.19**), which includes the Twin Platte, North Platte, and South Platte rivers.[5]

[4] www.weather.gov
[5] www.dnr.nebraska.gov/water-planning

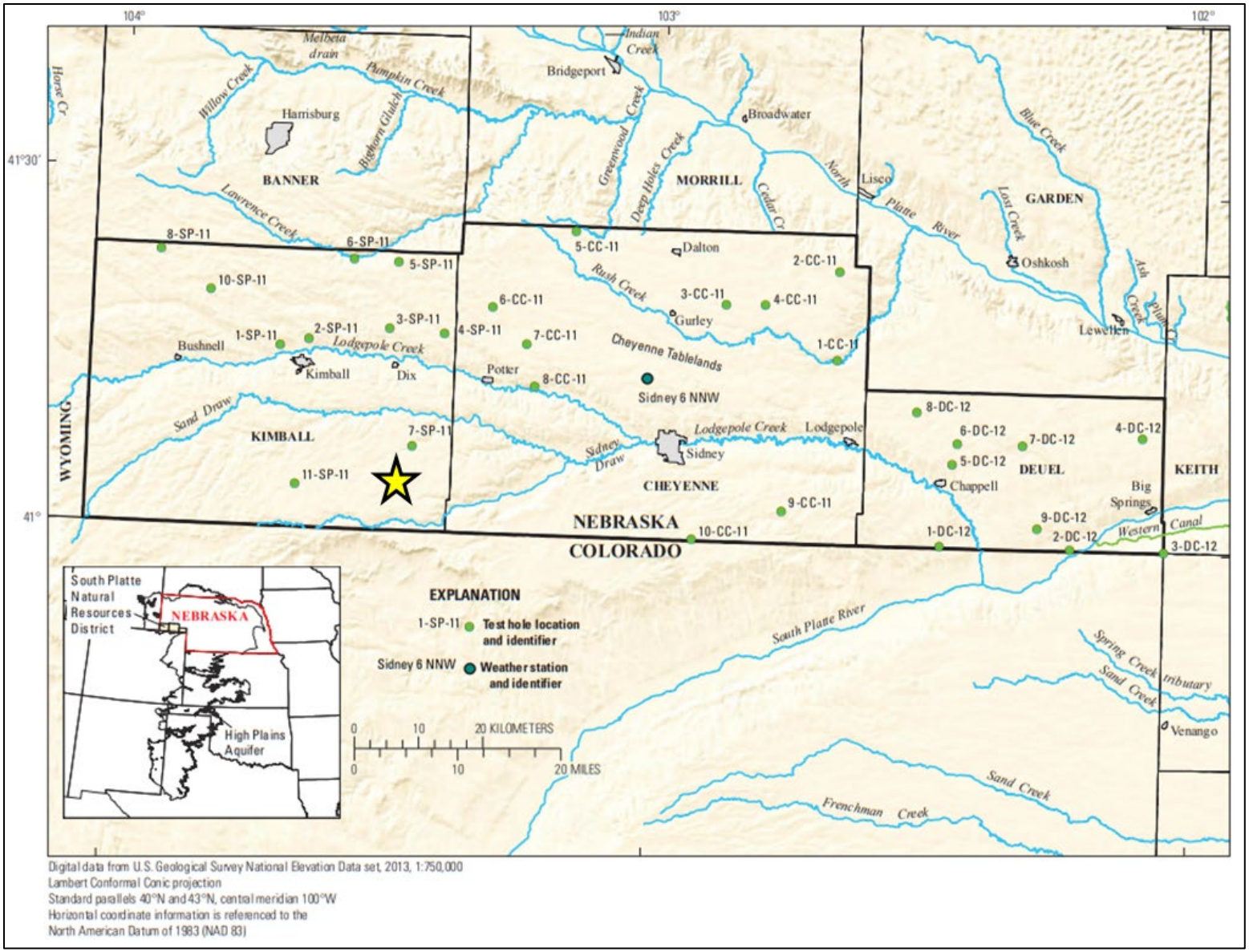


Figure 2.18—Surface water resources in western Nebraska (after Hobza and Sibray, 2014). The general location of the AoR is highlighted with a yellow star.

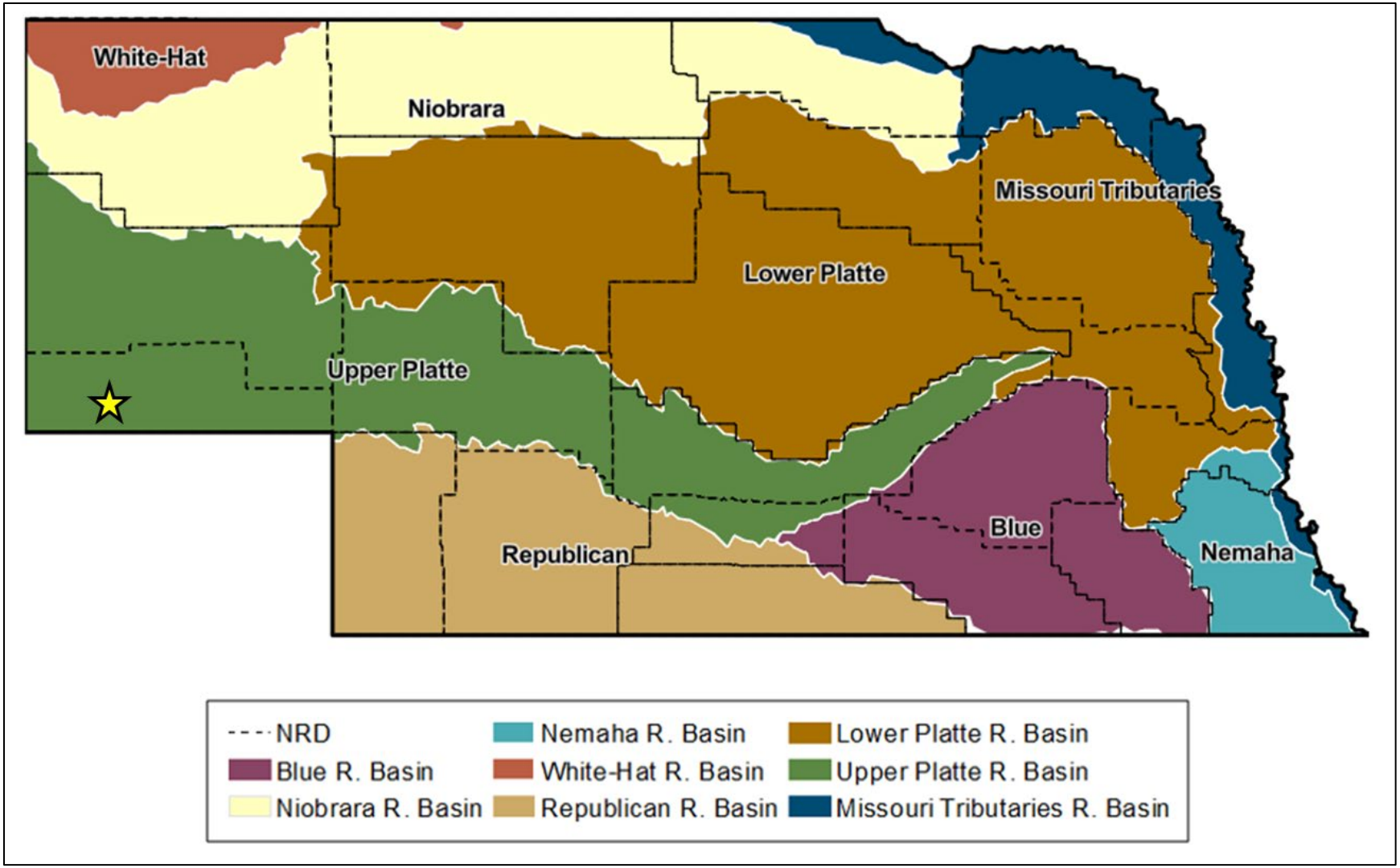


Figure 2.19—River basins of Nebraska. The general location of the AoR is highlighted with a yellow star (www.dnr.nebraska.gov/water-planning).

### *2.1.3.3 Regional Hydrogeology*

The High Plains Aquifer (HPA) is present within the AoR, which is the primary groundwater resource for agriculture, drinking water, industries, and ecosystems throughout the interior United States (**Figure 2.20**) and is the expected lowermost USDW. The HPA is considered one of the world's 37 mega-aquifer systems, covering an area of over 174,000 sq miles over eight states and hosts 129,000,000 $ft^3$ of groundwater (Korus and Joeckel, 2022). The HPA includes all Tertiary and Quaternary-age units that are hydrologically connected. The primary sandstone stratigraphic units that make up the HPA are the White River Formation, the Arikaree Formation, and the Ogallala Formation (**Figure 2.12**). The Brule Formation (of the White River Formation) is only considered part of the HPA when it contains saturated sandstones or interconnected fractures in massive siltstones. In western and central Nebraska, the HPA is about 1,000 ft thick and is predominantly the Ogallala and Arikaree formations. The Cenozoic units comprising the HPA were deposited as fluvial, eolian, and lacustrine sediments during the late Eocene to Pliocene. The Laramide Orogeny ended in the middle Eocene, coinciding with a period of volcanism throughout the southwestern USA that lasted through the early Miocene. The volcanic siltstone and tuffaceous sediments in the White River and Arikaree formations resulted from this. Following volcanism, the Rocky Mountains underwent a series of uplifts that increased the deposition of coarse-grained sediments, forming the Ogallala Formation.

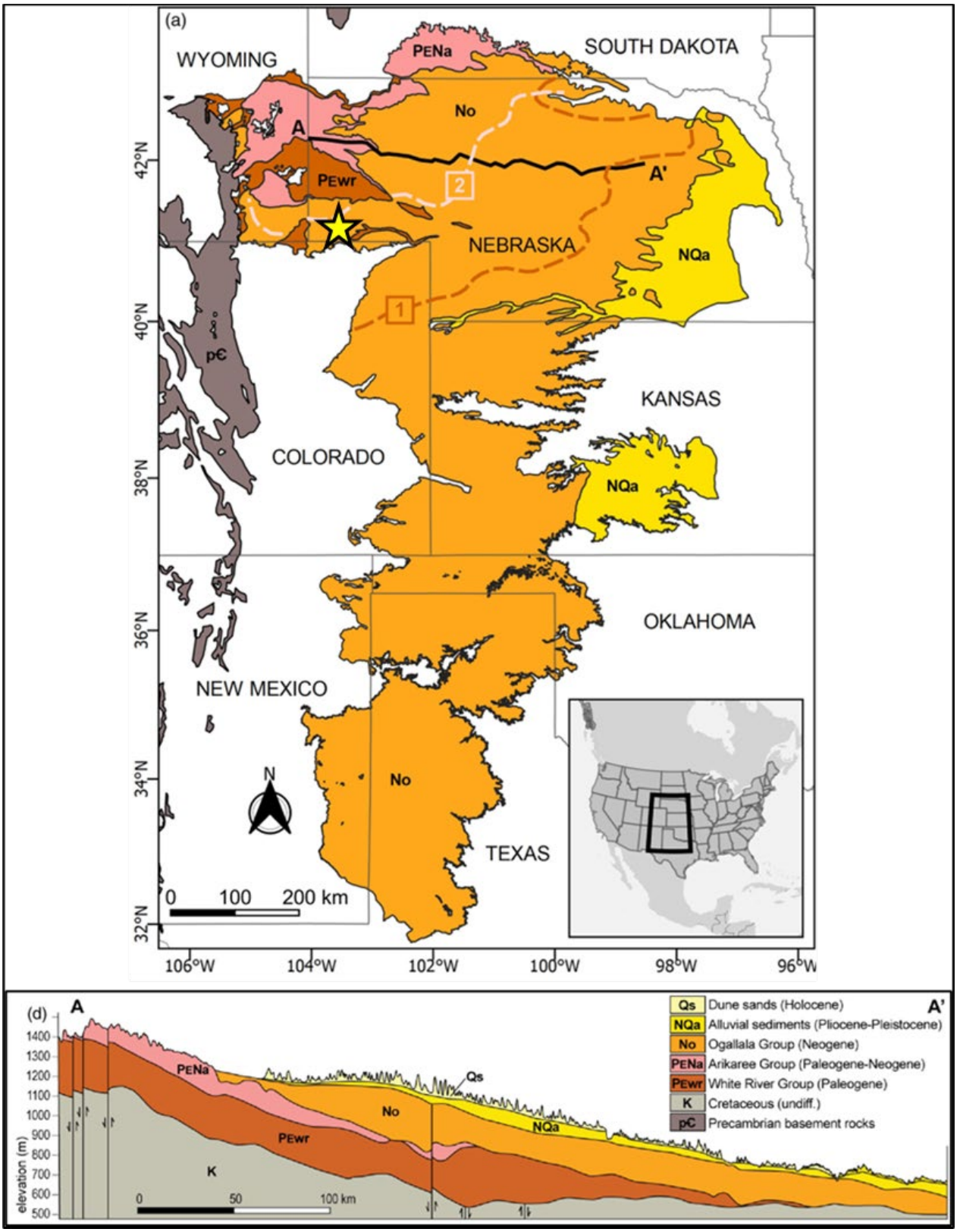


Figure 2.20—Surface geology and cross-section of the High Plains Aquifer system (after Korus and Joeckel, 2022).

### *2.1.3.4 Regional Aquifers and Confining Units/Aquitards*

The regional aquifers and confining units/aquitards are compiled and described in **Table 2.2** in descending age and are identified as major or minor aquifers or confining units (aquitards) within the basin. General lithologic descriptions of potential hydrogeologic units are provided in *Section 2.7.1*.

Table 2.2—Regional aquifers and aquitards (Korus and Joeckel, 2011; Taucher et al., 2013)

| **Major Aquifers** | | **Minor Aquifers** | | **Confining Units/Aquitards** | |
|---|---|---|---|---|---|
| **Hydrogeologic Unit** | **Age** | **Hydrogeologic Unit** | **Age** | **Hydrogeologic Unit** | **Age** |
| Alluvium and terrace deposits | Quaternary | *Inyan Kara Gp*: J-Sandstone | Lower Cretaceous | Pierre Shale | Upper Cretaceous |
| Ogallala Fm. | Miocene | *Inyan Kara Gp*: Dakota Fm. | Lower Cretaceous | Niobrara Fm. | Upper Cretaceous |
| Arikaree Fm. | Miocene | Sundance Fm. | Upper Jurassic | Carlile Shale | Upper Cretaceous |
| *White River Gp:* Brule Fm. | Oligocene | *Chase Grp:* Amazon Fm. | Lower Permian/Pennsylvanian | Greenhorn Fm. | Upper Cretaceous |
| *White River Gp:* Chadron Fm. | Oligocene | Fountain Fm. | Pennsylvanian | Huntsman Shale | Upper Cretaceous |
| Lyons Fm. | Permian | | | Mowry Shale | Upper Cretaceous |
| | | | | Skull Creek Shale | Lower Cretaceous |
| | | | | Morrison Fm. | Upper/Middle Jurassic |
| | | | | Chugwater Fm. | Upper Triassic |
| | | | | Goose Egg Fm. | Lower Triassic/Upper Permian |
| | | | | Satanka Fm. | Permian |
| | | | | Wolfcamp Fm. | Permian |

### *2.1.3.5 Regional Flow*

Groundwater in the lowermost USDW (HPA) generally moves from west to east in response to the slope of the water table (**Figure 2.21**). The velocity of water movement in this aquifer system is estimated to average about 1 ft/day (Miller and Appel, 1997). Recharge primarily occurs in uplifted and highland areas of southeastern Wyoming for two reasons. The climate transitions from semi-arid in the basin to humid-alpine in the mountains, where most atmospheric moisture is captured. Aquifers tend to exhibit increased faulting and fracturing associated with the structural uplift, and formations have the potential to be exposed at the surface. The combination of these factors allows precipitation and surface water to enter the system, the primary source of groundwater recharge to the HPA (Lee and Bethke 1994; Taucher et al. 2013).

In the Lyons Formation, basin fluids also migrated eastward from the Front Range due to the hydraulic gradient driven by Laramide orogeny uplift during the Eocene. Estimated flow velocities through the Lyons Sandstone in the Eocene are predicted at less than 20 m/year because of their

deep burial depth. This general flow direction of west to east, toward structural basin lows, continues today, but modern flow rates are presumably smaller due to erosion of the Front Range (Lee and Bethke 1994). **Figure 2.22** illustrates the potential groundwater recharge and flow within the Lyons Sandstone in the DJ Basin during the Eocene.

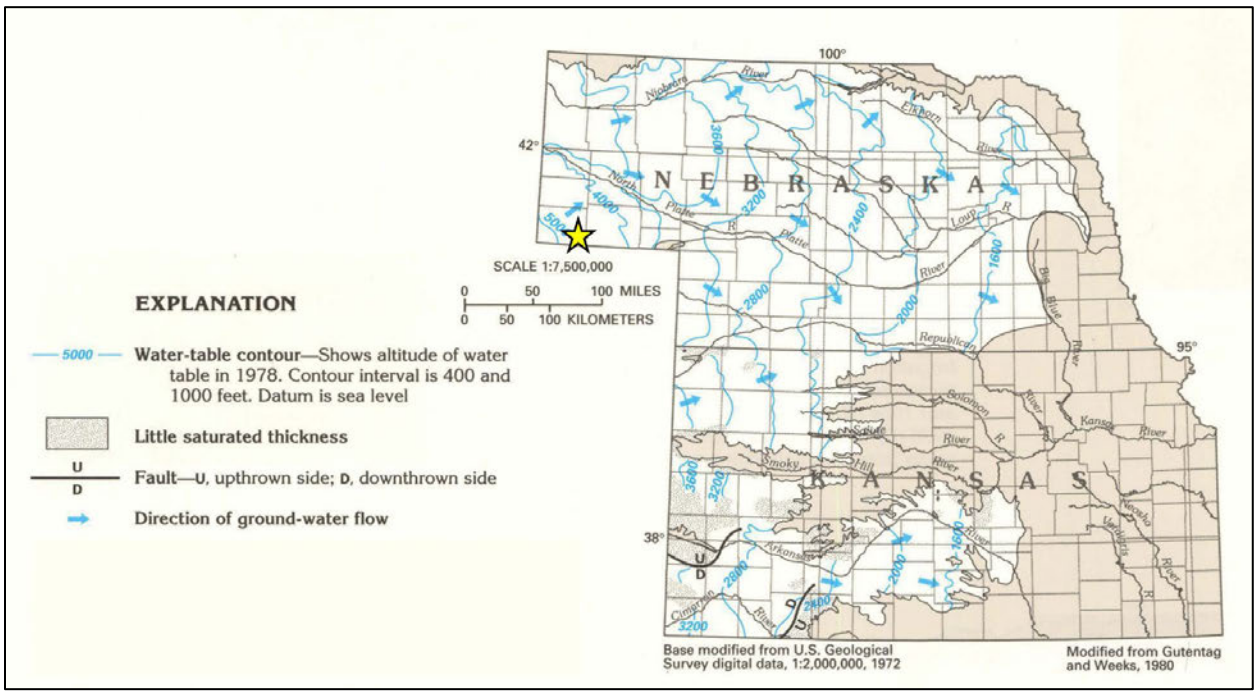


Figure 2.21—The water table of the lowermost USDW (High Plains Aquifer) generally slopes from west to east. The arrows show the general eastward direction of water movement, which is locally diverted by major streams (after USGS, 1997).

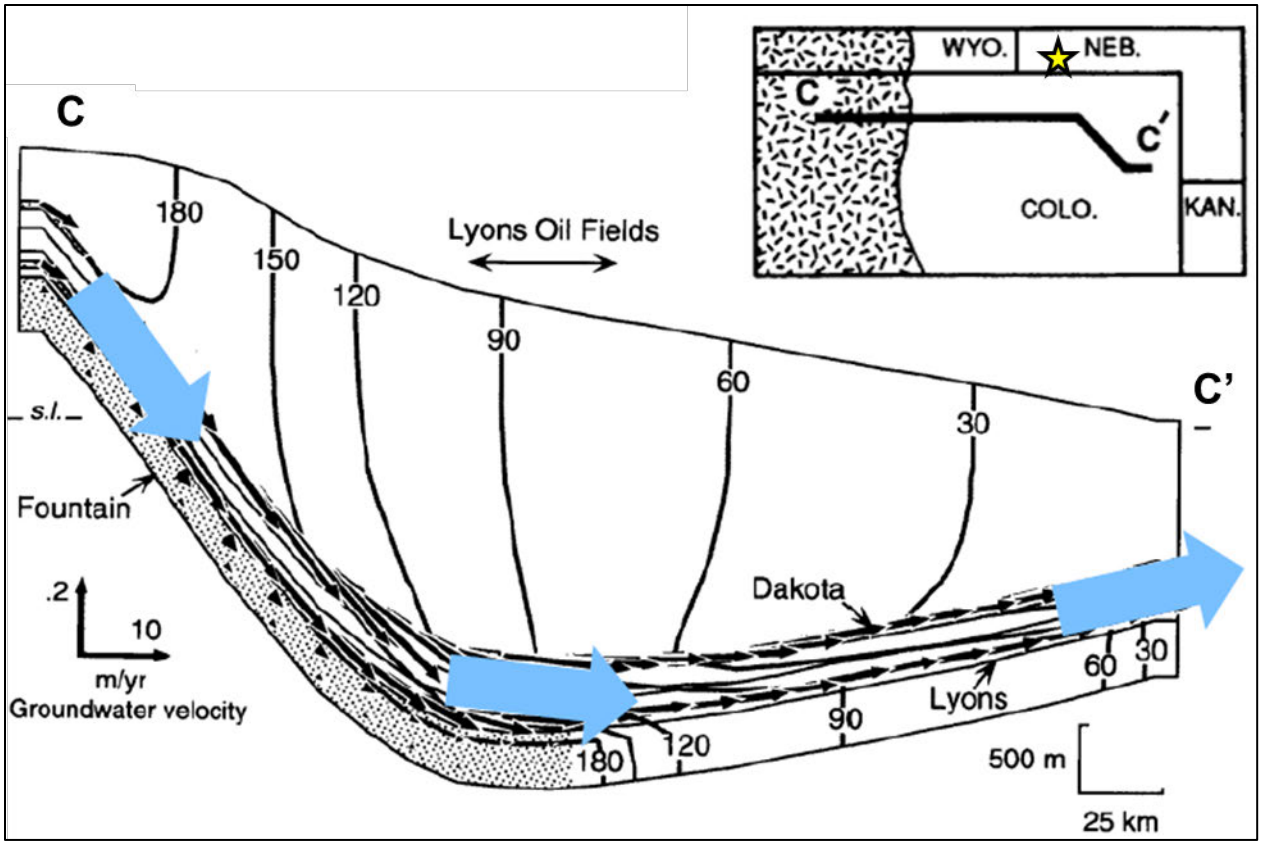


Figure 2.22—Schematic cross-section depicting calculated Eocene groundwater flow and hydraulic potential distribution of the DJ Basin (s.l. denotes sea level; gray contours in atmospheres). After Lee and Bethke (1994).

#### *2.1.3.6 Non-USDW Aquifers*

*Section 2.7—Hydrologic and Hydrogeologic Information [40 CFR 146.82(a)(3)(vi), 146.82(a)(5)]* provides a detailed discussion of the hydrologic properties of each USDW and non-USDW within the AoR. **Figure 2.9** provides a depiction of aquifers above the Lyons that are not USDWs within the AoR.

## 2.2 Maps and Cross Sections of the Area of Review [40 CFR 146.82(a)(2), 146.82(a)(3)(i)]

The Area of Review (AoR) is located in the northern Denver-Julesburg (DJ) Basin, which has a regional shallow dip to the east and exhibits no significant folding or faulting. Faulting in the DJ Basin occurs along the western margin of the basin against the Front Range uplift (see **Figure 2.2** and **Figure 2.3**).

A locator map (**Figure 2.5**) and regional cross-sections (**Figure 2.6 through Figure 2.9**) were constructed by High Plains with well logs to help convey the regional geologic interpretation of the WNS Hub. The regional cross-sections through the injection and confining zones demonstrate the consistent thickness of the confining and injection intervals. Locally observable changes in thickness in the Lyons Formation are attributed to the preservation of dune geometries.

### *2.2.1 Map of the Area of Review*

**2.2.1a_HighPlains_Conestoga_1_AoR_Map_Arch_D_1-20k _land-topo.pdf** is a map of the AoR with all required information per 14 CFR §146.82 at a scale of 1 in. to 1,667 ft (1:20,000). A smaller scale (1:75,000) version is also included in **Figure 2.23** below. A version at 1:16,000 scale with a recent satellite imagery basemap is provided in **2.2.1b_HighPlains_Conestoga_1_AoR_Map_ArchE_1-16k _SatImage.pdf**.

All data that informs the map is provided in an ESRI file geodatabase (**NE_Final_GDB.gdb**). Data sources of artificial penetrations, clean-up sites, hydrologic data, mines and quarries, faults, and structures are summarized as follows:

Artificial Penetrations

*Oil and Gas Wells*

Well locations, including production wells, abandoned wells, plugged wells, dry holes, stratigraphic boreholes, and injection wells, are sourced from the S&P Global Enerdeq well database[6] which was cross-checked for completeness and accuracy against the Nebraska Oil and Gas Conservation Commission (NOGCC) Nebraska Well Database.[7] For all wells identified, available files from the NOGCC were downloaded and reviewed to confirm total depths and zones penetrated. One well within the AoR penetrates the Goose Egg upper confining zone. A list of all [redacted] oil and gas wells within the AoR is provided in **3.4.1a_AoR Oil and Gas Well List_ (S&P Enerdeq)-dist.xlsx**. Historical well files for all wells within the AoR are provided in **3.4.1c_Oil and Gas Well Files_AoR_NOGCC_.zip**.

*Water Wells*

Water well locations were obtained from the Nebraska Registered Wells Inventory.[8] The records in this database are sourced and maintained by the Nebraska Department of Natural Resources.

Eight water wells located within the AoR were identified. Seven wells are active, and one is decommissioned; four are for livestock watering, three are for irrigation use, and one is for groundwater quality monitoring. The deepest well within the AoR is drilled to 400 ft below ground surface. A list of water wells within the AoR is provided in **3.4.1b_AoR Water Well List_NE_DNR-dist.xlsx**. Well files for all water wells within the AoR are provided in **3.4.1d_Water Well Files_NE_DNR.zip**.

Clean-Up Sites

EPA clean-up site data is from the United States Environmental Protection Agency (EPA) Geospatial Data of Regulated Facilities or Cleanup Locations database.[9] No EPA cleanup sites are identified within the mapped area.

[6] https://www.spglobal.com/commodityinsights/en/ci/products/oil-gas-tools-enerdeq-browser.html - Accessed 7/29/2024
[7] http://nogcc.ne.gov/data-publications/ - Accessed 7/29/2024
[8] https://www.nebraskamap.gov/datasets/groundwater-wells-dnr/explore - Accessed 7/26/2024
[9] https://www.epa.gov/frs/epa-frs-facilities-state-single-file-csv-download - Accessed 7/29/2024

State clean-up sites are sourced from the Nebraska Department of Environment and Energy Map Portal.[10] No active cleanup sites are present within the AoR or mapped area.

Hydrologic Data (Surface Waters and Springs)

Hydrologic data was sourced from the USGS 3D Hydrography Program (3DHP)[11] and the USGS National Hydrography Dataset (NHD).[12] Aside from seasonal/intermittent streams and ponds, no significant surface waters or springs are present within the AoR.

Mines and Quarries

The locations of mines and quarries were sourced from the USGS Mineral Resources Program (MRP).[13] There are no mines or quarries within the AoR. The nearest is an inactive gravel pit located approximately [redacted] miles from the proposed injection location.

Faults

Surface fault locations were sourced from the USGS Quaternary Fault Database[14] as well as regional geologic mapping by Scholle (2003). Neither source identifies surface faults within the AoR.

Structures Intended for Human Occupancy

There are [redacted] residential structures intended for human occupancy identified within the AoR. Potential structures were sourced from the FEMA Geospatial Resource Center's USA Structures database.[15] Points within the AoR were reviewed in conjunction with satellite imagery to confirm if a structure is present. The nearest potential structure for human occupancy is approximately [redacted] miles from the proposed injection site.

[10] https://deqmaps.nebraska.gov/deqmapportal/nebraskaMapPortal.html - Accessed 7/29/2024
[11] https://hydro.nationalmap.gov/arcgis/rest/services/3DHP_all/MapServer - Accessed 7/29/2024

[12] https://www.usgs.gov/national-hydrography/national-hydrography-dataset - Accessed 7/29/2024

[13] https://mrdata.usgs.gov/usmin/ - *Accessed 7/29/2024*

[14] U.S. Geological Survey, Quaternary fault and fold database for the United States, accessed August 1, 2024, at: https://www.usgs.gov/natural-hazards/earthquake-hazards/faults.
[15] https://gis-fema.hub.arcgis.com/pages/usa-structures - Accessed 7/29/2024

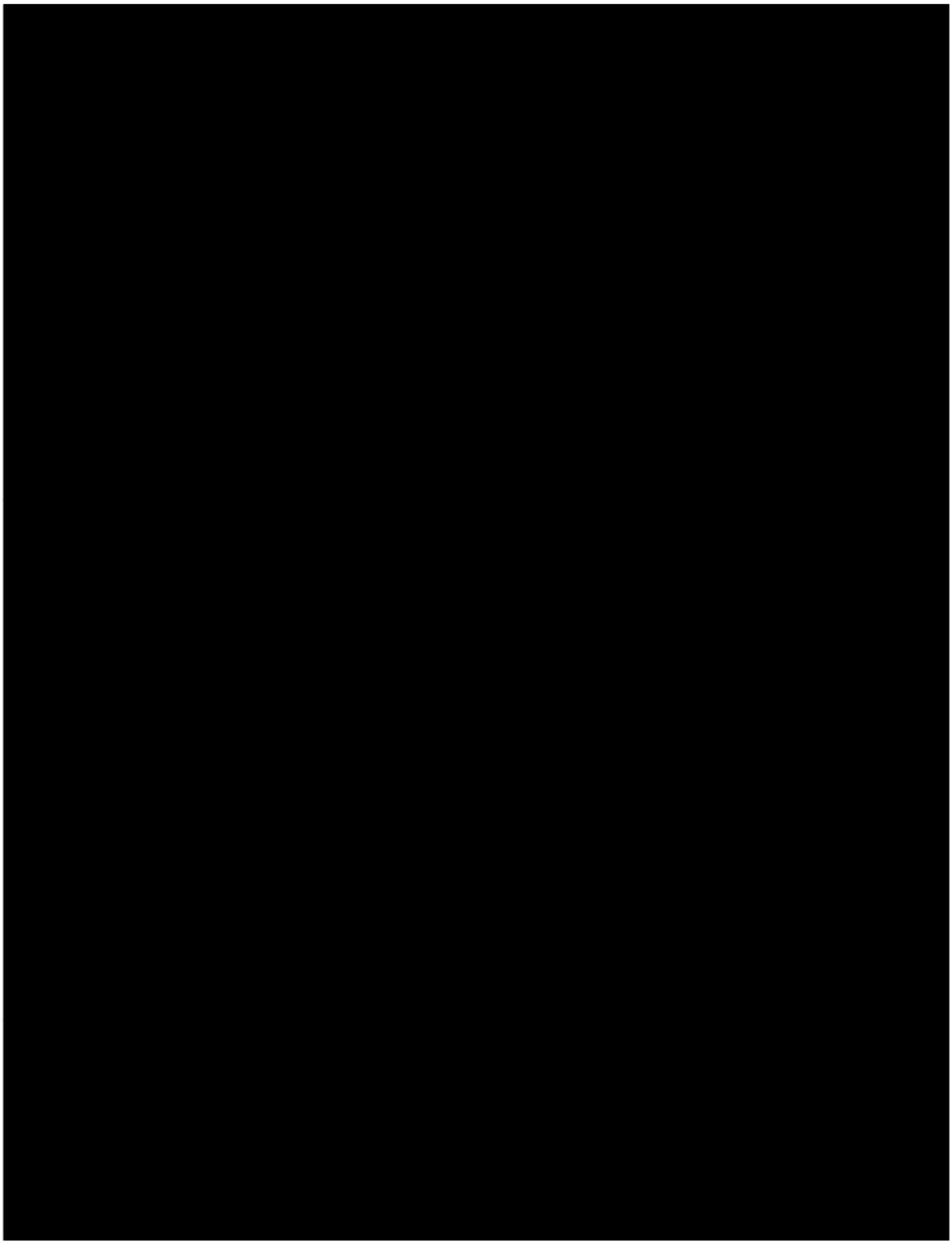

Figure 2.23—Area of Review basemap showing the location of the project wells: Conestoga I-1, Conestoga M-1, residential structures, and existing artificial penetrations in the mapped area, including oil and gas wells, water wells, and mines.

### *2.2.2 Maps of the Injection and Confining Zones*

#### *2.2.2.1 Lyons Formation (Injection Zone)*

Structure and isochore thickness maps in the vicinity of the AoR for the Lyons Formation (the injection zone) are shown in **Figure 2.24** and **Figure 2.25**. The Lyons has been mapped extensively across the entirety of the DJ Basin (**Figure 2.13**), as well as locally by High Plains, across a mapping domain of 12,300 sq miles to ensure reservoir quality and continuity. Electrical logs from [redacted] wells across the DJ Basin were used to pick formation tops and generate structure and isochore thickness maps of the Lyons Formation; [redacted] wells are within the WNS Hub static model domain (**Figure 2.10**). From this inventory, petrophysical analysis was conducted on [redacted] wells within the static model domain and used to generate porosity-height (PHI×H) maps across the northern-central DJ Basin (**Figure 2.26**). These maps demonstrate the relative pore volume across the mapping area.

The Lyons structure does not contain any significant structural traps within the AoR. It gently dips to the west at less than two degrees. Locally observable changes in thickness in the Lyons Formation are attributed to the preservation of Lyons dune geometries. Trapping within the AoR is driven by hydrodynamic and residual $CO_2$ trapping, further discussed in *Section 3.2.1.2*.

Figure 2.24—Structure contour map on the top of the proposed injection zone, the Lyons Formation. The yellow star denotes the proposed injector location. Each well location contains displayed data for the Lyons depth and respective well name.

Figure 2.25—Gross isochore map of the Lyons Formation. A yellow star denotes the proposed injection location. Squares represent true vertical thickness (gross) at each well penetration.

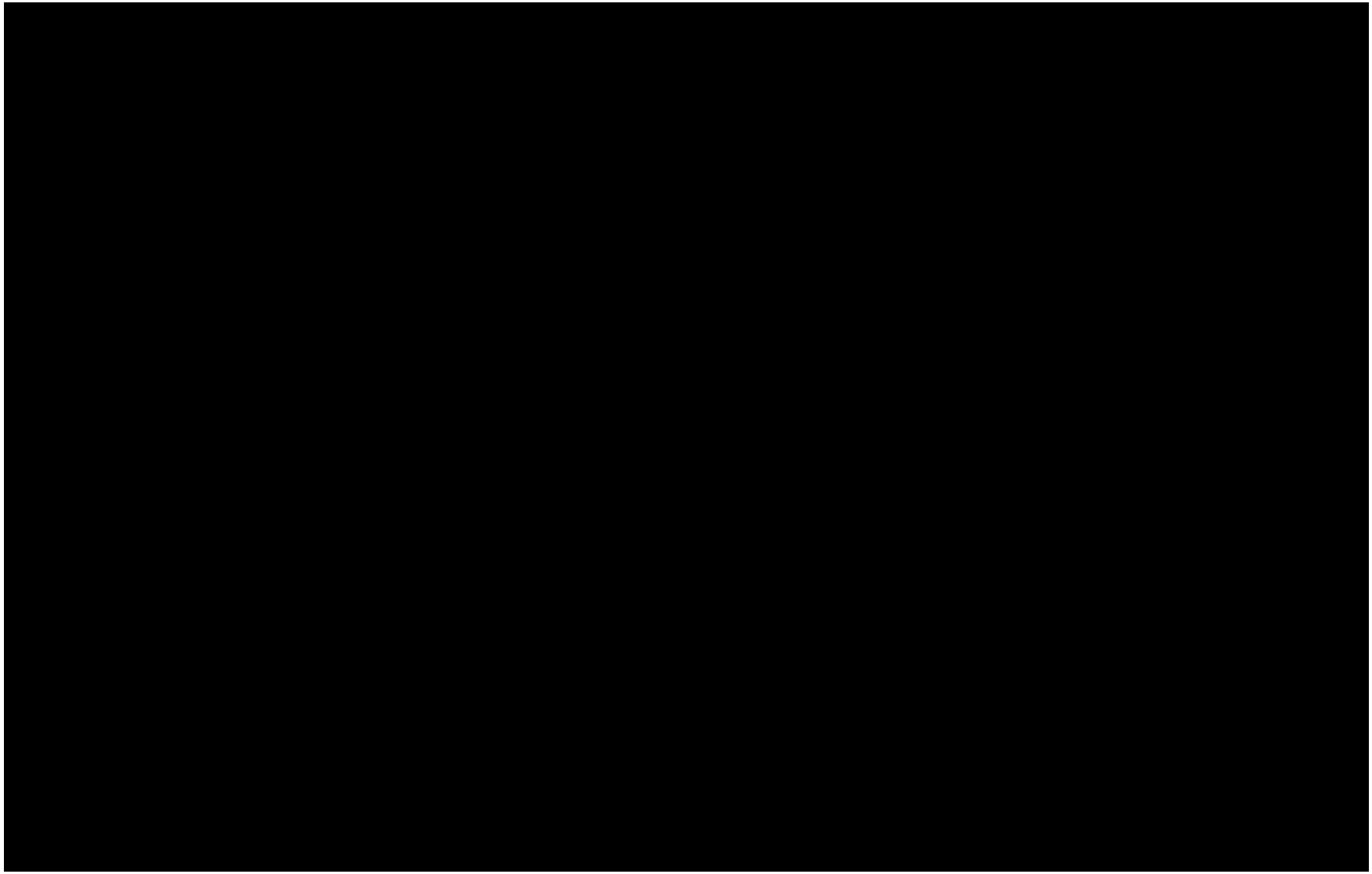

Figure 2.26—Porosity-height (PHI×H) map for the Lyons Formation within the AoR and surrounding locality.

#### *2.2.2.2 Goose Egg and Satanka Formations (Confining Zones)*

Structure maps on the top of the confining zones—the Goose Egg Formation (upper confining zone) in **Figure 2.27** and the Satanka Formation (lower confining zone) in **Figure 2.28**—are provided. Isochore thickness maps for the confining zones are shown in **Figure 2.29** for Goose Egg Formation and **Figure 2.30** for the Satanka Formation.

Both the Goose Egg and Satanka formations were deposited across the entirety of the DJ Basin and exhibit no major pinchouts, facies changes, or faulting within or adjacent to the AoR. **Figure 2.17** depicts the deposition of the Goose Egg Formation over the Lyons and the aerial extent of interbedded sabkha salt-flat facies. Both confining zones have consistently low porosity values across the basin and exhibit log characteristics indicating no significant lithologic changes that would modify the sealing ability within or outside the AoR.

Figure 2.27—Structure contour map on the top of the proposed upper confining zone, the Goose Egg Formation.

Figure 2.28—Structure contour map on the top of the lower confining zone, the Satanka Formation.

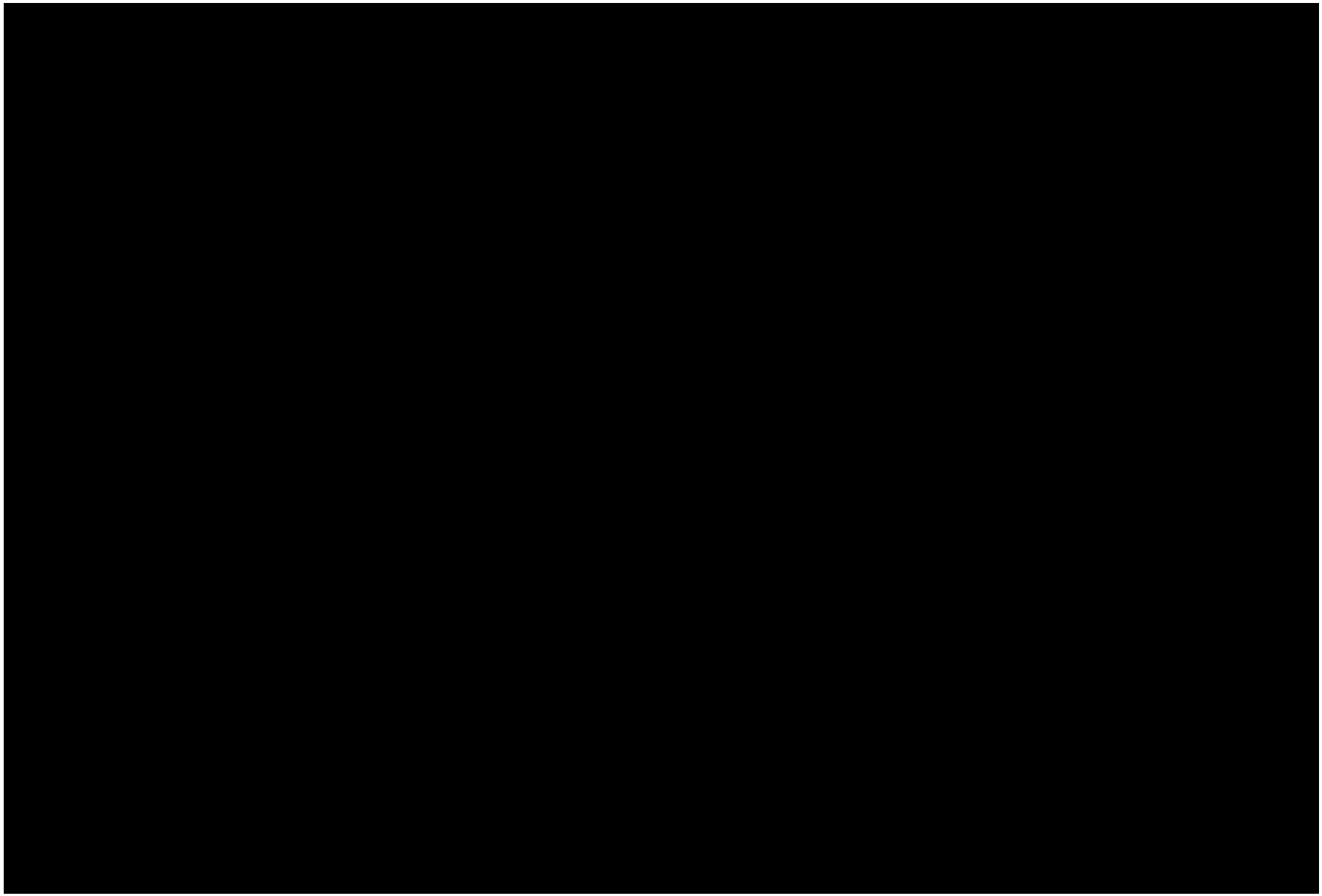

Figure 2.29—Gross Isochore map of the Goose Egg Formation, the upper confining zone.

Figure 2.30—Gross Isochore map of the Satanka Formation, the lower confining zone.

### *2.2.3 Cross Sections Through the AoR*

Cross-sections (and index map—**Figure 2.31**) comprising wells with penetrations into the injection interval that are adjacent to the proposed injection site are provided in **Figure 2.32** and **Figure 2.33**. **Figure 2.32** shows all intervals, including USDWs, from the ground surface to below the base of the storage complex. **Figure 2.33** is focused on the storage complex, extending from just above the confining zone (Goose Egg) to below the lower confining zone (Satanka). This section includes the proposed injection well location (Conestoga I-1) with interpolated tops. The cross-section includes petrophysically derived effective porosity logs and gamma ray logs to display the continuous tight characteristics of the confining zone rocks (Goose Egg and Satanka) and the porous nature of the Lyons Formation.

Figure 2.31—Location map for cross-section A-A′ through the Conestoga I-1 proposed location. The background colors are modeled porosity-height (PHI×H) as seen in **Figure 2.26**.

Figure 2.32—Local structural cross-section A-A′ through the Area of Review extending from the ground surface through the base of the lower confining zone.. The vertical distance between the lowermost USDW (the High Plains Aquifer) and the storage complex is displayed.

Figure 2.33—Local stratigraphic cross-section through Conestoga I-1 highlighting the storage complex, displaying the gamma ray log curve in the left column and the effective porosity petrophysical interpreted curve in the column on the right. The section is flattened on the Satanka Formation for viewing purposes and to emphasize variations in Lyons thickness. Surfaces have been interpolated through the Conestoga I-1 proposed location.

## 2.3 Faults and Fractures [40 CFR 146.82(a)(3)(ii)]

This section summarizes High Plains' current understanding of the distribution and characteristics of potential faults and fractures, including their density, spacing, orientation, transmissivity, and mode, along with any associated hazards related to $CO_2$ containment. It examines the influence of regional and local stresses and the tectonic history of the DJ Basin, supported by a review of relevant literature, seismic data, and well data from the Juniper M-1. The assessment of seismic-scale features within the AoR is based on available 2D seismic data.

This section also outlines how future data acquisition, including collecting whole cores, rotary sidewall cores, and image logs from Conestoga I-1, will enhance the characterization of subseismic natural faults and fracture density within the AoR. High Plains' current understanding of subseismic fault and fracture characterization near the Conestoga I-1 well is primarily derived from core samples and openhole wireline log data (e.g., sonic and resistivity images) collected from the Juniper M-1 well, located approximately 41 miles west of the Conestoga I-1. Current 2D seismic shows no evidence of seismic-scale faults or fractures within or through the proposed injection or confining units in the AoR.

### *2.3.1 Literature Review*

The AoR is located within the DJ Basin, just east of the basin axis, in an area without significant documented faulting and gentle westerly dips. The DJ Basin has a structurally and tectonically complex history (refer to *Section 2.1.1—Tectonic and Structural History*). It is bound on the west by the Rocky Mountain Front Range, on the northwest by the Hartville Uplift, on the northeast by the Chadron Arch, on the southeast by the Las Animas Arch, and on the southwest by the Apishapa Uplift.

In 2020, Lundstern and Zoback published an article on multiscale variations of the crustal stress field throughout North America. They produced an updated stress map of North America by incorporating more than 300 new, measured stress orientations, relative stress magnitudes from earthquake focal mechanisms, and recent fault-slip measurements from almost 2,000 locations. Then, in 2022, Lundstern and Zoback researched maximum horizontal stress orientations, specifically in unconventional oil and gas reservoirs, including the DJ Basin. Their findings indicate a west-northwest to east-southeast maximum horizontal stress orientation near the AoR, as shown in **Figure 2.34**. Additionally, their research identifies this region as an area of extensional faulting based on focal mechanism analysis. This data may be further refined if wireline data, such as resistivity imaging, reveals wellbore breakouts within the Conestoga I-1 after well construction.

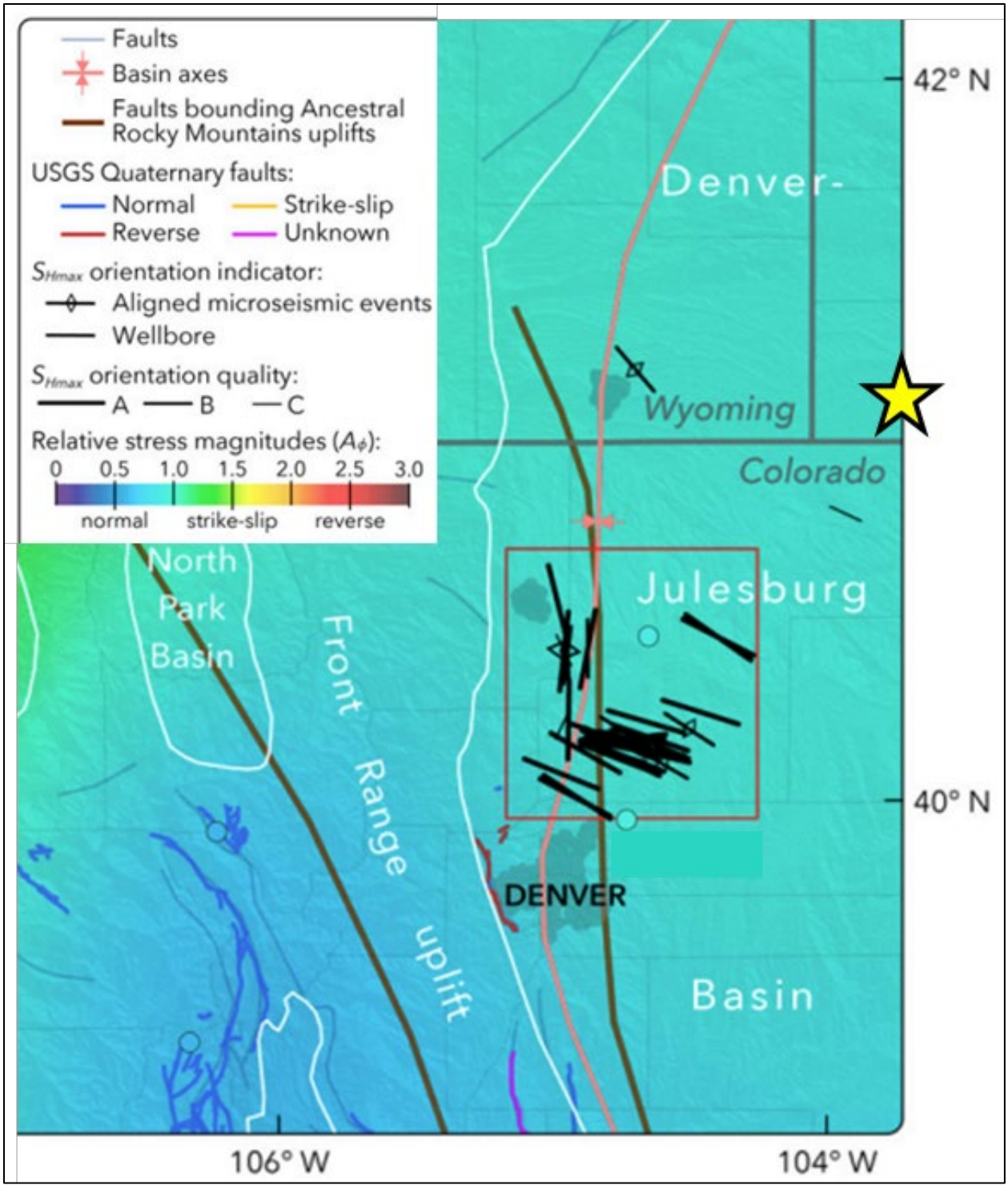


Figure 2.34—Map showing the state of stress across the Denver-Julesburg Basin, with maximum horizontal principal stress (SHmax) shown as black lines (after Lundstern and Zoback, 2022). Most SHmax orientations across this region are from Lundstern and Zoback (2020). Light blue faults are from Marshak et al. (2000), and Garrity and Soller (2009), and bold, brightly colored faults are from the United States Geological Survey (USGS) Quaternary Faults and Folds Database (Crone and Wheeler, 2000). The general location of the AoR is highlighted with a yellow star.

According to the USGS Quaternary Fault Map (Crone and Wheeler, 2000), shown in **Figure 2.35**, there are no active surface faults near the AoR. Furthermore, subsurface faulting is restricted to primarily the Upper Cretaceous rocks, such as the shallower Niobrara and Codell formations (Downard, 2021).

Figure 2.35—Quaternary faults near AoR. Green faults: middle and late Quaternary; purple faults: late Quaternary; teal blue faults: latest Quaternary. The location of the AoR and Conestoga I-1 well are shown.[16]

Faults southwest of the WNS Hub could represent deep shear zones associated with the Colorado mineral belt. Pre-Cambrian shear zones have been noted across the DJ Basin and broader Rocky Mountain region. The regional isostatic gravity anomaly map shown in **Figure 2.36** (after Downard, 2021) depicts the Colorado mineral belt and identifies the locations of nearby oil and gas fields. Boundaries of the Colorado mineral belt run from southwest to northeast, suggesting that shear zones may extend roughly five miles south of Conestoga I-1. Shear zones contain areas of structural basement weakness that have the potential to be reactivated over time (Downard, 2021). Downard identified possible faulting within the Precambrian basement in Hereford field in Colorado, located more than 50 miles southwest of the WNS Hub, with a general east-to-west orientation. These subsurface features do not appear to extend to the Project's AoR.

[16] Fault data is from *https://www.usgs.gov/natural-hazards/earthquake-hazards/faults*

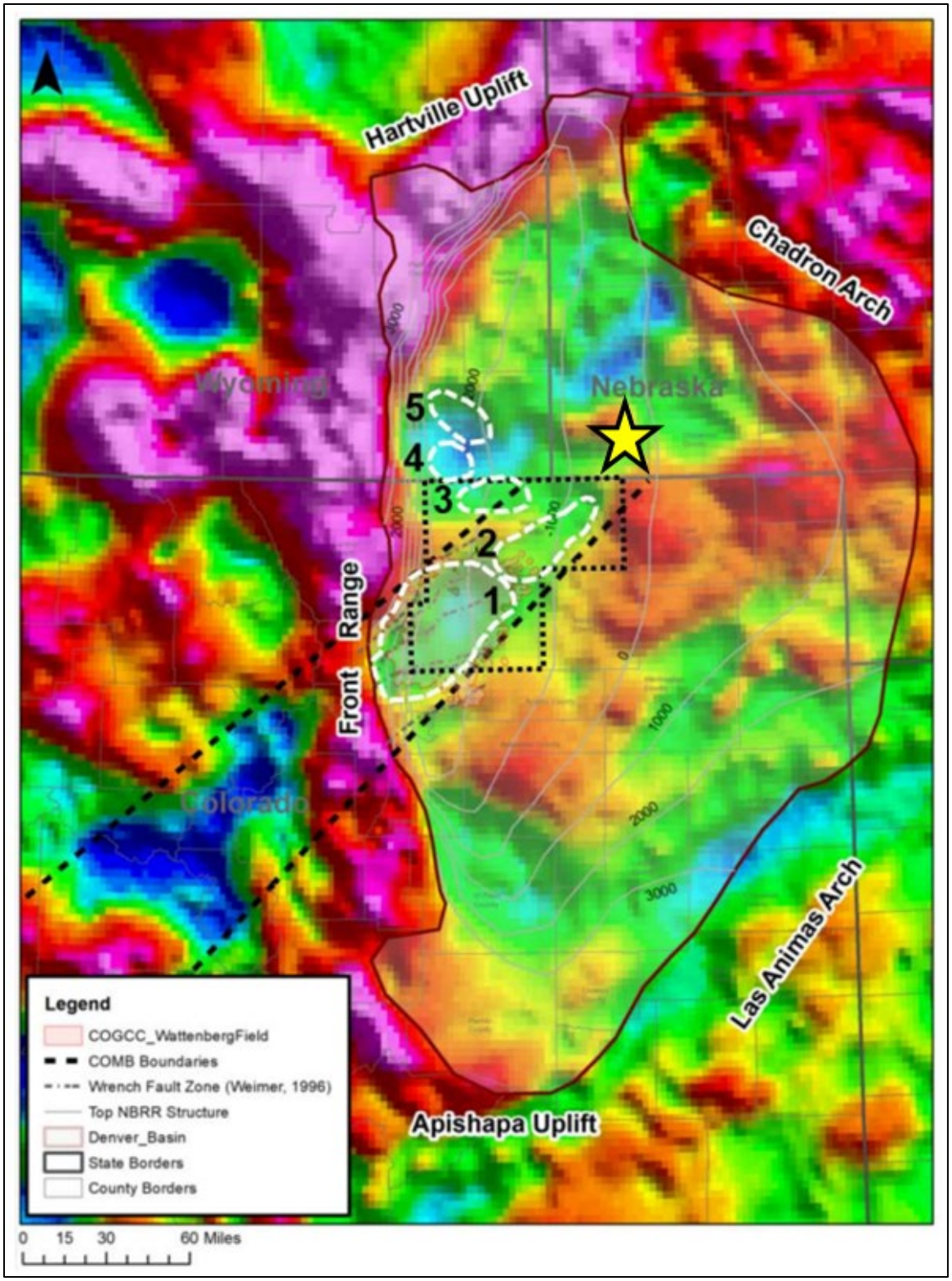


Figure 2.36—Regional isostatic gravity anomaly map showing five of the main producing fields in the DJ Basin, including (1) Wattenberg field, (2) Wattenberg extension, (3) Hereford field, 4) Fairway field, and 5) Silo field. Note the gravity lows that underlie all five fields. The USGS has interpreted these as magma chambers, igneous intrusions, or batholiths. The general location of the AoR is highlighted with a yellow star (after Downard, 2021).

### *2.3.2 Seismic Data*

High Plains evaluated four 2D seismic lines licensed within the region of the WNS Hub to confirm structural mapping and locate any potential faulting or fracturing within the area. A map of reviewed 2D lines relative to the WNS Hub location is displayed in **Figure 2.37**.

Figure 2.37—Map showing the location of the four 2D seismic lines (pink lines) reviewed for the Project.

The quality, resolution, and fold, of the 2D seismic data was sufficient to map key formation tops and faulting that may be present at the depth of the injection complex). Seismic interpretation identified faults in shallower intervals that do not appear to be present in the injection and confining layers (**Figure 2.38**). No faulting of the injection or confining zones was identified by the seismic evaluation within the Conestoga I-1's plume boundary (the AoR).

2D seismic lines from the northern DJ Basin in Sioux County, Nebraska show faulting in the Precambrian basement and Cretaceous rocks and no faulting in the Permian, Triassic, or Jurassic formations (**Figure 2.39**; Burberry et al., 2014).

Figure 2.38—2D seismic line across the AoR demonstrating the absence of interpreted faulting across the injection interval and the upper and lower confining zones.

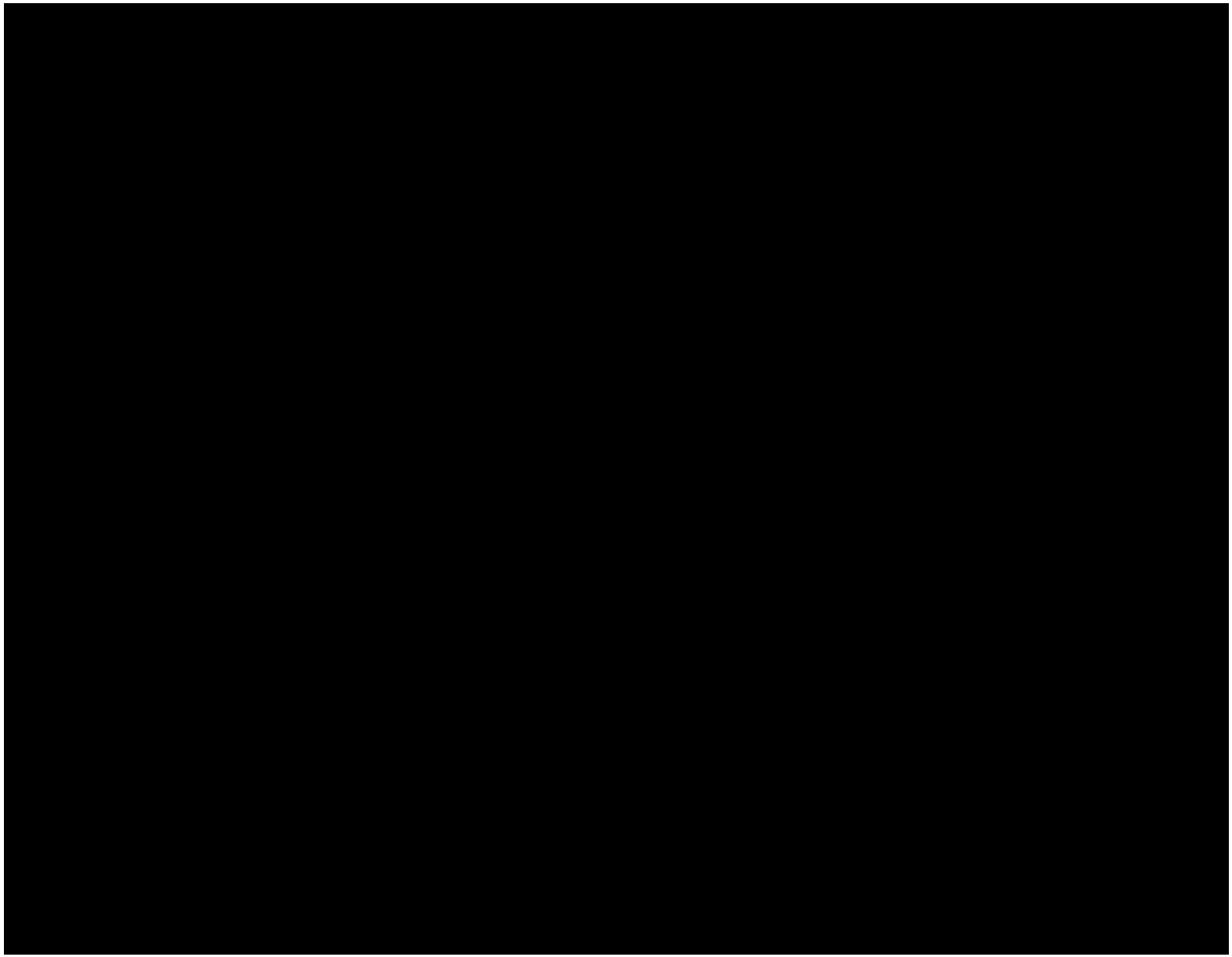

Figure 2.39—2D seismic lines from southern Sioux County, Nebraska with faults and the Lyons Formation highlighted (after Burberry et al., 2014).

### *2.3.3 Well Data*

High Plains utilized SLB's oil-based, openhole resistivity imaging log (QuantaGeo™) and sonic imaging tools in the Juniper M-1 stratigraphic test well to gather site-specific orientations of the WNS Hub. It is assumed that regional stresses are consistent between the Juniper M-1 and the proposed Conestoga I-1 well location (**Figure 2.40**). Consequently, the Juniper M-1 image log data offers insights into the presence and density of faults and fractures within the injection and confining layers at the WNS Hub. Additional image log data will be collected in the Conestoga I-1 to incorporate locally influenced natural stresses. Furthermore, [redacted]—surround the proposed well location, and no transmissive or significant faults have been identified from the correlation of these well logs.

Figure 2.40—Reference Wells ( basemap. The location of the Juniper M-1 characterization well, the proposed Conestoga I-1, and the AoR are also shown.

#### *2.3.3.1 Image Log Analysis and Interpretation*

High Plains ran oil-based resistivity (QuantaGeo™) and Ultrasonic Borehole Imager (UBI) logs and dipole sonic logs across the injection and confining intervals in Juniper M-1 to determine if these intervals contain transmissive faults or fractures.

**Figure 2.41** presents the interpretation from the QuantaGeo™ image. All fracture features observed are at bedding scale and do not cross-cut formational thicknesses. This observation is consistent with the lack of seismic-scale features noted in *Section 2.3.2*. The QuantaGeo™ and UBI image-based fracture interpretation, along with a quick look Stonely Fracture Analysis, supports an interpretation of generally limited natural fracture openness.

Within the Goose Egg upper confining zone, the top [redacted] ft of the section shows healed fractures and healed minor faults. The remainder of the confining zone contains occasional interpreted partly and fully open fractures and minor faults, none of which are interpreted as being transmissive. This lack of transmissivity was based on the anisotropic response from the dipole sonic Stoneley waves (depth of investigation 2 to 3 ft). Stoneley wave response can help verify whether fractures and minor faults identified in the resistivity tool are open past the borehole. Additionally, the dipole sonic tool provides a wider horizontal depth of investigation than the oil-based and ultrasonic image logs, which allows the dipole tool to collect data from deeper in the formation and infer whether open fracturing continues away from the wellbore. In the Juniper M-1, limited attenuation of the Stonely wave was observed across the storage complex, supporting an interpretation of little to no transmissivity.

Figure 2.41—SLB borehole image interpretation from the Juniper M-1 (API No. 49-021-29548).
Track 1: gamma ray; Track 2: zones; Track 3: spectroscopy track (dry weight anhydrite: yellow, dry weight quartz: lime green, dry weight pyrite: orange, dry weight kerogen: medium green; dry weight illite: cyan, dry weight dolomite: medium blue, dry weight calcite: dark blue); Track 4: borehole shape, Track 5: static-scaled image and image orientation; Track 6: high resolution resistivity generated from processed QuantaGeo; Track 7: dynamic-scaled image and image orientations; Track 8: tadpole interpreted classification of fractures; Track 9: Azimuth fan plot of bedding Track 10: Strike fan plot of interpreted fractures Track 11: P32 (i.e. area per unit volume) sum of all fractures; Track 12: P32 (i.e. area per unit volume) sum of open and partially-open fractures; Track 13: acoustic anisotropy (Sloani); Track 14: inversion processes quanta geo standoff image; Track 15: spacer track (no data) Track 16: static amplitude from the Ultrasonic Borehole Imager (UBI); Track 17: UBI static amplitude image, Track 18: UBI dynamic amplitude image; Track 19: UBI radius image of borehole shape; Track 20: SLB sonic processing formation resistivity perpendicular to bedding.

## 2.4 Injection and Confining Zone Details [40 CFR146.82(a)(3)(iii)]

The proposed storage reservoir for the WNS Hub is the Lyons Formation. Sonnenberg and Weimer (1981) reviewed outcrops of the Lyons section (including the original quarry type section) near Lyons, Colorado, and described the formation as a well-sorted, fine-grained, eolian quartzose sandstone. Modeling performed by High Plains demonstrates that the Lyons Formation is well-suited for injection due to the presence of a regional sand body with sufficient porosity and permeability, confined by regionally extensive impermeable intervals. Representative properties of the Lyons Sandstone at the WNS Hub location are listed in **Table 2.3** and **Table 2.6**. **Figure 2.42** depicts openhole logs through the Lyons Formation and its confining layers, along with predicted porosity and mineralogy from the nearest offsetting Lyons penetration, the [redacted]

Figure 2.42—Openhole log from the nearest offsetting Lyons penetration, the [redacted] to the proposed Conestoga I-1 location. The proposed injection zone (Lyons Formation) and its confining layers (Goose Egg and Satanka) and shown. The yellow circle on the locator map indicates the location of the Mathewson 1. The blue teardrop indicates the proposed Conestoga I-1 injector location. Track 1: The Lyons (injection zone) and the Goose Egg and Satanka (confining zones); Track 2: gamma ray (in green) and caliper (half-track in dash) shows the distinctive character of the Lyons blocky sands. Track 3: Deep (RT) and shallow (RXO) resistivity; Track 4: Overlay of neutron porosity (on sandstone matrix) (NPHI_SS) and bulk density (RHOB); Track 5: Total porosity; Track 6: Predicted lithology volumes normalized to 100% of the rock matrix and includes quartz volume (vqtz_norm), clay volume (vclay_norm), K-feldspar volume (vkspar_norm), anhydrite volume (vanhy_norm), and dolomite volume (vdol_norm).

Within six miles of the Conestoga I-1 well location, there are [redacted] wells penetrating the confining and/or injection zones: [redacted] (**Figure 2.40**). These wells, collectively referred to as the "Reference Wells," each have openhole wireline logs (**Figure**

**2.32 and Figure 2.33**) providing crucial insights for the geologic and petrophysical models and understanding the reservoir properties of the injection and confining zones within the AoR.

The injection zone, the Lyons Formation, shown in the cross-section (**Figure 2.32** and **Figure 2.33**), is dominated by quartzose sand of good reservoir quality. The Lyons is bounded by two confining zones: the Goose Egg Formation above (upper confining zone) and the Satanka Formation below (lower confining zone), as illustrated in the cross-section shown in **Figure 2.33**.

The wireline log and core data from the Juniper M-1 were used to calibrate the petrophysical model. The Juniper M-1, whose location is shown in **Figure 2.40,** serves as an appropriate calibration set for the WNS Hub, as the dune facies observed in the M-1 are likely present in the WNS Hub based on log response and correlation to the Reference Wells. Additionally, log responses also suggest that Lyons within the AoR may contain a higher proportion of good-quality facies compared to those in the Juniper M-1 (**Figure 2.8 and Figure 2.9**). **Table 2.3** displays the average property ranges of the Juniper M-1 and the Reference Wells, reflecting the increased porosity and reservoir quality observed in the AoR.

Table 2.3—Average petrophysically-modeled properties within the Reference Wells in AoR and the calibration well (Juniper M-1).

| WELL | FM. | PHIT_RES[1] (v/v) | PERM_RES[2] (mD) | VQTZ[3] (v/v) | VKSPAR[4] (v/v) | VDOL[5] (v/v) | VCLAY[6] (v/v) | VANHY[7] (v/v) |
|---|---|---|---|---|---|---|---|---|
| JUNIPER M-1 | Goose Egg | [redacted] | | | | | | |
| | Lyons | | | | | | | |
| | Satanka | | | | | | | |
| **REFERENCE WELLS:** | | | | | | | | |
| [redacted] | | | | | | | | |

[1] PHIT_RES = total porosity prediction in volume fraction at reservoir conditions;
[2] PERM_RES = permeability prediction at reservoir conditions, Lyons permeability is Klinkenberg-corrected;
[3] VQTZ = predicted volume fraction of quartz,
[4] VKSPAR = predicted volume fraction of potassium feldspar;
[5] VDOL = predicted volume fraction of quartz;
[6] VCLAY = predicted volume fraction of total clay (does not differentiate clay species);
[7] VANHY = predicted volume fraction of anhydrite.
**Weighted average accounts for the distance of the Reference Well from the Conestoga I-1 location. Weighting multipliers [redacted], based on distance from Conestoga I-1 location (e.g. [redacted]; the weighting multipliers above reflect this) were applied during the summation.

### *2.4.1 Data on the Injection Zone (Lyons Formation)*

#### *2.4.1.1 Depth, Areal Extent, and Thickness*

A structure map was generated on the top of the Lyons Formation from offset formation tops where openhole logs were publicly available (**Figure 2.24**). To confirm structural interpretation and improve the detail of the structural understanding, 2D seismic lines were also reviewed (see *Section 2.3.2*). The Lyons structure strikes north-south and has a general dip to the west of approximately 1 to 2 degrees. A list of Lyons Formation tops utilized to generate the top of the Lyons structure map is provided in **Appendix 2.2**.

Offset openhole logs were also utilized to construct a gross isochore of the Lyons Formation (**Figure 2.25**). Conestoga I-1 is anticipated to encounter the Lyons at a depth of [redacted] ft TVD with a gross vertical thickness of approximately [redacted].

The Lyons gross isochore thickness ranges from [redacted] ft across the mapping area, with thicknesses within the AoR ranging from [redacted] ft. Unlike marine deposits, which typically exhibit sheet-like geometry, dune architecture can be highly variable, leading to significant local thickness variations depending on which parts of the dune are preserved (i.e., the crest or the trough). Once the Conestoga I-1 well is constructed and characterized, the Lyons thickness at the well location will be incorporated into the static and dynamic models.

#### *2.4.1.2 Porosity*

The Juniper M-1 well provides the data, including basic and advanced wireline logs and core, to calibrate the log response from standard logs (GR, resistivity, RHOB, NPHI, PEF, and sonic) for use in predictive, quantitative porosity model. This calibration is particularly valuable for legacy wells with only standard log suites.

Routine core measurements of total porosity (PHIT) at reservoir conditions, along with a wireline nuclear magnetic resonance (NMR) log, are used to calibrate the total porosity model of the Lyons Formation injection zone. The Lyons exhibits a narrow range in grain densities [redacted] due to minimal mineralogic variability. However, the petrophysical porosity model accounts for slight variations in mineralogy to optimize the accuracy of PHIT estimations. The Reference Wells, listed in **Table 2.3**, show lower porosity (PHIT = [redacted]%) in the upper [redacted] ft of the Lyons, possibly due to increased clay or dolomitic cementation. The remaining [redacted] ft—comprising the majority of the Lyons Formation—consists of massive sandstone, with all intervals showing a PHIT of around [redacted]

**Figure 2.43** illustrates the calibration of wireline and core measurements with petrophysical modeling from the quad combo. Wireline NMR porosity is measured by binning the time it takes for polar hydrogen molecules to relax; the tool acquisition settings take these wait times into account. NMR wireline porosity is slightly underestimated (i.e., it did not measure an accurate total porosity) in the Lyons and Satanka due to insufficient wait times during log acquisition. The insufficient wait times make measuring this slow porosity population (large pores with high permeability) from the acquisition across the Lyons rock impossible. Within the Satanka, NMR porosity is also underestimated, but for a different reason: the tool's acquisition parameters do not allow sufficient time to capture the fast-relaxing signals from the small, low-permeability pores.

Despite these challenges, the NMR still accurately captures overall porosity trends. Core PHIT data further confirms that the NMR wireline captured the majority of the porosity present in all zones despite the data clipping. Porosity within the Lyons Formation is well-constrained.

**Figure 2.43** will be discussed in more detail in subsequent subsections. Tracks 5 to 9 show the elemental log measurements (in blue), core XRD data (red dots), and the modeled mineralogy (color-filled black line). Track 10 is the core RCAL permeability at reservoir effective stress (NCS) and Klinkenberg-corrected (red dots) and High Plains' permeability model (described in *Section 2.4.1.3*).

**Figure 2.43** also illustrates the vertical distribution of core-derived porosity and permeability from the Juniper M-1 stratigraphic test well.

Figure 2.43—Juniper M-1 (API No. 49-021-29548) wireline and core calibration data with petrophysical model. Track 1: Gamma ray (GR); Track 2: Facies A and B dominated intervals defined; Track 3: Deep (RT) and shallow (RXO) resistivities; Track 4: neutron porosity on sandstone matrix (NPHI_ss) and density (RHOB) crossplot; Track 5: Total porosity (PHIT) model and core-measured total porosity at reservoir net confining stress (PHI_RES); Track 6: modeled quartz volume fraction of matrix (VQTZ_NORM), Quartz volume fraction from core XRD (Quartz), & elemental wireline measurement of quartz, feldspar, and lithics (WQFM_INCP); Track 7: modeled clay volume fraction of matrix (VCLAY_NORM), Total clay volume fraction from core XRD (Illite_mica), & elemental wireline measurement of total clay (WCLA_INCP); Track 8: modeled anhydrite volume fraction of matrix (VANHY_NORM), anhydrite volume fraction from core XRD (Anhydrite), & elemental wireline measurement of anhydrite (WANHY_INCP); Track 9: modeled dolomite volume fraction of matrix (VDOL_NORM), dolomite volume fraction from core XRD (dolomite), & elemental wireline measurement of dolomite (WDOL_INCP); Track 10: modeled potassium feldspar volume fraction of matrix (Vkspar_NORM) & potassium feldspar volume fraction from core XRD (k_spar); Track 11: permeability predictive model and core-measured permeability at reservoir conditions and Klingenberg-corrected as point data.

### *2.4.1.3 Permeability*

The porosity-permeability relationship (**Figure 2.44**) within the Lyons Formation is determined from routine core analysis (RCAL) core measurements (n = 42) within the Juniper M-1 well. Two sand-bearing facies, "Facies A" and "Facies B," were identified in the Juniper M-1, both exhibiting good reservoir quality and present in roughly equal proportions. Facies B contains a higher proportion of potassium feldspar, resulting in higher GR readings. GR is currently being used to differentiate these two sand facies, but High Plains is in the process of developing a predictive facies model.

Facies B shows a slightly higher permeability for a given porosity than Facies A, leading to distinct porosity-permeability trends for each facies. Within the AoR, based on Reference Well logs (**Figure 2.9**), the gamma ray values in high porosity zones are higher than at Juniper M-1, indicating that Facies B is likely the dominant facies present.

Figure 2.44—Routine core porosity and permeability data relationships by facies.

Porosity and permeability distributions generated from geocellular modeling are displayed in **Figures 3.19** and **3.20** in *Section 3.1.3*. These distribution plots demonstrate that log-derived porosity and permeability values are consistent with core-derived values of the Lyons sandstone (**Table 2.3**). Vertical and lateral heterogeneity may be present within the Lyons Sandstone due to the interfingering of facies commonly associated with the deposition of eolian sands (**Figure 2.45**). According to Kendigelen's 2016 thesis, better reservoir-quality facies (e.g., High Plains' Facies A and B) of the Lyons Formation are associated with better reservoir-quality sand development. Kendigelen (2016) also points out that damp or wet interdune deposits, when present, can

detrimentally affect reservoir quality. Core and log data acquired in the Conestoga I-1 will confirm the facies present within the AoR.

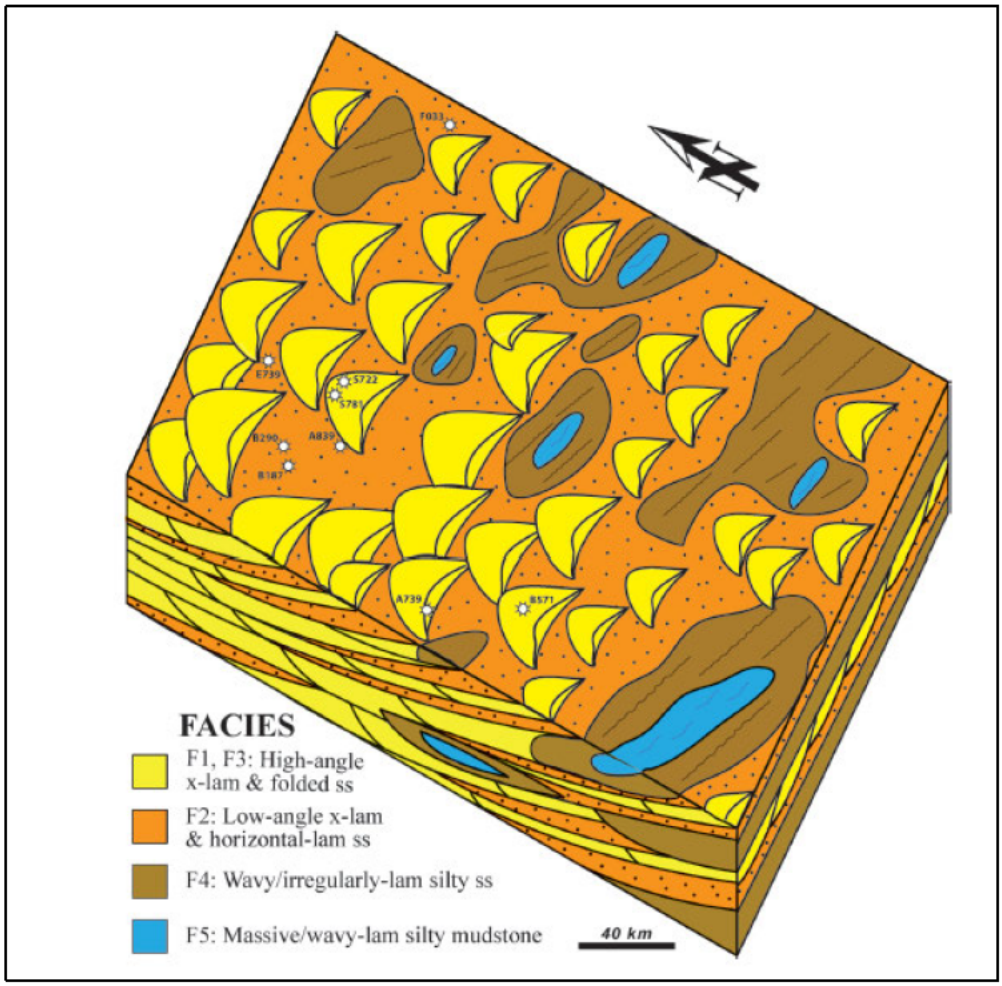


Figure 2.45—Hypothesized facies model of dune paleoenvironments and facies associations based on Lyons core study in northern Colorado (Kendigelen et al., 2023). Facies 1 and Facies 3 are described as "high-angle, cross-laminated (x-lam), and folded sandstone (ss)," related to "dry" barchan dune deposition. Facies 2 is "low-angle, cross-laminated, and horizontal laminated (-lam) sandstone" related to dry interdune deposits. Facies 4 is described as "wavy/irregularly limited silty sandstone" related to damp interdune deposits. Facies 5 is "massive/wavy laminated silty mudstone" related to wet interdune deposits.

### *2.4.1.4 Minerology*

In the Juniper M-1 well, the Lyons Formation is comprised of fine-grained to very fine-grained eolian sands. The mineralogic composition was measured in the Juniper M-1 both in core (x-ray diffraction [XRD], and x-ray fluorescence [XRF]) and by wireline (elemental spectroscopy logs) (refer to **Figure 2.43**, tracks 5 to 10). Quartz is the dominant mineralogy ([redacted]) followed by feldspars (potassium feldspar = [redacted] wt% and plagioclase = [redacted]). Anhydrite and dolomitic cement can be found at the top and bottom of the Lyons Formation. Petrophysical modeling in the Reference Wells suggests Conestoga I-1 will have a similar composition and vertical distribution to what is seen in the Juniper M-1 (**Figure 2.43**). The Reference Wells suggest the presence of clay-rich or dolomite cement intervals within the

uppermost [redacted] ft of the Lyons Formation within the AoR, which were not observed in the Juniper M-1 well.

#### *2.4.1.5 Potential for Geochemical Interactions*

Based on comprehensive analyses of Lyons core samples from the Juniper M-1 characterization well, High Plains is confident that no significant reactions between the injectate stream and the formation mineralogy will adversely impact injectivity, storage potential, or containment. A detailed formation damage test was conducted on a Lyons core sample, where the plug was saturated with synthetic brine, and permeability was measured across varying injection rates. After injecting approximately 100 pore volumes of brine, minor permeability reductions were observed at higher injection rates (above 50 $cm^3$/min), likely due to turbulence or fines migration. However, reducing the injection rate restored permeability to near-original levels. Furthermore, a reverse formation brine salinity (post-$CO_2$ relative permeability) test showed consistent permeability at 100% brine saturation, confirming minimal geochemical reactivity that might affect the injection zone's permeability.

Coupled with geochemical modeling of long-term $CO_2$ storage (see *Section 2.8.3*), these results suggest no concerns regarding the compatibility of the Lyons reservoir and the injectate stream. *Sections 2.8.1.1* and *2.8.2.1* provide more details on the injection reservoir's fluid and solid geochemistry.

#### *2.4.1.6 Additional Data Collection Plans*

High Plains is currently utilizing the Juniper M-1 data as the characterization well but will acquire additional geomechanical (**Table 2.4**) and rock property (**Table 2.5)** data in the Conestoga I-1 to confirm results. See *Section 6.0—Pre-Operational Logging and Testing Program* for more details.

Table 2.4—Summary of required geomechanical characterization per 40 CFR 146.82(a)(3)(iv), and forthcoming data to address requirements.

| UIC Class VI Requirements for 40 CFR 146.82(a)(3)(iv) | Data Acquisition Planned for Conestoga I-1 | |
|---|---|---|
| | Wireline | Core |
| Fractures | [redacted] | |
| Rock Strength | | |
| In-Situ Stress Field | | |
| Pore Pressure | | |

Table 2.5—Summary of required rock properties of the confining and injection zone per 40 CFR 146.82(a)(3)(iii) and forthcoming data to address requirements.

| UIC Class VI Required Data [40 CFR 146.82(a)(3)(iii)] | Data Acquisition Planned for Conestoga I-1 | |
|---|---|---|
| | Wireline | Core |
| Mineralogy | [redacted] | |
| Porosity | | |
| Permeability | | |
| Capillary Pressure | | |
| Geology/Facies Changes | | |

### *2.4.2 Data on the Confining Zone(s)*

The Project's upper confining zone (UCZ) is the Goose Egg Formation; the lower confining zone (LCZ) is the Satanka Formation. Based on High Plains' evaluation of the Reference Wells within the AoR, the Satanka Formation is a low permeability, dolomitic, mudstone and siltstone with approximately [redacted] anhydrite cement. The Goose Egg Formation consists of interlayered anhydrites with low permeability mudstone and siltstone beds. Dolomitic cementation [redacted] can also be present. The properties of the confining zones indicate significant sealing capacity. Both formations exhibit extensive thicknesses (**Figure 2.29**, **Figure 2.30**), have low porosity and permeability (*Section 2.4.2.2*), and exhibit geomechanical properties (*Section 2.5*) that provide robust confinement for fluids in the Lyons Formation.

### *2.4.2.1 Depth, Areal Extent, and Thickness*

Within the AoR, the Goose Egg Formation UCZ is predicted to be predominantly muddy siltstone with layers of massive anhydrite and some dolomitic cements. The geologic type log for the Goose Egg Formation is in central Wyoming and contains an interbedded sequence of silty shales, carbonate, and evaporites that are red to ocher in color and Permian to Lower Triassic in age (**Figure 2.46** from Burk and Thomas, 1956).

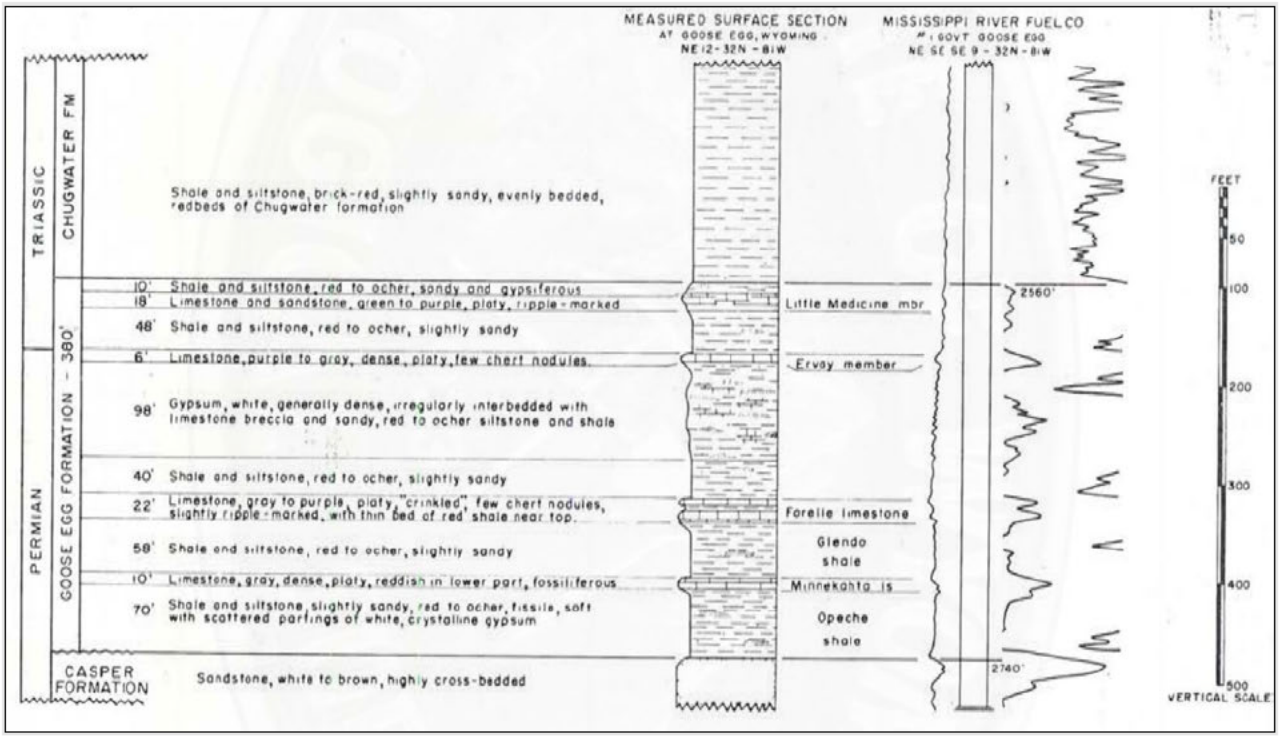


Figure 2.46—Generalized Goose Egg and Chugwater lithology at type location (NW1/4, Sec.12, T32N, R81W) with electric log character of formation in the nearby subsurface (Burk and Thomas, 1956).

The Goose Egg Formation overlies the Lyons Formation injection interval and is expected to be encountered at approximately [redacted]) in the Conestoga I-1 well, with a gross thickness of [redacted] (**Table 2.6**). The schematic cross-sections displayed in **Figure 2.47** illustrate the stratigraphic relationships among Goose Egg members and clarify nomenclature changes across regions. At the WNS Hub location, the Forelle and Minnekahta limestone tongues are anticipated to be present.

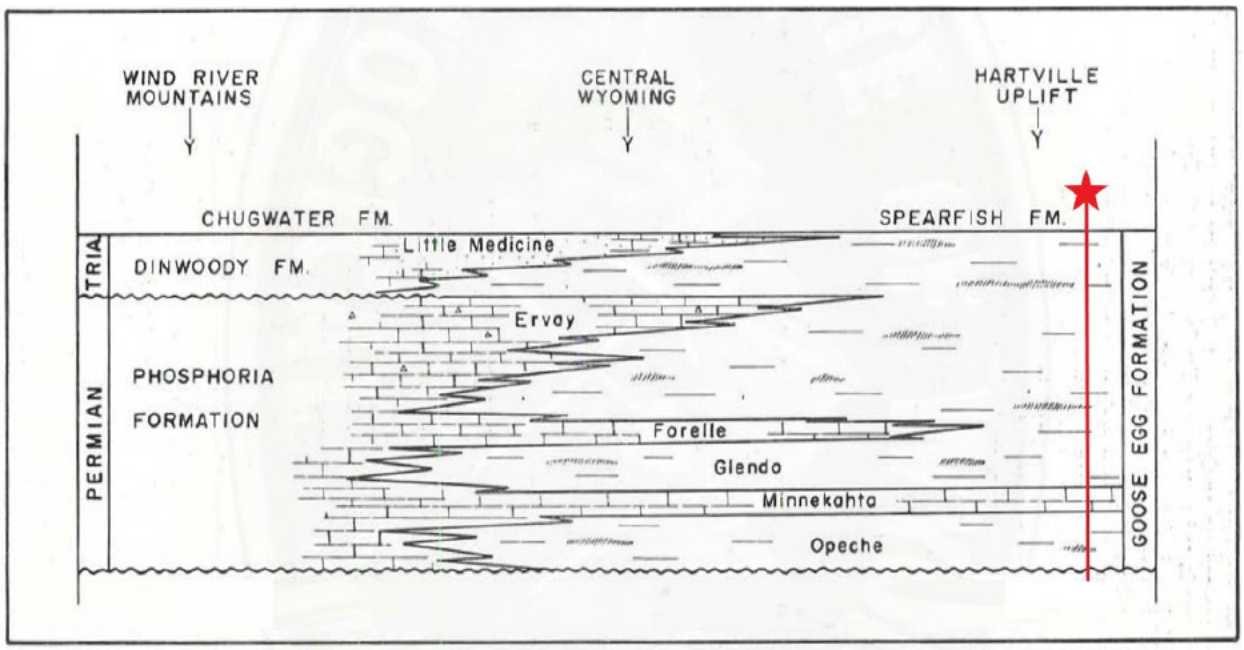


Figure 2.47—Schematic cross-section depicting the stratigraphic relationship of Goose Egg Formation with the time-equivalent Phosphoria and Dinwoody formations from the Wind River Mountains to the Hartville Uplift, Wyoming (after Burk and Thomas, 1956). The red star and line represent the approximate location of the WNS Hub.

Table 2.6—Summary of predicted subsurface properties in AoR over the injection zone and upper and lower confining zones.

| Confining Zone Properties | Upper Confining Zone | Injection Zone | Lower Confining Zone |
|---|---|---|---|
| Formation Name | Goose Egg | Lyons | Satanka |
| Lithology | Interbedded anhydrite and silty mudstone | Eolian quartzose sandstone | Dolomitized silty mudstone |
| Formation Top Depth (ft, MD) | [redacted] | | |
| Gross Thickness (ft) | | | |
| Net Thickness > 10% PHIE (ft)** | | | |
| Total Porosity (%) (avg. from logs*) | | | |
| Permeability (mD average from logs*) | | | |
| Capillary entry pressure (gas-water; psi) (estimated from core) | | | |
| Depth below the base of the lowest confirmed USDW (ft) | | | |

* Weighted average porosity and permeability from petrophysical models in Reference Wells based on models calibrated from Juniper M-1 well. Weighting multipliers [redacted] based on distance from Conestoga I-1 location.
** Calculated for net reservoir quality rock > 10% porosity (net to gross [redacted]

Carbonate beds of the Goose Egg Formation primarily consist of finely crystalline dolomite to dolomitic limestones, with some finely crystalline limestone. These carbonate tongues are distributed within a sequence of red beds and evaporites. The red sediments of the Goose Egg consist of nonresistant shales, mudstones, and siltstones that generally lack any prominent structure. Typical detrital constituents of the red sediments are quartz and feldspar with some mudstone, shale fragments, mica, carbonate grains, and magnetite-ilmenite-leucoxene. Beds are poorly developed and grade vertically and laterally into the evaporites of the Goose Egg depositional sequence (Campbell, 1963).

Core crushed rock analysis (CRA) at the Juniper M-1 well confirmed that all facies within the Goose Egg Formation exhibit very low porosity and permeability (see *Section 2.4.2.2)* for more discussion). A Review of regional literature and site-specific characterization of the thick, regionally extensive geologic sequence suggests that the Goose Egg Formation effectively acts as the upper confining layer for the injection zone.

The lower confining zone, the Satanka Formation, was deposited in a more arid environment than the Goose Egg Formation, across a dry salt-pan playa. The Satanka Formation is composed primarily of red siltstones and mudstones, which exhibit low porosity and permeability, as evidenced by log characteristics and core data (**Figure 2.48**). Core observations reveal minimal sedimentary structures, except for occasional haloturbation and small teepee structures. These features indicate cycles of hydration and expansion, followed by evaporation and salt precipitation, leading to sediment buckling. The Satanka exhibits minor log character and thickness changes across the DJ Basin and is a reliable LCZ.

#### *2.4.2.2 Porosity and Permeability*

CRA was performed on the Juniper M-1 whole core in the confining intervals. This method allows for proper cleaning of the samples, enabling accurate measurement of matrix porosity and grain density in low-permeability samples (**Figure 2.49**). Permeability is assessed semi-quantitatively through this technique and is further validated by estimates from high-pressure mercury injection (HPMI). In the Juniper M-1 stratigraphic well, all data sources—nuclear magnetic resonance (NMR) wireline porosity, core porosity and permeability, and HPMI porosity and permeability—consistently indicate that both confining layers (the Satanka and Goose Egg Formations) exhibit very low porosity (< 5%) and permeability (in low microdarcy range).

Figure 2.48—Porosity-permeability crossplot for low permeability samples from crushed rock analysis (CRA).

For the Goose Egg Formation, porosities range from [redacted] v/v, with an average porosity of [redacted] Permeability in Goose Egg rock ranged from [redacted] mD, with an average of [redacted]. The anhydrite beds have nearly no porosity or permeability and, in the Juniper well, can be up to [redacted] ft thick. In the Reference Wells, anhydrite beds are generally thinner, averaging around [redacted], but often occur in clusters of [redacted] ntervals. The average modeled porosity in the Goose Egg within the Reference Wells is [redacted] v/v (**Table 2.3**). For the Satanka Formation, the dolomitic mudstones are relatively consistent throughout, with a porosity range of [redacted]. The low permeabilities are also remarkably consistent, with a [redacted] permeability range. Below the Satanka, at the Satanka-Wolfcamp transition, there is a massive zone of anhydrite with a thickness of up to [redacted] Within the AoR extent, Goose Egg and Satanka porosity is generally low and does not exhibit much variation.

Figure 2.49—Juniper M-1 (API No. 49-021-29548) well crushed rock porosity and permeability results (blue dots in Tracks 5 and 8). Track 1 shows intervals dominated by Facies A and B, respectively; Track 2: Log Gamma (GR) and Caliper (Cali). Track 3: deep (RT) and shallow (Rxo) resistivity. Track 4: Density (RHOB) and Neutron (NPHI) crossplot at a Lyons sandstone compatible scale. Track 5: Porosity track that includes helium porosity (PHIT_HE, as blue dots)) from crushed rock analysis (CRA), reservoir porosities from RCAL (PHI_RES, as red dots), NMR (purple line), and modeled porosity (PHIT); Tracks 7 and 8 show the permeability model on two scales; Track 7 is on a scale suitable for the permeable Lyons RCAL samples; Track 8 is on a scale suitable for the low permeability, crushed rock samples for the confining zones.

#### *2.4.2.3 Minerology*

**Table 2.3** highlights the stark contrast in mineralogical composition between the confining zones and the Lyons Formation. The confining Satanka and Goose Egg Formations show a significant increase in clay and dolomite within the siltstones, along with a greater presence of anhydrite beds, compared to the Lyons Formation injection zone. These mineralogical characteristics enhance the integrity of the confining zones by reducing porosity and permeability, as discussed in *Section*

*2.4.2.2*. The anhydrite beds of the Goose Egg are interbedded with dolomitic mudstone and siltstones. The Satanka is finely interbedded dolomitic mudstones and siltstones with some anhydrite cement. **Figure 2.42** illustrates the vertical distribution of these minerals within the nearest offset well (Mathewson 1).

**Table 2.3** illustrates the marked contrast in mineral composition between the confining zones and the Lyons Formation. The primary differences between the confining layers—the Satanka and Goose Egg formations—and the Lyons Formation (injection zone) include a pronounced increase in clay and dolomite content within the siltstones, as well as a more frequent occurrence of anhydrite beds. These distinctions from the Lyons Formation enhance the integrity of the confining zones and contribute to a reduction in porosity and permeability, as detailed in *Section 2.4.2.2*.

### *2.4.2.4 Potential for Geochemical Interactions*

The confining zones above and below the Lyons Formation play a critical role in ensuring the containment of injected $CO_2$. Understanding the mineralogical makeup of these zones is essential to evaluate potential geochemical reactions that might impact the storage integrity and long-term stability of the injection site.

The average clay content in the Juniper M-1 core XRD samples is [redacted]% in the Goose Egg Formation and [redacted] in the Satanka Formation. All Satanka samples (n = 8) contain more than [redacted]% clay, the majority [redacted] of which is illite/mica. The remaining clay species are dominated by corrensite, an intermediate form between trioctahedral chlorite and trioctahedral smectite (Brigatti and Poppi, 1984). Of the Goose Egg samples (n = 24), 13 of the mudstone samples have a clay content greater than 20%, with illite/mica ([redacted] being the predominant clay mineral, followed by corrensite [redacted] Small amounts [redacted] of chlorite and mixed-layer illite-smectites are also present. Corrensite's expandability is [redacted] which can create gum-balling while drilling. In the Satanka samples, corrensite averages [redacted] of the clay species, ranging from [redacted] while chlorite comprises [redacted] of the remaining clay content.

While expandable clays like corrensite can potentially react with $CO_2$, leading to issues such as fines migration, High Plains believes that several factors will mitigate the likelihood of significant adverse geochemical interactions. These factors include the negligible amounts of corrensite in the injection zone, the interbedded nature of the confining zones with the corrensite and other clay species restricted to specific beds, the presence of anhydrite beds isolating these clay-rich layers, and the inherently low permeability of the confining zones. These characteristics should minimize $CO_2$ interactions with the clays in the confining layers. For further details on the geochemistry of the confining zones, refer to *Section 2.8.2.2*; for details on the geochemical modeling conducted, see *Section 2.8.3*.

### *2.4.2.5 Capillary Pressure and Integrity of the Confining Zone*

The capillary pressure data from HPMI (also known as mercury injection capillary pressure [MICP]) for the confining zones demonstrates effective seals. In the Goose Egg Formation, mudstone samples show Swanson permeability values (Swanson, 1981) of [redacted]

[redacted] The sealing capacity of the Goose Egg samples varies slightly with permeability. These column heights indicate that upper confining zone leakage due to capillary failure is highly unlikely.

#### *2.4.2.6 Additional Data Collection Plans*

As discussed above (*Section 2.4.1.6*) and in *Section 6.0—Pre-Operational Logging and Testing Program*, additional site-specific data for the upper confining zone will be collected while drilling the Conestoga I-1 well. Please refer to the listed sections for details on the data collection plans and to **Table 2.4** for a list of additional geomechanical data to be collected and **Table 2.5** for a list of rock property data to be collected.

## 2.5 Geomechanical and Petrophysical Information [40 CFR 146.82(a)(3)(iv)]

High Plains has developed a geomechanical model to predict in-situ stresses (pore pressure and minimum horizontal stress) across the Lyons Formation and its confining zones. This model was developed using data from the Juniper M-1 well, including wireline log responses calibrated to core geomechanical measurements and pressure gradients from the Modular Formation Dynamics Tester (MDT). The MDT pressure gradients constrain the pore pressure at the Juniper M-1 and provide calibration to a log model of a compacted shale at both hydrostatic pressures and sub-hydrostatic conditions. Geomechanical measurements conducted on the Juniper M-1 core allowed for the creation of quantitative, predictive models for stress moduli within the AoR. The [redacted] provided the required sonic logs. Logs and core from Conestoga I-1 will be used to cross-check the model as applied to Reference Wells.

The pore pressure gradient in the Lyons Formation (0.343 to 0.345 psi/ft), measured via MDT in the Juniper M-1, shows that the Lyons is naturally under-pressured at the Juniper M-1 location. This means the Lyons Formation is in a rock package below the hydrostatic gradient. Natural hydrostatic gradients typically range from 0.433 psi/ft (equivalent to zero TDS) to 0.510 psi/ft (equivalent to 260,000 mg/L). Birchall et al. (2022) comprehensively reviews multiple mechanisms responsible for producing naturally occurring underpressured reservoirs.

Belitz and Bredehoeft (1988) attribute the under-pressure in the Dakota Sands in Wyoming and Colorado to a combination of highly permeable sands, which are isolated from the surface by a thick package of impermeable Cretaceous strata, and further isolated by regional faulting. These permeable sands are regionally hydraulically connected to low-elevation outcrops hundreds of miles away. **Figure 2.22** is a cartoon depiction of this potential connection (over long geologic timescales) with a lower-elevation outcrop.

Pore pressure is predicted from **Equation 2.1** (Eaton, 1969; Anderson et al., 1973). Values predicted for Lyons in the AoR can be found in **Table 2.7**.

Equation 2.1—Predicted pore pressure.

$$PP_{grad} = OB_{grad} - [(OB_{grad} - hydrostatic_{grad}) \times (\frac{DTC_{np\ shale}}{DTC})^3]$$

Where,
$PP_{grad}$ = Pore pressure gradient
$OB_{grad}$ = Overburden gradient ≈ 1.02 psi/ft
$DTC_{np\ shale}$ = compressional slowness of a normally compacted shale
DTC = sonic slowness log

Acoustic logs show that the compaction trend of a normally pressured shale in the Juniper M-1 well differs from that in the Conestoga Reference Wells. It appears that pore pressure within the Lyons sands in the Conestoga I-1 is closer to normal pressure (0.443 psi/ft). Since the lithologies are the same, the relationship between pore pressure and horizontal minimum stress will likely be similar.

Representative core samples from the Lyons, Goose Egg, and Satanka formations, from the Juniper M-1 core, underwent a series of geomechanical analyses, including triaxial compressive strength, pore volume compressibility, Brazil tensile strength, and fracture toughness. High Plains incorporated these vertical and horizontal measurements of geomechanical moduli (e.g., Young's modulus, Poisson's ratio, and Biot's coefficient alpha. These moduli also played a crucial role in minimum horizontal stress determination. They were incorporated into the geomechanical modeling to move from a predicted log-based pore pressure to a horizontal minimum stress (**Equation 2.2**) (Thiercelin and Plumb, 1994). The pore elastic stress model was calculated to determine the minimum horizontal stress for the Lyons Formation, incorporating regional tectonic stresses, following the industry-standard methodology described by Zhang (2019, *Applied Petroleum Geomechanics*, Chapter 6). An isotropic model was applied due to the Lyons' isotropy and only slight anisotropy in the confining zones to predict minimum horizontal stress. This method estimated the fracture gradient to be approximately 0.74 to 0.76 psi/ft within the Lyons and confining zones.

Equation 2.2—Minimum horizontal stress.

$$\sigma_h = \frac{\nu}{(1-\nu)}(\sigma_V - \alpha P_p) + \alpha P_p + \frac{E_{sta} \times \varepsilon_{Hmin}}{(1-\nu^2)} + \frac{\nu \times E_{sta} \times \varepsilon_{Hmax}}{(1-\nu^2)})$$

Where,
$\sigma_h$ = minimum horizontal stress (psi)
$\nu$ = Poisson's ratio
$\sigma_V$ = overburden pressure (psi)
$\alpha$ = Biot's coefficient alpha
$P_p$ = pore pressure (psi)
$E_{sta}$ = Young's modulus (Mpsi or GPa)
$\varepsilon_{Hmin}$ = tectonic strain in minimum horizontal stress direction (millistrain)= 9.9E-05
$\varepsilon_{Hmax}$ = tectonic strain in maximum horizontal stress direction (millistrain) = 0.00057

The model can only estimate the minimum pressure for the rock to fail (fracture). This method does not necessarily tell the *exact* minimum pressure at which the rock will fail but rather the boundary that the minimum pressure should not exceed. A normal faulting regime was assumed for this method based on a literature review of the region (Lundstern and Zoback, 2022). For the AoR, a hydrostatic gradient of 0.443 psi/ft (equivalent to approximately 32,000 mg/L) was

assumed due to a compaction response in the sonic data that differed from the Juniper M-1 and more closely resembled hydrostatic pressures.

Table 2.7—Predicted ranges of modeled geomechanical properties and stresses for the Lyons Formation within the AoR.

| Formation | Poisson's Ratio (n) | Biot's (a) | Young's ($E_{sta}$) (Mpsi) | Pore Pressure ($P_p$) (psi/ft) | Minimum Horizontal Stress (SHmin) (psi/ft) | Overburden ($s_V$) (psi/ft) |
|---|---|---|---|---|---|---|
| Lyons | [redacted] | [redacted] | [redacted] | [redacted] | [redacted] | [redacted] |

### *2.5.1 Fractures*

At the Juniper M-1, non-transmissive natural fractures were observed in the image log data (as described in *Section 2.3.3*). Core geomechanical tests were conducted on carefully selected samples using micro-CT scans to ensure the samples were free of fractures and microfractures. The core-determined elastic properties of these fracture-free samples were used to estimate minimal horizontal stress (SHmin) (**Equation 2.2**). Based on these calculations, High Plains predicts the SHmin to range from [redacted] psi/ft. The injection test indicated that SHmin is above [redacted] psi/ft. The close alignment of these values suggests that the impact of non-transmissive fractures on the geomechanical properties of the injection zone and its confining layers is minimal.

### *2.5.2 Pore Pressure*

High Plains calibrated its pore pressure model through multiple approaches. Regionally, the American Institute of Formation Evaluation's (AIFE) online DST database was utilized to access proprietary data from wells penetrating the Lyons and Sundance formations. Formation pressures were interpreted from the AIFE data. At the injection wells, a combination of pressure gauges, formation tester gradients, DFITs, and injection testing provided measured calibration points for both pore pressure and minimum horizontal stress. The Lyons' pore pressure is anticipated to be higher (at hydrostatic, 0.443 psi/ft) at the Conestoga I-1 than at the Juniper M-1 (underpressured, 0.344 psi/ft), potentially due to different compaction histories or connections to outcropping rock in the region.

During the injection phase, advanced geomechanical modeling, in combination with reservoir modeling, will be used to better understand injection responses and plume migration over time. Once measured pore pressure data (e.g., formation tester) from the Conestoga I-1 well has been analyzed, reservoir models and associated tables will be updated with site-specific values. **Table 2.8** provides the estimated pressure gradients (with an uncertainty range) for the Lyons and Sundance formations.

Table 2.8—Formation pressure and pressure gradient estimations.

| Formation | Test Depth (TVD, ft) | Estimated Formation Pressure (psi) | Mean Pressure (psi) | Gradient (psi/ft) |
|---|---|---|---|---|
| Sundance | [redacted] | | | |
| Lyons | | | | |

Pore pressure gradients measured in the Juniper M-1 for the Sundance sands (0.328 to 0.332 psi/ft) and J Sand (0.271 psi/ft) vary from those of the Lyons Formation. This variation suggests that

these sands are fully isolated from one another and from the Lyons Formation, further demonstrating the sealing capacity of the Goose Egg Formation.

### *2.5.3 Stress*

Two of the Reference Wells for the Conestoga I-1 [redacted] have slightly different acoustic log responses. The estimation of minimum horizontal stress described in this section is determined from the average of the Reference Wells. Reservoir models and associated tables will be updated with site-specific values once measured stress gradients (e.g., formation tester, step-down tests, minifracture tests) from the Conestoga I-1 well have been analyzed. **Table 2.9** summarizes the predicted fracture gradient (with an uncertainty range) within the Lyons Formation.

Table 2.9—Estimated minimum stress of the injection formation (Lyons).

| Depth (TVD ft) | Closure Pressure (psi) | Average Minimum Stress (psi) |
|---|---|---|
| [redacted] | | |

#### *2.5.3.1 Vertical Stress*

Overburden stress, or vertical stress, was calculated from bulk density (**Equation 2.3**). The density is converted to pressure below ground level. A density ($\rho$) of [redacted] g/cm$^3$ was used for shallow, missing values. To convert bulk density to pressure, 1 kg/cm is the equivalent of 14.22 psi. The overburden gradient for the Conestoga I-1 well is estimated to be approximately [redacted] psi/ft.

Equation 2.3—Bulk density.

$$\sigma_V = \rho_a \times g \times Z$$

Where,

$\rho_a$ = average density per foot (where 1 kg/cm$^2$ = 14.22 psi)
$g$ = acceleration due to gravity, 32.174 ft/sec$^2$
$Z$ = true vertical depth (ft)

#### *2.5.3.2 Minimum Horizontal Stress or Fracture Gradient*

The Lyons Formation has little to no variation in its elastic properties and stresses. The confining zones exhibit more variability in elastic properties, with the more anhydrite and/or dolomite present, the greater the differentiation between the Lyons and the confining layers. At the Conestoga I-1 location, averaging formation properties from the References Wells leads to a similar pore pressure and minimum horizontal stress/fracture gradient. However, the anhydrite and dolomite layers increase the fracture gradient in the confining zones. The anhydrite beds, in particular, on the bedding scale are stiffer than the mudstones in the confining zones. These stiff anhydrite beds (some regionally continuous), along with the interbedded mudstones, help contribute to the Goose Egg's confining capacity. Estimated ranges of predicted variables for **Equation 2.2** can be found in **Table 2.7**.

#### *2.5.3.3 Maximum Horizontal Stress*

Predicting the maximum horizontal stress is more challenging than predicting the minimum horizontal stress. If stress-induced features (e.g., breakouts on image logs or leak-off tests) are

present, they can be used to estimate maximum horizontal stress (Davidson et al., 2012; Li and Purdy, 2010). In the Juniper M-1, High Plains did not have wellbore breakouts to use in this estimation. Based on **Equation 2.4**, maximum horizontal stress is predicted to be approximately 50 psi above minimum horizontal stress. Zhang and Zhang (2017), in their summary of in-situ stress state with fault regimes interaction, that, in a normal-faulting regime σV ≥ σH ≥ σh.

Equation 2.4—Maximum horizontal stress.

$$\sigma_H = \frac{\nu}{(1-\nu)}\left(\sigma - \alpha P_p\right) + \alpha P_p + \frac{E_{sta} \times \varepsilon_{Hmax}}{(1-\nu^2)} + \frac{\nu \times E_{sta} \times \varepsilon_{Hmin}}{(1-\nu^2)})$$

Where,

$\sigma_H$ = minimum horizontal stress (psi)
$\nu$ = Poisson's ratio
$\sigma_V$ = overburden pressure (psi)
α = Biot's coefficient alpha
$P_p$ = pore pressure (psi)
$E_{sta}$ = Young's modulus (Mpsi or GPa)
$\varepsilon_{Hmin}$ = tectonic strain in minimum horizontal stress direction (millistrain)
$\varepsilon_{Hmax}$ = tectonic strain in maximum horizontal stress direction (millistrain)

#### *2.5.3.4 Stress Orientation*

According to the World Stress Map (Heidbach et al., 2016) and the USGS (Lundstern and Zoback, 2023), the AoR is tectonically quiescent but is in an extensional regime within the DJ Basin with a maximum horizontal stress orientation of northwest-southeast (**Figure 2.50**). This is consistent with Juniper M-1 data where limited tensile, drilling-induced fracturing, and borehole breakouts indicated a WNW-ESE orientation.

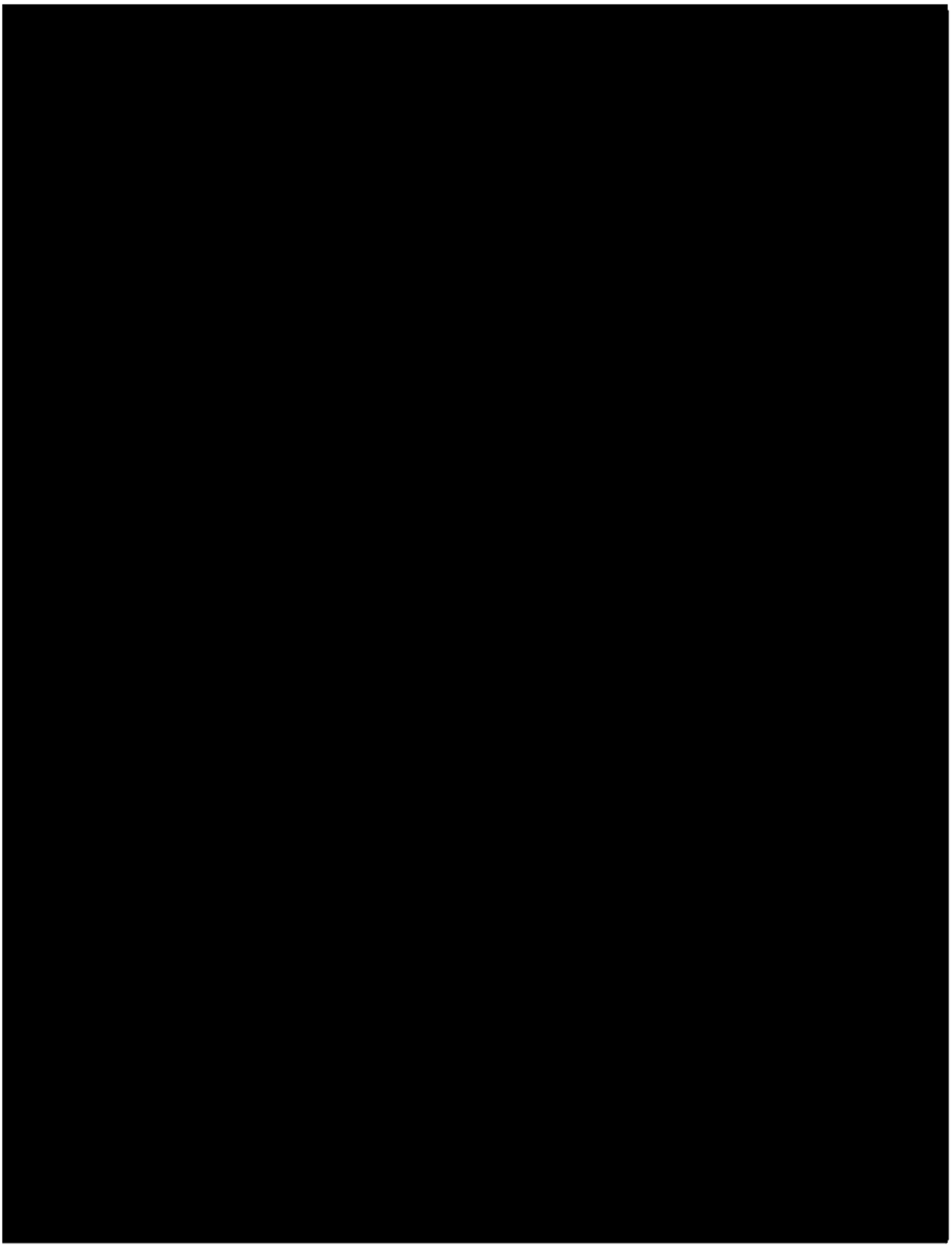

Figure 2.50—World Stress Map (Heidbach et al., 2016; Lundstern and Zoback, 2023) with the Conestoga I-1 well location shown.

### *2.5.4 Ductility*

Biot's coefficient alpha for the Lyons Formation is measured at [redacted] and approximately [redacted] for the confining zone rocks. Refer to **Table 2.10** for a comprehensive list of all geomechanical core measurements from the Juniper M-1. The bulk densities of [redacted] $g/cm^3$ or greater are anhydrite beds.

Table 2.10—Juniper M-1 (API No. 49-021-29548) geomechanical core data.

| Formation | Core Depth (ft) | Sample Orientation | Bulk Density ($g/cm^3$) | Young's Modulus (psi) | Poisson's Ratio A | Poisson's Ratio B | Bulk Modulus (psi) | Bulk Compressibility (1/psi) | Grain Compressibility (1/psi) | Biot's Alpha (1-Cg/Cb) |
|---|---|---|---|---|---|---|---|---|---|---|
| Goose Egg | [redacted] | | | | | | | | | |
| Lyons | | | | | | | | | | |
| Satanka | | | | | | | | | | |

### *2.5.5 Rock Strength*

The Lyons Formation core sample exhibits distinct geomechanical properties compared to the confining layers, both in its overall elastic properties and its isotropic nature. In contrast, the confining formations show slight anisotropy. The Young's Modulus (vertical) for the Lyons Formation is 1.74 Mpsi, significantly less than the confining zone shales, which range from [redacted]

### *2.5.6 In-Situ Fluid Properties*

The Lyons Formation exhibits very low deep resistivities [redacted]) in the Reference Wells, indicating that the pore space is likely fully saturated with brine. Based on the estimated porosity and reservoir temperature, the salinity (NaCl-equivalent) of the brine in the Lyons Formation is estimated to range from [redacted] mg/L. If present, the Sundance Formation is estimated to have pore water salinity of [redacted] mg/L (NaCl-equivalent).

### *2.5.7 Geothermal Gradient*

Drilling mud temperatures were gathered from log header data, and mud circulation time was considered. Plotting all available temperature data with depth yielded a regional thermal gradient of 2.4°F/100 ft, which was adopted for the area. **Table 2.11** shows the predicted formation temperatures based on this temperature gradient.

Table 2.11—Formation temperature measurements and calculated temperature gradients.

| Formation | Test Depth (TVD, ft) | Temperature (°F) | Mean Surface Temp. (°F) | Gradient (°F/100 ft) |
|---|---|---|---|---|
| Sundance | [redacted] | | | |
| Lyons | | | | |

## 2.6 Seismic History [40 CFR 146.82(a)(3)(v)]

### *2.6.1 Summary of Seismic History and Available Data*

Historical earthquakes with magnitudes greater than 2.5 for the past 100 years were obtained from the USGS Earthquake Hazards database, focusing on recorded earthquakes within a 100-mile radius of the proposed Conestoga I-1 well.[17] The search results, shown in **Figure 2.51** and **Table 2.12**, indicate that the WNS Hub is located in a very low-risk area that has experienced no seismic activity over the past 100 years. The most recent earthquake within 100 miles of the proposed location occurred northeast of Greeley, CO, on March 30, 2019, approximately 75 miles southwest of Conestoga I-1, with a magnitude of 2.9 and a focal depth of four miles.

[17] Retrieved at: https://www.earthquake.usgs.gov/earthquakes/search

The search results identified several seismic events from 2014 to 2019 with magnitudes of less than 3.2 near Greely, Colorado, approximately 75 miles southwest of the AoR. Modeling conducted by Brown et al. (2017) suggests this seismicity was due to wastewater injection into deep fractured reservoirs in close vertical proximity to the crystalline basement.[18]

Plume modeling of the Conestoga I-1 injection suggests the plume will likely migrate no more than ten miles in diameter, which results in more than 60 miles between the modeled plume extents and the nearest recorded seismic activity. In addition, as discussed in *Section 2.3.2,* interpretation of 2D seismic data indicated the absence of faulting at the storage complex level and, therefore, most likely, the absence of earthquake sources within the AoR and regionally. Therefore, the Project has a low risk of impacts due to natural seismicity.

**Figure 2.51** identifies the WNS Hub's location relative to historical seismic events. The figure also shows SHmax orientations and the location of existing seismic monitoring stations.

[18] www.inducedearthquakes.org

Figure 2.51—USGS reported earthquakes (≥ M2.5) between 1934 and 2024, as well as seismic monitoring stations and SHmax directions. The yellow cross star is the approximate location of the WNS Hub.

Table 2.12—Summary of earthquakes of magnitude of 2.5 and above from January 1900 to August 2024, within a 100-mile radius of WNS Hub.

| Date | Magnitude | Depth (miles) | Longitude* | Latitude* | City or Vicinity of Earthquake | Distance to Conestoga I-1 (miles) |
|---|---|---|---|---|---|---|
| 3/30/2019 | 2.9 | 4.0 | -104.631 | 40.4634 | 4.4 miles NE of Greeley, CO | 75 |
| 11/6/2016 | 3.0 | 4.2 | -104.6214 | 40.4557 | 5 miles ENE of Greeley, CO | 75 |
| 11/6/2016 | 2.7 | 4.3 | -104.6208 | 40.4576 | 5 miles ENE of Greeley, CO | 75 |
| 8/23/2016 | 2.6 | 6.1 | -104.7029 | 40.5055 | 1.2 miles SSE of Eaton, CO | 75 |
| 6/23/2014 | 2.5 | 3.1 | -104.5397 | 40.4414 | 3.7 miles NNE of Kersey, CO | 71 |
| 6/1/2014 | 3.2 | 0.7 | -104.6079 | 40.4674 | 5.6 miles NNW of Kersey, CO | 75 |
| 8/9/1967 | 5.5 | 6.2 | -104.661 | 39.957 | 4.4 miles SE of Lochbuie, CO | 100 |
| 9/14/1965 | 3.6 | 3.1 | -104.6 | 39.9 | 9.3 miles SE of Lochbuie, CO | 100 |
| 12/5/1962 | 3.8 | 20.5 | -104.6 | 39.9 | 9.3 miles SE of Lochbuie, CO | 100 |

*NAD83

In their comprehensive study of Nebraska's historical seismicity, Filina et al. (2018) generated an earthquake database for Nebraska and its neighboring states. This database included earthquakes from the USGS online earthquake catalog,[19] the International Seismological Centre (ISC) Bulletin,[20] the North American Moment Tensor catalog from Saint Louis University (SLU),[21] older Nebraska earthquake catalogs (Rothe and Lui, 1983; Burchett, 1990) and articles from local newspapers (the Lincoln Journal Star). This study shows that the WNS Hub AoR is located in a region with very low earthquake activity in magnitude and occurrence and minimal seismicity risk. The most recent clusters of earthquakes with magnitudes between 2.6 and 4.1 were more than 200 miles from the AoR.

### *2.6.2 Seismic Risk*

The USGS released an updated National Seismic Hazard Model (NSHM) in 2023 to improve earthquake-resilient construction in the United States (Petersen et al., 2023; **Figure 2.52**). This

[19] https://earthquake.usgs.gov
[20] http://www.isc.ac.uk
[21] http://www.eas.slu.edu/eqc/

probabilistic model incorporates all known earthquake sources, their distances to sites, and other seismological and geological information to project the potential maximum expected ground motions in an area over 10,000 years. The model predicts less than ten occurrences of "damaging earthquake shaking" will occur within the AoR over this period. Thus, the AoR is in a region of the United States that is very unlikely to be impacted by damaging earthquakes.

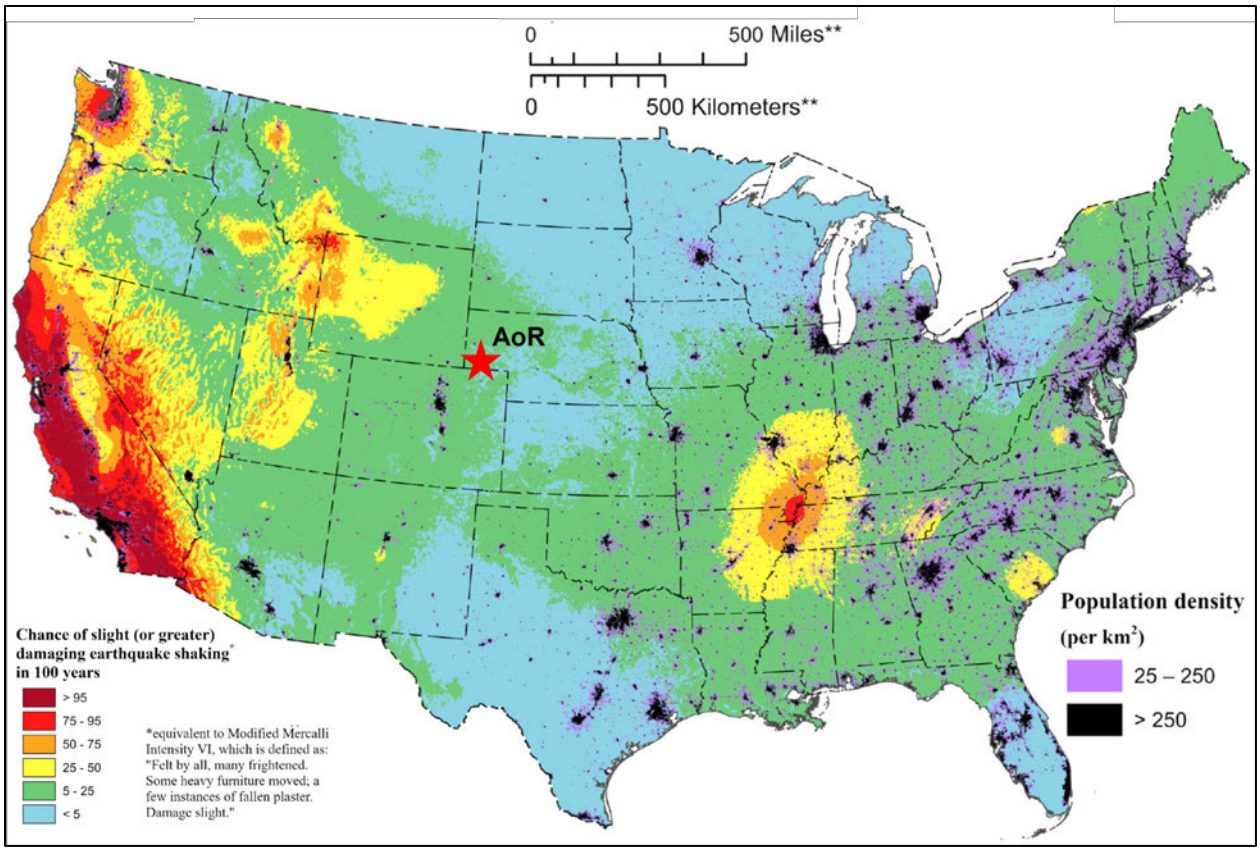


Figure 2.52—Map showing the chance of a slight (or greater) damaging earthquake shaking in 100 years from the 2023 NSHM (after Petersen et al., 2023). The red star indicates the location of the AoR.

## 2.7 Hydrologic and Hydrogeologic Information [40 CFR 146.82(a)(3)(vi), 146.82(a)(5)]

### *2.7.1 Hydrostratigraphy and Underground Sources of Drinking Water*

Following a review of major aquifers, minor aquifers, marginal aquifers, and aquitards identified in (Miller and Appel, 1997), Diving and Sibray (2017), Bartos et al. (2021), Wildgust et al. (2018), Taucher et al. (2013), Sibray et al. (2020), and Korus and Joeckel (2011), the High Plains Aquifer (HPA) is the primary USDW, and likely lowermost, in the AoR. The HPA is composed of the following hydrogeologic units:

- Quaternary unconsolidated deposits
- Ogallala Formation
- Arikaree Formations
- White River Formation (including the Brule and Chadron members)

A comprehensive review of the above publications indicates that the HPA is the lowermost freshwater aquifer at the proposed injection location. The formations that comprise the HPA serve as the primary aquifers for water wells within the AoR. Proper USDW designations of potential hydrogeologic units from the review are summarized in the stratigraphic column in **Figure 2.12**. **Figure 2.53** displays the important aquifers across Nebraska, showing the HPA as the primary source within the AoR.

**Figure 2.21** shows the water table depth (with sea level datum) for the HPA. The direction of groundwater flow is indicated by the blue arrows, showing a general easterly flow direction. A more detailed map on the base of the HPA and an associated geologic cross-section can be found in **Figure 2.54** and **Figure 2.55** from Sibray et al. (2020). Sibray et al.'s (2020) study utilized 2,097 logs across the HPA to construct a regional base surface for the HPA.

A map of all local water well locations and their associated total depths is shown in **Figure 2.56**.

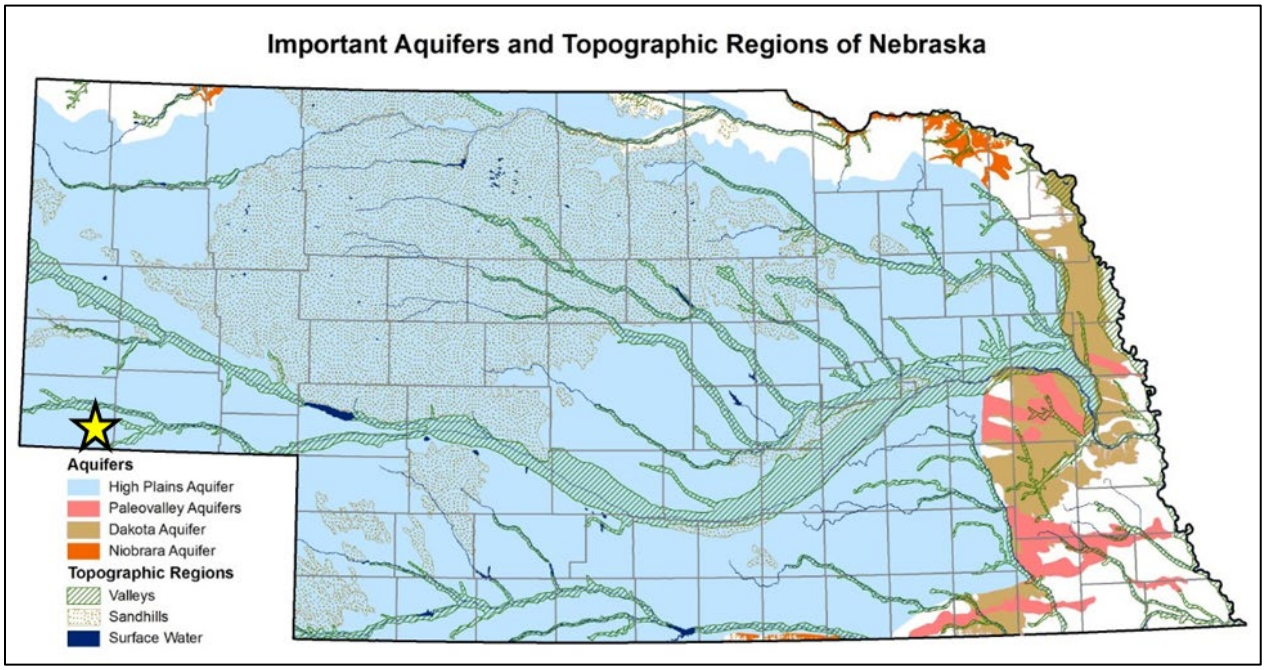


Figure 2.53—Map of important aquifers and topographic regions of Nebraska (after Korus and Burbach, 2009, p. 3). The yellow star indicates the location of AoR.

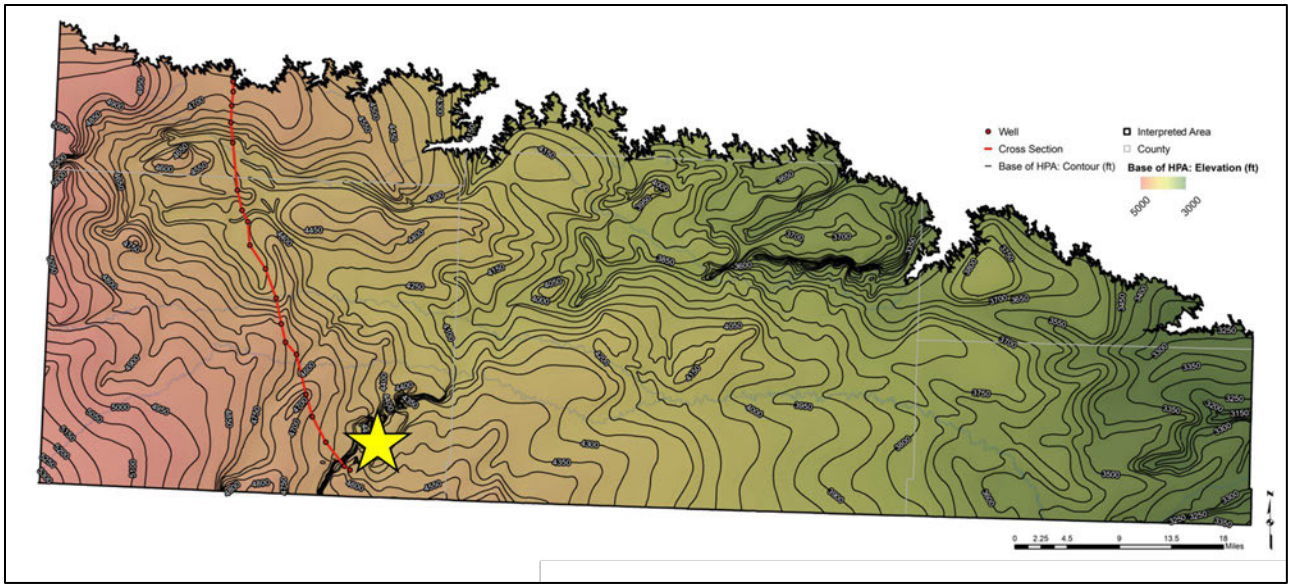


Figure 2.54—Colored contour map of the base of the High Plains aquifer (after Sibray et al., 2020). The yellow star denotes the approximate location of the Conestoga I-1, and the red line is the path of the cross-section shown in **Figure 2.55**.

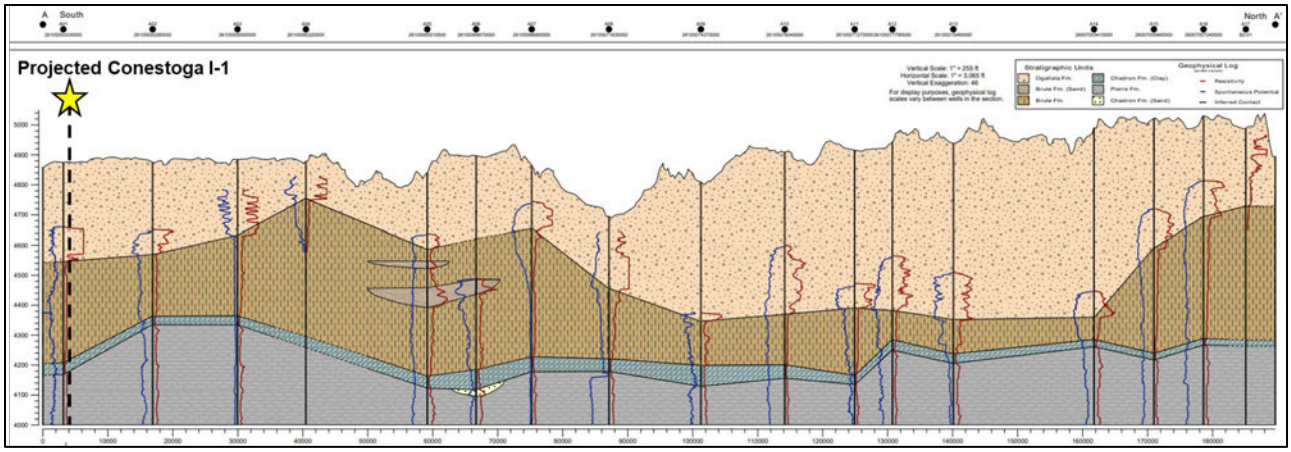


Figure 2.55—Geologic cross-section (south-north) of the High Plains Aquifer across the southern panhandle of Nebraska, showing the location of the proposed Conestoga I-1 well (after Sibray et al., 2020).

General lithologic descriptions of hydrogeologic units are provided along with supporting information to determine if the zones meet the criteria for designation as a USDW, as defined in 40 CFR 144.3. Descriptions and regional designations are based on work performed by Taucher et al. (2013) unless otherwise noted. Additional discussions and data regarding the criteria for USDW designation can be found in the summary following the subsequent descriptions.

### *2.7.1.1 High Plains Aquifer System*

The USGS groups the White River, Arikaree, and Ogallala formations, as well as any Quaternary deposits, into the "High Plains Regional Aquifer System" or "Tertiary Aquifer System" (Brendecke and Hinckley, 2014). Reported data on containing formations may be specific or generalized to one of these nomenclatures. These aquifer systems and formations are USDWs and

likely the lowest USDW within the AoR. Openhole logging, petrophysical analysis, and fluid analysis will be conducted on the underlying, likely saline aquifers, to improve the modeling of the WNS Hub and ensure the protection of all USDWs. The base of the High Plains aquifer is estimated to be at [redacted]) at the WNS Hub location (**Figure 2.54**).

*Major Aquifer: Quaternary Alluvium and Terrace Deposits*

The Quaternary alluvium in this region consists of highly permeable, uncemented, well-sorted sand, silt, and gravel stream deposits primarily from the Ogallala Formation. The alluvium varies in thickness from 60 to 200 ft (Babcock et al., 1952). This unit is not considered a major water source for high-capacity wells as it is generally thin throughout this region. The alluvium provides the important function of capturing water to recharge the underlying Brule Formation (Brendecke and Hinckley, 2014). This aquifer is anticipated to be present at the WNS Hub and is a USDW.

*Major Aquifer: Ogallala Aquifer*

The Tertiary Ogallala Formation consists of sand, gravel, and poorly to moderately sorted calcium-carbonate cemented sandstone and unconformably overlies the Arikaree Formation or Brule Formation. The Ogallala Formation was deposited in a fluvial environment that also included eolian and lacustrine settings. The Ogallala Formation is the principal geologic unit in the High Plains Aquifer that provides water to domestic and stock wells, with yields to wells dependent on local geology (Babcock et al., 1952). Water levels vary from land surface to greater than 250 ft (Brendecke and Hinckley, 2014). This aquifer is anticipated to be present at the WNS Hub and is a USDW.

*Major Aquifer: Arikaree Aquifer*

The Tertiary Arikaree Formation includes very fine to fine-grained, friable, volcaniclastic sandstones, conglomerates, and siltstone that is up to 400 ft thick in outcrop and pinches out to the southeast. The Arikaree was deposited in a fluvial and eolian environment. It is topographically high with only the lower part of the formation becoming saturated with water. It is considered capable of yielding moderate amounts of water to wells but is not typically the target of high-capacity wells (Brendecke and Hinckley, 2014). The Arikaree is a USDW if encountered at the WNS Hub.

*Marginal Aquifer: White River Aquifer*

The White River Aquifer is commonly subdivided into the upper “Brule Aquifer” and the lower “Chadron Aquifer.” The Brule and Chadron sandstone aquifers are restricted to thin, highly permeable sand lenses deposited as alluvial valley fill within the White River Group.

The Chadron aquifer is utilized in western Nebraska and is present in southwestern South Dakota, eastern Wyoming, and northeastern Colorado (Devine and Sibray, 2017). It is overlain by a regional aquitard, also part of the “Chadron Formation,” consisting of greenish bentonitic clay and some white, reddish, and yellowish clays.

There are currently about 163 active registered wells completed in the Chadron aquifer. These wells are used for domestic, livestock, and irrigation purposes. As of 2015, 51 registered irrigation wells were screened across other units of the High Plains Aquifer and the Chadron Aquifer (Devine

and Sibray, 2017). The average depth of Chadron aquifer wells is 353 ft, with an average depth to water of 144 ft. The average depth of Brule aquifer wells is 246 ft, with an average depth to water of 73 ft.

Recharge of the Brule and Chadron aquifers is thought to occur near outcrops in eastern Wyoming, with discharge occurring to the east. The water quality of the Chadron aquifer is generally poor, with TDS values averaging 750 mg/L in Scotts Bluff and southern Sioux counties. The water quality of the Brule aquifer is generally good, with low TDS values reported in Cheyenne County, NE (Steele et al., 2007).

*Aquitard: White River Aquitard*

The Tertiary White River Formation is composed of partially consolidated to consolidated argillaceous volcaniclastic mudrocks, including siltstone, mudstone, and claystone. The diagenesis devitrified White River volcaniclastic sediments over most of the region, converting the other clay species to montmorillonite and kaolinite. These clay species are known for their profound confining properties and act as an aquitard within the formation (Taucher et al., 2013).

The White River Formation is commonly subdivided into the upper "Brule" and lower "Chadron" members. The productive freshwater aquifer portion of the White River is found within localized permeable sand lenses within the Brule and Chadron, but the majority of the lithology is composed of clay and silt that acts as an aquitard to lateral and vertical flow outside of isolated aquifer sand bodies. The White River aquifer is anticipated to be present at the WNS Hub and is a USDW.

#### *2.7.1.2 Lance Aquifer*

The Lance Formation is Upper Cretaceous in age. Aquifers of the Lance are found within fine- to medium-grained permeable sandstones interbedded with low-permeability gray shale, black carbonaceous shale, and coal (Brendecke and Hinckley, 2014). The gross thickness of the Lance Formation ranges from 200 feet in eastern Laramie County, Wyoming, to zero feet in the western portion of Kimball County, Nebraska (Brendecke and Hinckley, 2014; Bartos et al., 2021). The aquifers are used for stock or domestic purposes due to poor water quality and moderate yields (Taucher et al., 2013). Similar to the Fox Hills, the Lance aquifer is not anticipated to be present at the WNS Hub.

#### *2.7.1.3 Fox Hills Aquifer*

The Fox Hills Formation is Upper Cretaceous in age and composed of friable sandstone interbedded with dark sandy shale. Sandstone beds are typically gray to white or yellow to brown. The thickness ranges from 40 to 250 ft in Laramie County, Wyoming (Brendecke and Hinckley, 2014); however, the Fox Hills appears to thin across Kimball County, NE, eventually pinching out west of the AoR (Bartos et al., 2021; Sibray et al., 2020). In the unlikely event that the Fox Hills aquifer is present at the WNS Hub and contains water with TDS concentrations below 10,000 mg/L, it would likely be considered the lowermost USDW.

#### *2.7.1.4 Pierre, Niobrara, Carlile, Greenhorn, Huntsman, and Mowry Aquitards*

Pierre, Niobrara, Carlile, Greenhorn, Huntsman, and Mowry formations are thick, regionally extensive, confining units that prevent groundwater from flowing between or into aquifers due to

reduced vertical hydraulic conductivity. The Pierre Formation is dark-gray shale with interbedded thin to moderately thick sandstone beds. The Niobrara is dark-gray calcareous shale with light-colored limestone, chalk, and sandstone interbeds. The Carlile, Greenhorn, and Huntsman units are primarily shale with some limestone and sandstone. The Late Cretaceous Mowry is siliceous shale that ranges from dark gray to deep brown to black and contains numerous bentonite interbeds (Taucher et al., 2013). The section consists of low permeability aquitards; therefore, individual formations are not USDWs.

#### *2.7.1.5 Muddy Sandstone Aquifer*

The Early Cretaceous Muddy Sandstone ("J-Sand" or "Muddy-J") aquifer lies between the Huntsman and Skull Creek shales and is a fine- to medium-grained silty sandstone with buff to gray color. Permeability is low due to tight cementation and silty matrix; however, the formation has been found suitable for domestic, irrigation, and livestock use in some regions outside of the AoR (Taucher et al., 2013). The Muddy sandstone is an exempt aquifer in portions of adjacent counties in Wyoming and Colorado for Class II injection and is oil and gas bearing. The Muddy Sandstone is heavily drilled and exploited in Kimball County, including within the AoR, for oil and gas production.

#### *2.7.1.6 Skull Creek Aquitard*

The Early Cretaceous Skull Creek Shale is described as a dark gray to black shale with thin beds of sandstone, siltstone, and bentonite (Taucher et al., 2013). This zone functions as a low-permeability aquitard and, therefore, does not meet the criteria for USDW designation.

#### *2.7.1.7 Inyan Kara Aquifer (Minor)*

Minor aquifers were differentiated because they are thinner than major aquifers, more diverse in nature, yield less water, and are contained within relatively limited lateral extents.

The Early Cretaceous Inyan Kara/Dakota minor aquifer consists of rusty to light-gray sandstone and cherty-pebble conglomerate interbedded with variegated bentonitic claystone. The Inyan Kara group has a complicated naming convention due to regional unconformities within the section. Depending on the extent of local sand bodies, it can also be referred to as the Lakota, Dakota, Fall River, or Cloverly formations. The local log resolution of these discontinuous sandstone bodies is too thin to get an accurate petrophysically-derived salinity estimate. The Dakota is oil and gas bearing and an exempt aquifer in Kimball County, NE, and therefore is not a USDW.

Water chemistry changes within Inyan Kara group must be well understood to ensure proper protection of any potential USDWs. Therefore, site-specific stratigraphy and fluid chemistry of the Conestoga I-1 location will be confirmed via openhole logging, petrophysical analysis, and fluid analysis to confirm if any zones meeting the criteria of a USDW are present.

#### *2.7.1.8 Morrison Aquitard*

The Late Jurassic Morrison Formation consists of laterally discontinuous siltstones, marlstones, and claystones that occur in various dull colors. Intervals high in claystone and mudstone content represent the confining layers of the Morrison Formation. Minor aquifers of the Morrison are limited to thin, gray, silty-sandstone, and massive limestone beds where porosity tends to develop.

The Morrison can yield small quantities of water for stock or domestic use when a porous, permeable reservoir is present and saturated with adequate water (Love and Christiansen, 1985; Taucher et al., 2013).

Regional mapping performed by High Plains indicates the WNS Hub location will exclusively encounter confining shales within the Morrison Formation. No water wells within Kimball County penetrate the Morrison Formation. Silty sandstones associated with minor aquifers of the Morrison Formation are not anticipated to be encountered at the proposed Conestoga I-1 location; therefore, the Morrison is not a USDW within the AoR.

#### *2.7.1.9 Sundance Aquifer*

The Middle to Late Jurassic Sundance Formation primarily consists of light-tan sandstone with greenish-gray, glauconitic sandy shale, underlain by red to gray, non-glauconitic sandy shale. Aquifers occur within the intergranular porosity and permeability of well-sorted, well-rounded sandstone intervals (Lowry and Crist, 1967; Love and Christiansen, 1985; Taucher et al., 2013).

At the proposed injection site, the Sundance Formation thins and may pinch out on top of a major Triassic unconformity, exhibiting moderate to low-quality reservoir properties in offset well logs. Petrophysical log data indicates a highly interbedded siltstone and sandstone mix, resulting in low permeability. This makes the Sundance an unsuitable aquifer within the AoR and, therefore, is not designated as a USDW. Openhole logging, petrophysical analysis, and fluid analysis will be conducted on the Sundance to confirm the TDS of contained pore water and ensure the protection of USDWs.

#### *2.7.1.10 Chugwater Aquitard*

The Triassic Chugwater Formation consists of red siltstone and shale with a few strata of purple, yellow, and green; it also contains beds of gypsum, sandstone, and limestone. (Love and Christiansen, 1985). This zone is expected to be minimally present across the WNS Hub AoR, acts as a vertical and lateral barrier to flow, and is not a USDW.

#### *2.7.1.11 Goose Egg Aquitard (Upper Confining Zone)*

The Triassic Goose Egg Formation confining unit is composed of red sandstone and siltstone with interbeds of white gypsum/anhydrite, halite, and purple to white dolomite and limestone (Love and Christiansen, 1985). This zone is present across the WNS Hub AoR and acts as the upper confining unit to the proposed Lyons Formation injection zone. Therefore, the Goose Egg Formation is a confining interval and not a USDW.

#### *2.7.1.12 Lyons Formation – Major Saline Aquifer (Proposed Injection Zone)*

The hydrogeologic role of the Lyons Formation was not identified in the 2013 WWDC report. However, High Plains analyzed regional data from the USGS National Produced Water Geochemical Database[22] and found a strong trend of salinity increasing with depth and along the eastern flank of the basin. Freshwater is found only along the western edge of the DJ Basin, where meteoric recharge along outcrops adjacent to the Front Range plays a dominant role. To the east,

[22] Retrieved at: https://www.usgs.gov/data/us-geological-survey-national-produced-waters-geochemical-database-v23

salinity increases due to the presence of evaporites and brines in the Paleozoic section (**Figure 2.14**).

Petrophysical interpretation across the Lyons Formation estimates the WNS Hub location to have a range of salinity from 83,000 to 90,000 mg/L NaCl equivalent, classifying the Lyons as a highly saline to brine formation water. The Lyons is, therefore, not a USDW. Furthermore, Lyons water samples acquired from the Juniper M-1 characterization well indicated TDS concentrations of 120,000 to 200,000 mg/L, further supporting that the Lyons is not a USDW.

#### *2.7.1.13 Satanka Formation Aquitard (Lower Confining Zone)*

The Early-Permian Satanka confining unit consists of silty red shale and siltstone interbedded with fine-grained sandstone, gypsum, and anhydrite beds (Taucher et al., 2013). As the zone is a low permeability confining interval, the Satanka unit is not a USDW.

### *2.7.2 Springs*

No natural springs exist within the AoR. Data from the USGS 3D Hydrography Program dataset[23] and the USGS National Water Information System dataset[24] was reviewed to confirm the absence of documented springs.

### *2.7.3 Water Wells Within the Area of Review*

Water well locations were obtained from the Nebraska Registered Wells Inventory.[25] The records in this database are sourced from the Nebraska Department of Natural Resources.

There are [redacted] water wells identified that are located within the AoR (**Figure 2.56**). [redacted] A list of water wells within the AoR is provided in **3.4.1b_AoR Water Well List_NE_DNR-dist.xlsx**. Well files for all water wells within the AoR are provided in **3.4.1d_Water Well Files_NE_DNR.zip.**

[23] https://hydro.nationalmap.gov/arcgis/rest/services/3DHP_all/MapServer/20 - Accessed 7/26/2024
[24] https://maps.waterdata.usgs.gov/mapper/index.html - Accessed 7/26/2024
[25] https://www.nebraskamap.gov/datasets/groundwater-wells-dnr/explore - Accessed 7/26/2024

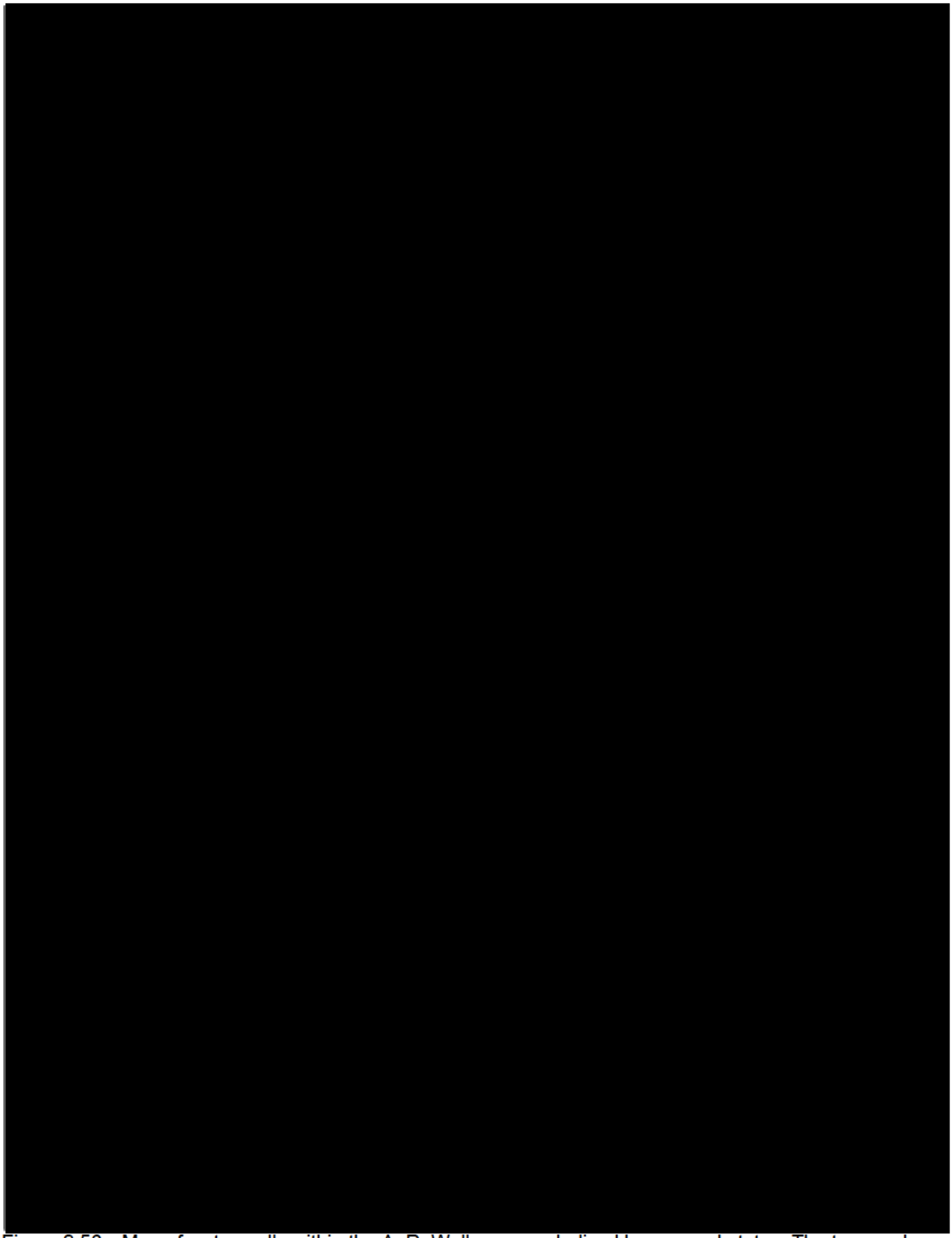

Figure 2.56—Map of water wells within the AoR. Wells are symbolized by use and status. The top number is the well registration number, and the bottom number is the well's measured depth.

## 2.8 Geochemistry [40 CFR 146.82(a)(6)]

Understanding the existing fluid- and solid-phase geochemistry of aquifers and confining layers is essential to evaluating the suitability of $CO_2$ storage sites. Identifying potential geochemical reactions that could affect $CO_2$ trapping mechanics, confining zone integrity, and storage capacity at the proposed Project site is essential.

Rock matrix mineralogy (core and wireline) and aquifer fluid samples have been collected from the stratigraphic characterization well, Juniper M-1, located approximately 41 miles west of the AoR. Conventional core was taken across the Sundance Sandstone, the first permeable unit above the upper confining zone, and the Goose Egg Formation. Core plugs were taken to evaluate porosity, permeability, and water content. Petrographic thin-section analysis, electron microscopy, and XRD were used to assess mineralogy and elemental composition. Elemental wireline logs were also acquired to verify vertical mineralogic variability in both cored and uncored sections of the Juniper M-1. The Juniper results indicate that the Lyons Formation has sufficient storage capacity for the planned $CO_2$ injection volumes. It also shows minimal potential for deleterious chemical interaction between the formation's mineralogy and the injectate, an insignificant risk of releasing trace elements, and is vertically bound by confining layers capable of effectively containing $CO_2$ over long periods.

These conclusions will be further confirmed via future site-specific data collection from dedicated wells drilled within the AoR. Solid- and fluid-phase geochemistry data will be collected from High Plains' proposed Conestoga I-1 during and post-drilling, providing baseline geochemical information within the proposed AoR (Refer to *Section 6.0—Pre-Operational Logging and Testing*). Wireline data, core, and fluid samples will be collected from the Lyons Sandstone in Conestoga I-1 to confirm its salinity and that it is not a USDW. Fluid samples from the Lyons Sandstone will also provide baseline geochemical information including the major ions, pH, alkalinity, total organic carbon, trace metals, stable isotopes, and evaluate $CO_2$ solubility.

No solid- or fluid-phase geochemical data currently exists in the injection or confining zones within the AoR. For solid-phase mineralogy prediction, High Plains is using petrophysical modeling of the reference wells (**Figure 2.40**) calibrated to the mineralogy seen in the core and logs of the Juniper M-1. For fluid-phase salinity prediction, salinity values are calculated from the Reference Wells assuming 100% brine saturation in the aquifers using the empirical relationship between total resistivity and porosity to calculate water resistivity (Rw) (Archie, 1941). Empirical relationships of temperature-resistivity-salinity were then used to derive salinity in equivalent NaCl concentrations (Warren and Smalley, 1994). High Plains will update the solid- and fluid-phase geochemical with data obtained from within the AoR when available.

Salinity may be derived in one of two ways: total dissolved solids (TDS) or equivalent NaCl concentrations. TDS is defined as the sum of all cations and anions in solution and is measured either by weighting the amount of solid present from a dried volume (e.g., EPA Method 160.1, SM2540 C -2015, ASTM D5907-13, USGS I-1750-85), from measuring ionic concentrations of a solution (sum of EPA Method 200.7or 200.8 from cation measurements with 300 and SM2320B for anion measurements), or by summing all ionic concentrations within solutions using ICP-AES or ICP-MS measurements from a single solution. Equivalent NaCl concentrations are a weighted sum of all ionic concentrations to convert them back to NaCl equivalent solutions with known resistivity (Warren and Smalley, 1994; Desai and Moore, 1969). Depending on the TDS concentration, the equivalent NaCl concentration may be greater than, equal to, or less than the

TDS concentration. This variation occurs because most ionic species have correction multipliers to convert to NaCl that are typically less than 1.0 (examples of variable multipliers by TDS can be found in Desai and Moore, 1969).

### *2.8.1 Fluid Chemistry*

**Table 2.13** summarizes High Plains' understanding of aquifer salinity within the AoR based on publicly available salinity data measurements and log-based NaCl equivalent estimations. Within a 20-mile radius, there is a large variability in the salinity concentrations reported in the available public data (**Table 2.13**). High Plains notes that in hydrocarbon-bearing rock, large pores have been filled with hydrocarbons, while smaller pores (at irreducible water saturation) may show a fresher TDS than their 100% brine-saturated counterparts. A Pickett Plot can be used to estimate brine salinity when hydrocarbons are present, but that salinity is only of brine-filled pores and does not give the complete picture of those aquifers. High Plains will collect and update this salinity data with the results from sampling and wireline calculations conducted within the AoR.

Table 2.13—Summary table of measured and calculated TDS values for relevant zones within a 20-mile buffer of the Conestoga I-1 well.

| Zone | Significance | Depth to Top of Zone (TVD, ft) | Measured TDS (mg/L)[1] | Log Calc. NaCl Equivalent [2] (mg/L) |
|---|---|---|---|---|
| HPA | USDW | [redacted] | [redacted] | [redacted] |
| Muddy Fm - J | Non-USDW | | | |
| Inyan Kara Group-Dakota Fm | Non-USDW | | | |
| Sundance Formation | First Permeable Zone Above the Confining Layer | | | |
| Lyons Sandstone | Injection Zone | | | |

Depths are the predicted Conestoga I-1 penetration depths inferred from the geomodel.
[1a] Wortmann, 2021; Bartos et al., 2021
[1b] Lab-measured TDS from wells within a 15-mile radius of the proposed Conestoga I-1 (USGS National Produced Waters Geochemical Database).
[2] Estimated from available wireline in the Reference Wells via relationships established in Schlumberger (2005).

#### *2.8.1.1 Injection Zone—Lyons Sandstone*

A search of the USGS National Produced Waters Geochemical Database[26] did not identify any fluid analysis for the Lyons Formation within the extent of the WNS Hub.

The last two columns of **Table 2.13** are log-derived equivalent NaCl concentrations from the Reference Wells. The range of salinities within column "Log Calc. Equivalent" is the salinity range calculated among the Lyons Formation sands in the Reference Wells. These predict the Lyons Formation to be relatively saline [redacted] mg/L). In the last column of **Table 2.13**, the

[26] retrieved at: https://www.usgs.gov/data/us-geological-survey-national-produced-waters-geochemical-database-v23

predicted salinities from each Reference Well are weighted by each well's distance from the Conestoga I-1 location. High Plains plans to collect Conestoga I-1 site-specific Lyons Formation fluid sample to confirm its TDS concentration.

#### *2.8.1.2 Upper Confining Layer—Goose Egg Formation*

No Goose Egg Formation fluid sample analyses are available from the DJ Basin. Within the AoR, the expected Goose Egg porosity ranges from [redacted] and permeability ranges from [redacted] mD, making it difficult to collect water samples using conventional sampling methods.

#### *2.8.1.3 First Permeable Zone Above the Confining Layer—Sundance Sandstone*

A search of the USGS National Produced Waters Geochemical Database[27] did not identify fluid analysis for the Sundance Formation within the AoR or near the WNS Hub. The calculated equivalent NaCl concentrations from the Reference Wells are [redacted] mg/L. The Sundance is not expected to be a USDW. High Plains plans to collect a site-specific Sundance Formation fluid sample from the Conestoga I-1 to confirm its TDS concentration and to verify that it is not a USDW.

#### *2.8.1.4 USDWs Within the Area of Review*

##### 2.8.1.4.1 Lowermost Underground Source of Drinking Water – High Plains Aquifer

A 2021 groundwater quality study by the University of Nebraska-Lincoln, using data from 642 irrigation wells penetrating the HPA across Nebraska, identified several groundwater wells in close proximity to the AoR (**Figure 2.57**). The TDS concentration in these wells was less than 443 mg/L (Wortmann, 2021).

[27] Retrieved at: https://www.usgs.gov/data/us-geological-survey-national-produced-waters-geochemical-database-v23

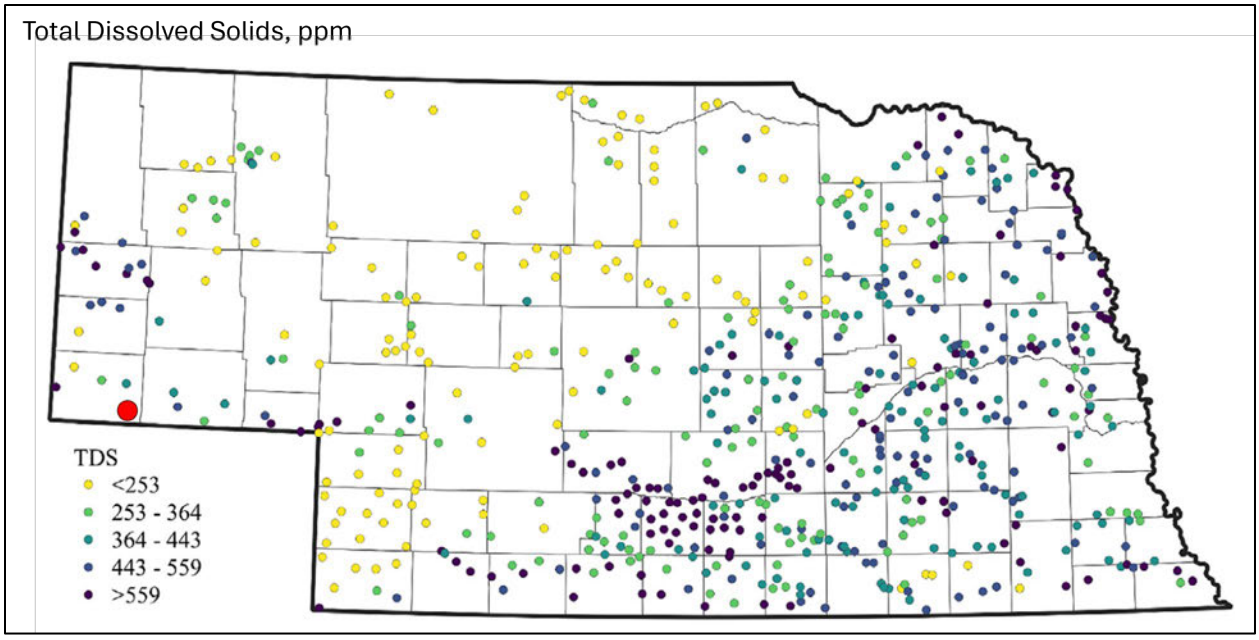


Figure 2.57—Map of total dissolved solids (TDS) concentrations (mg/L) from High Plains Aquifer (HPA) irrigation wells in Nebraska. The red circle shows the approximate location of the AoR. (after Wortmann, 2021).

2.8.1.5 Non-USDWs Within the Area of Review

2.8.1.4.2 Muddy Group (J Sand) – Non-USDW

Using a 10-mile search radius around the Injector well, a search of S&P Global-Enerdeq's database[28] found 172 wells that produced hydrocarbons from the J-Sand interval (**Appendix 2.1**). The closest producer is [redacted] miles away from the Conestoga I-1 location. Since this interval is not 100% brine-saturated (due to hydrocarbon presence), the equivalent NaCl salinity from wireline resistivity cannot be accurately calculated.

2.8.1.4.3 Inyan Kara Group, Dakota Formation – Non-USDW

The estimated equivalent NaCl concentrations from the three Reference Wells suggest a range of 21,000 to 23,000 (**Table 2.13**), classifying the Dakota as a highly saline formation.

### *2.8.2 Solid Phase Geochemistry*

#### *2.8.2.1 Injection Zone*

Conventional core was collected in the Juniper M-1 from the injection and confining zones. XRD, XRF, and thin section petrography were utilized to determine the mineralogic composition of the Lyons Sandstone. **Table 2.14** shows the mineralogy (from XRD) present within the Lyons Formation. Note that the XRD values provided are the average percent by weight for each mineral across all samples; therefore, the total of the averages will not equal 100%.

[28] https://www.spglobal.com/commodityinsights/en/ci/products/oil-gas-tools-enerdeq-browser.html

Table 2.14—Measured XRD within the Juniper M-1 Lyons Formation.

| Mineral | Lyons Sandstone (n = 31) Average wt% | Std Dev |
|---|---|---|
| QUARTZ | [redacted] | |
| K-FELDSPAR | | |
| PLAGIOCLASE | | |
| DOLOMITE | | |
| CHLORITE | | |
| ILLITE/MICA | | |
| CORRENSITE | | |
| HEMATITE | | |
| ANHYDRITE | | |

High Plains does not anticipate any adverse chemical reactions from $CO_2$ injection in the Lyons Sandstone. XRD results from Juniper M-1 indicate the Lyons does not contain trace metals that could be liberated from formation solids by the injectate. The framework grain mineralogy of the Lyons Sandstone is largely non-reactive or has very slow kinetics under injection conditions (Black et al. 2015; Palandri and Kharaka 2004). Further, High Plains utilized PHREEQC to model any potential chemical reactions in the Lyons Sandstone (refer to *Section 2.8.3*).

#### *2.8.2.2 Confining Layers*

No publicly available core data from the Goose Egg Formation were identified near the WNS Hub location. Therefore, modeling parameters were based on the data collected from the Juniper M-1. **Table 2.15** and **Table 2.16** show the mineralogy (from XRD) present within the Goose Egg Formation and Satanka Formation.

Once the Conestoga I-1 well has been approved, drilled, and evaluated, core-derived, site-specific mineralogy values will be collected and analyzed from the upper confining interval.

Table 2.15—Measured XRD within the Juniper M-1 Goose Egg Formation.

| Mineral | Goose Egg Formation (n = 31) Average wt% | Std Dev |
|---|---|---|
| QUARTZ | [redacted] | |
| K-FELDSPAR | | |
| PLAGIOCLASE | | |
| DOLOMITE | | |
| CHLORITE | | |
| ILLITE/MICA | | |
| CORRENSITE | | |
| HEMATITE | | |
| ANHYDRITE | | |

Table 2.16—Measured XRD within the Juniper M-1 Satanka Formation.

| Mineral | Satanka Formation (n = 9) Average wt% | Std Dev |
|---|---|---|
| QUARTZ | [redacted] | |
| K-FELDSPAR | | |
| PLAGIOCLASE | | |
| CALCITE | | |
| DOLOMITE | | |
| CHLORITE | | |
| ILLITE/MICA | | |
| CORRENSITE | | |
| HEMATITE | | |
| ANHYDRITE | | |

#### *2.8.2.3 First Permeable Zone Above Confining Layer - Sundance Formation*

No publicly available core data from the Sundance Formation was identified near the WNS Hub location. Therefore, modeling parameters were based on the data collected from the Juniper M-1. **Table 2.17** shows the mineralogy (from XRD) present within the Sundance Formation.

Table 2.17—Measured XRD within the Juniper M-1 Sundance Formation

| | Sundance Formation (n = 45) | |
|---|---|---|
| Mineral | Average wt% | Std Dev |
| QUARTZ | [redacted] | |
| K-FELDSPAR | | |
| PLAGIOCLASE | | |
| CALCITE | | |
| DOLOMITE | | |
| CHLORITE | | |
| ILLITE/MICA | | |
| HEMATITE | | |

#### *2.8.2.4 Underground Source of Drinking Water – High Plains Aquifer*

No publicly available core data or wireline logs for mineralogy determination from the High Plains Aquifer were identified near the WNS Hub location. Samples will be taken from a proposed USDW monitoring well prior to injection.

### *2.8.3 Geochemical Modeling*

This section summarizes the geochemical modeling used to determine the compatibility of the $CO_2$ stream, pore fluids, and host mineralogy of the injection and confining zones. A detailed geochemical report, including geochemical interactions, is provided in **Appendix 2.3—Geochemical Modeling Report**. This model was run for the site characterization well (Juniper M-1); it has not been updated with the numbers provided in the above sections for estimated salinity. It will be updated with site-specific data from the Conestoga I-1. However, the results are expected to be similar.

A geochemical analysis was performed to model potential interactions between the injected $CO_2$ stream, in-situ fluids, and minerals proximal to injection. Four models were run to evaluate independent mineral facies distributions identified within the Satanka, Lyons, Goose Egg, and Chugwater formations.

The brine composition used for the simulations is derived from water samples acquired from the Lyons Formation during the Juniper M-1 testing program. In the testing process, the well was perforated in the Lyons interval between the depths of 9,165 to 9,171 ft. SLB's Single-Phase Reservoir Sampler (SRS) tool was then placed at three depths while the well was pumped, resulting in samples from the target injection interval. A subset of anions and cations relevant to mineral-brine-$CO_2$ interactions are summarized for each sample in **Table 2.18.** The available analytical values were averaged for each mineral facies to create a composite brine composition that was used in each model (**Table 2.19**).

Data from 71 core plug samples obtained during the Juniper M-1 testing program across the injection and confining intervals were used in this analysis. Those samples were used in conjunction with XRF core data and elemental wireline logs to develop a predictive mineral volumes model from triple combo wireline data. The predicted Conestoga I-1 average mineralogy volumes (based on the predictive mineral model) are shown in **Table 2.20**.

Table 2.18—Composition of Lyons water samples.

| Formation | Depth (TVD, ft) | pH | TDS (mg/L) | $HCO_3$ (%) | $SO_4$ (%) | Cl (mg/L) | I (mg/L) | Ca (mg/L) | Fe (mg/L) | K (mg/L) | Mg (mg/L) | Na (mg/L) |
|---|---|---|---|---|---|---|---|---|---|---|---|---|
| [redacted] | | | | | | | | | | | | |

Table 2.19—Average brine composition by mineral facies.

| Mineral Facies | Facies Name | Depth (TVD, ft) | Strat Interval | pH | TDS (mg/L) | $HCO_3$ (%) | $SO_4$ (%) | Cl (mg/L) | I (mg/L) | Ca (mg/L) | Fe (mg/L) | K (mg/L) | Mg (mg/L) | Na (mg/L) |
|---|---|---|---|---|---|---|---|---|---|---|---|---|---|---|
| [redacted] | | | | | | | | | | | | | | |

Table 2.20—Mineral composition of facies clusters.

| Mineral Facies | Facies Name | Modeled Depth (TVD, ft) | Stratigraphic Interval | Quartz (wt%) | Dolomite (wt%) | K-spar (wt%) | Clay (wt%) | Anhydrite (wt%) |
|---|---|---|---|---|---|---|---|---|
| [redacted] | | | | | | | | |

The Lyons Formation models were evaluated at its average depth. The Goose Egg model was evaluated at the Goose Egg-Lyons interface. The Satanka model was evaluated at the Lyons-Satanka interface. Across all the models, the simulations show a net mineral change of less than 8%. Reactions begin to occur after a few seconds of contact and accelerate through the first several hundred years. From 1,000 to 10,000 years, the reactions reach equilibrium.

The largest constituent (quartz) in the Lyons injection interval shows net precipitation. However, within the minor constituents, anhydrite, k-feldspar, plagioclase (albite), and illite dissolve, while kaolinite and calcite precipitate. Mild net precipitation in the injection facies will reduce porosity over time, especially at the upper confining zone-injection zone interface. Geochemical modeling indicates that the net precipitation and alteration of illite to smectite at the Goose Egg-Lyons interface supports seal capacity over the course of injection.

The casing that will be exposed to the injection zone was selected to resist the potential corrosion caused by exposure to carbonic acid created by the interaction between $CO_2$, $O_2$, and brine in the injection formation. The use of acid-resistant casing will be sufficient to withstand the corrosive effects on the casing.

Four water samples were collected from the Lyons Formation between the perforated depths of 9,165 to 9,171 ft in the Juniper M-1 well. Analysis of the four samples were averaged and are provided in **Table 2.21.**

Table 2.21—Formation water chemistry from the injection formation.

| Parameter | Results (mg/L) |
|---|---|
| Alkalinity, as Bicarbonate ($HCO_3^-$) | [redacted] |
| Alkalinity, as Carbonate ($CO_3^{2-}$) | |
| Alkalinity, as Hydroxide ($OH^-$) | |
| Boron | |
| Barium | |
| Bromide | |
| Calcium | |
| Chloride | |
| Dissolved Inorganic Carbon (DIC) | |
| Dissolved Organic Carbon (DOC) | |
| Iron | |
| Lead | |
| Lithium | |
| Magnesium | |
| Potassium | |
| Sodium | |
| Sulfate | |
| Strontium | |
| TDS | |
| Zinc | |

The expected $CO_2$ stream composition at the WNS Hub is provided in **Table 2.21**.

Table 2.22—Expected $CO_2$ stream composition that will be injected into the Lyons Formation.

| Component | ppm | mol% |
|---|---|---|
| Carbon Dioxide ($CO_2$) | [redacted] | |
| Oxygen ($O_2$) | | |
| Nitrogen Oxides (NOx) | | |
| Total Hydrocarbons (as $CH_4$) (Maximum cricondentherm dew point of hydrocarbon mix -20°F) | | |
| Total Sulfur (S) | | |
| Water ($H_2O$) | | |
| Carbon Monoxide (CO) | | |

## 2.9 Other Information

Not applicable. No surface air and/or soil gas monitoring is proposed or planned by High Plains at this time.

## 2.10 Site Suitability

This section will demonstrate that the massive Lyons Sandstone has sufficient reservoir quality, thickness, and lateral continuity to support the proposed $CO_2$ injection volumes (27.1 million metric tons [Mt]). The confining layers, with thick interbedded low permeability mudstone and anhydrite beds, also have sufficient sealing capacity to support the injected column at the proposed injection rates and ensure continued isolation of the injected plume.

### *2.10.1 Structural and Tectonic Suitability*

The extent and structure of the DJ Basin and its tectonic setting make it an ideal location for $CO_2$ storage. The proposed injection site is located within the north-central portion of the DJ Basin. The geologic setting in this area of the DJ Basin is well defined, with thousands of wellbore penetrations from oil and gas exploration and production. Unlike the basin's western edge, which is characterized by significant faulting and tectonic uplift along the Front Range, this portion of the basin has not undergone significant deformation, with gently dipping formations and no significant faulting or tectonic activity. The Lyons Sandstone (injection zone) and overlying Goose Egg Formation (confining zone) dip less than one degree towards the west (**Figure 2.24 and Figure 2.27**). Well log correlation has not revealed any faults or open fractures in the Lyons or Goose Egg formations within or near the AoR.

No significant seismic hazards have been identified within the AoR, and no earthquakes with epicenters within the AoR have been recorded. According to the USGS Earthquake database,[29] no earthquakes are known to have occurred in the Nebraska portion of the DJ Basin. The most recent earthquake of magnitude 2.5 or greater near the AoR occurred approximately 158 miles northeast near Merriman, Nebraska, in July 2024, with a magnitude of 2.6. The closest earthquake near the AoR occurred approximately 75 miles southwest near Greeley, Colorado, in 2019, with a magnitude of 2.9. Therefore, the proposed injection site is at minimal risk of natural or induced seismicity, and no seismically resolvable faults were interpreted within or around the AoR. High

[29] https://earthquake.usgs.gov/earthquakes/map/?extent=-54.36776,-179.12109&extent=81.38765,-10.72266

Plains has thus determined that the AoR and surrounding area are considered structurally and tectonically suitable for the geologic storage of $CO_2$.

### *2.10.2 Storage Reservoir Suitability (Injection Zone)*

The proposed storage reservoir for the WNS Hub is the Lyons Formation. Sonnenberg and Weimer (1981) reviewed outcrops of the Lyons section near Lyons, Colorado, and described the formation as a well-sorted, fine-grained, eolian quartzose sandstone. Mapping and modeling conducted by High Plains indicate that the Lyons Formation is well-suited for geologic sequestration. This suitability is due to the presence of a regionally extensive sand body with sufficient porosity and permeability encased within equally extensive confining intervals. Representative properties of the Lyons sandstone at the WNS Hub location are listed in **Table 2.3** and, in *Section 2.4.1.1*, **Table 2.6**.

The Lyons Formation is a well-known saline aquifer, with regional measurements in some areas exceeding 200,000 TDS. At the proposed EWS Hub, High Plains anticipates a water salinity range of [redacted] mg/L NaCl equivalent, well above the 10,000 mg/L TDS threshold required for an aquifer to be classified as a USDW.

High Plains does not anticipate any adverse chemical reactions from $CO_2$ injection in the Lyons Sandstone. A detailed geochemical report, including geochemical interactions, is provided in **Appendix 2.3—Geochemical Modeling Report**.

#### *2.10.2.1 Storage Capacity of the Injection Zone*

The Lyons Formation is a highly porous and permeable basin-wide interval spanning thousands of square miles (**Figure 2.25**). As the formation is an open aquifer, there are no stratigraphic, structural traps, or spill points to use to define a storage area. Thus, the potential storage volume is primarily a function of the area where the operator desires the plume to be contained. The calculated storage volume estimated at increasing radii from the proposed injection well is provided in **Table 2.23**. These capacities are estimated based on a methodology after Bachu (2006) (**Equation 2.5**). Note that this method does not account for rock compressibility nor migration due to buoyancy; it is simply a volumetric analysis.

Equation 2.5—$CO_2$ storage volume calculation (after Bachu 2006).

$$V_{CO2} = (A \times H \times \emptyset \times (1 - Sw_{irr}) \times \rho_{CO2} \times EF) \times 10^{-6}$$

Where:

$V_{CO2}$ = $CO_2$ Storage Volume (Mt)
$A$ = area ($m^2$)
$H$ = net thickness (m)
$\emptyset$ = porosity (v/v)
$Sw_{irr}$ = irreducible water saturation
$\rho_{CO2}$ = density of $CO_2$ (reservoir conditions)
$EF$ = Efficiency Factor – defined here as the ratio of the volume of $CO_2$ injected to the net pore volume (pore volume excluding irreducible water) at the final storage pressure.

Solid-phase geochemical analysis of Lyons Formation core, as well as pore water chemistry collected from the Juniper M-1 well, coupled with geochemical modeling (*Section 2.8.3*), indicated no significant potential for interactions between the carbon dioxide steam and the formation or dissolved minerals that could impact storage capacity.

Table 2.23—Potential $CO_2$ storage volumes within the Lyons Formation inside increasing radii calculated from the proposed injection well. At two miles, the Lyons Formation has the capacity to store more $CO_2$ than the amount proposed by this Project.

| Radius (miles) | Area ($m^2$) | Gross Thickness (m) | Net Thickness (m) | Avg. Porosity (v/v) | $Sw_{irr}$ (%) | Net Volume ($m^3$) | $CO_2$ Density (tonnes/$m^3$) (supercritical @ res cond.) | Theoretical Stor. Volume (tonnes) | Est. Efficiency Factor (EF, %) | Storage Volume (Mt) | Multiple of Anticipated Inj. Volume |
|---|---|---|---|---|---|---|---|---|---|---|---|
| 1 | 8,136,681 | [redacted] | | | | 62,462,694 | 0.4325 | 27,015,115 | [redacted] | 14 | 0.5x |
| 2 | 32,546,723 | | | | | 249,850,777 | 0.4325 | 108,060,461 | | 54 | 2.0x |
| 3 | 73,230,127 | | | | | 562,164,249 | 0.4325 | 243,136,038 | | 122 | 4.5x |
| 4 | 130,186,892 | | | | | 999,403,110 | 0.4325 | 432,241,845 | | 216 | 7.8x |
| 5 | 203,417,019 | | | | | 1,561,567,359 | 0.4325 | 675,377,883 | | 338 | 12.5x |

Based on the calculation results, which use conservative inputs for $Sw_{irr}$ [redacted]%) and Efficiency Factor [redacted]%), within a two-mile radius of the proposed injection well, the Lyons Formation has the capacity to store approximately twice the anticipated volume of $CO_2$ to be injected by this project (27.1 Mt). The available volume increases exponentially with distance from the injection well. Simulation results indicate that the Efficiency Factor used here may be a significant underestimation.

### *2.10.3 Confining Zone Suitability*

#### *2.10.3.1 Upper Confining Zone Suitability (Goose Egg Formation)*

The Goose Egg Formation is the upper confining zone at the WNS Hub location. The lithology consists of thick siltstone and mudstone beds interbedded with massive anhydrite, with an average thickness of [redacted] ft at the WNS Hub site. The nature of deposition of the Goose Egg across a broad low-relief evaporite basin created a continuous regional seal across a majority of the DJ Basin with minor lithologic variations. High Plains petrophysical and seismic analysis further indicates that the Goose Egg is a tight low-permeability zone that is regionally extensive, without any observed faults or other vertical migration pathways. Geochemical analysis from core collected from the Juniper M-1 characterization wells, coupled with geochemical modeling (see *Section 2.8.3*), indicates no concerns for adverse interactions with the formation and the carbon dioxide stream that could impact confinement.

The Goose Egg Formation upper confining zone exhibits robust mechanical integrity, ensuring its effectiveness as a top seal for geologic sequestration. Capillary pressure data from mercury injection capillary pressure (MICP) tests show that the Goose Egg Formation has very low permeability, with Swanson permeability values under 0.0004 mD and high mercury entry pressures. These characteristics, combined with the formation's ability to retain a significant $CO_2$ column height (calculated to be approximately [redacted] ft), indicate a low risk of a breach, supporting the mechanical integrity of the zone.

In summary, Goose Egg has been thoroughly characterized as a robust confining zone. While no secondary confinement is necessary to ensure USDW protection, in addition to the Goose Egg, approximately [redacted] ft of overlying, low permeability shale formations through the Upper Cretaceous separate the Lyons injection zone from the lowermost USDW (High Plains Aquifer).

#### *2.10.3.2 Lower Confining Zone Suitability (Satanka Formation)*

The Satanka Formation is the lower confining zone at the WNS Hub location. Lithologies of the Satanka consist primarily of red siltstones and mudstones and exhibit low porosities and permeabilities in wireline log and core data. The Satanka was deposited in an arid environment across a large low-angle salt-pan playa, and High Plains regional mapping has confirmed the Satanka (with thicknesses of 60 to 160 ft TVT in the basin and [redacted] ft TVT in the AoR) is a regionally extensive formation of low permeability. These characteristics make the Santanka a suitable lower confining zone for the injection zone.

## 2.11 References

Adams, J., and Patton, J., 1979, Sebkha-Dune Deposition in the Lyons Formation (Permian) Northern Front Range, Colorado: *The Mountain Geologist*, v. 16, no. 2, p. 47-57.

Ajayi, T., Gomes, J.S., and Bera, A., 2019, A review of CO2 storage in geological formations emphasizing modeling, monitoring and capacity estimation approaches: *Petroleum Science*, v. 16, no. 5, p. 1028–1063, https://doi.org/10.1007/s12182-019-0340-8.

Anderson, R.A., Ingram, D.S., and Zanier, A.M., 1973, Determining fracture pressure gradients from well logs: *Journal of Petroleum Technology*, v. 25, no. 11, p. 1259–1268, https://doi.org/10.2118/4135-PA.

Archie, G.E., 1941, The electrical resistivity log as an aid in determining some reservoir characteristics: *Transactions of the AIME*, v. 146, p. 54-62, https://doi.org/10.2118/942054-G.

Babcock, H.M., Visher, F.N., and Durum, W.H., 1952, Reconnaissance of the geology and ground-water resources of the Pumpkin Creek area, Morrill and Banner Counties, Nebraska, with a section on the chemical quality of the water: U.S. Geological Survey Circular 156, 40 p., https://doi.org/10.3133/cir156.

Bachu, S., and Adams, J.J., 2003, Sequestration of CO2 in geological media in response to climate change: capacity of deep saline aquifers to sequester CO2 in solution: *Energy Conversion and Management*, v. 44, no. 20, p. 3151–3175, https://doi.org/10.1016/S0196-8904(03)00101-8.

Bachu, S., 2006, The Capacity for Carbon Dioxide Storage in Oil and Gas Pools in Northeastern Alberta: Alberta Energy Research Institute, 120 p.

Bartos, T.T., Galloway, D.L., Hallberg, L.L., and others, 2021, Geologic and hydrogeologic characteristics of the White River Formation, Lance Formation, and Fox Hills Sandstone, northern greater Denver Basin, southeastern Laramie County, Wyoming: U.S. Geological Survey Scientific Investigations Report 2021–5020, 219 p., https://doi.org/10.3133/sir20215020.

Belitz, K., and Bredehoeft, J.D., 1988, Hydrodynamics of Denver Basin: explanation of subnormal fluid pressures: *AAPG Bulletin*, v. 72, no. 11, p. 1334-1359, https://doi.org/10.1306/703C999C-1707-11D7-8645000102C1865D.

Birchall, T., Senger, K., and Swarbrick, R., 2022, Naturally occurring underpressure – a global review: *Petroleum Geoscience*, v. 28, p. 1-22, https://doi.org/10.1144/petgeo2021-051.

Black, J., Carroll, S., and Haese, R., 2015, Rates of mineral dissolution under CO2 storage conditions: *Chemical Geology*, v. 399, p. 134-144, https://doi.org/10.1016/j.chemgeo.2014.09.020.

Brendecke, C.M., and Hinckley, B.S., 2014, Hydrogeologic Study of the Laramie County Control Area: Final Report, Prepared for the Wyoming State Engineer's Office, March 2014, 52 p.

Brigatti, M.F., and Poppi, L., 1984, Crystal Chemistry of Corrensite: A Review: *Clays and Clay Minerals*, v. 32, no. 5, p. 391-399, https://doi.org/10.1346/CCMN.1984.0320507.

Brown, M.R.M., Ge, S., Sheehan, A.F., and Nakai, J.S., 2017, Evaluating the effectiveness of induced seismicity mitigation: Numerical modeling of wastewater injection near Greeley, Colorado: *Journal of Geophysical Research: Solid Earth*, v. 122, p. 6569–6582, accessed August 22, 2024, https://doi.org/10.1002/2017JB014456.

Burberry, C.M., Joeckel, R.M., Korus, J.T., and Peppers, M.H., 2014, Multiphase deformation of the Paleozoic and Mesozoic units within the Panhandle of Nebraska: Paper presented at AAPG Rocky Mountain Section Meeting, Denver, Colorado, July 20-22, 2014.

Burchett, R.R., 1990, Mineral Facts for Nebraska: Nebraska Geological Survey Report.

Burk, C.A., and Thomas, H.D., 1956, The Goose Egg Formation (Permo-Triassic) of Eastern Wyoming: Geological Survey of Wyoming, Report of Investigations No. 6.

Campbell, J.A., 1963, Permo-Triassic Red Beds Northern Denver Basin: Rocky Mountain Association of Geologists, *Geology of the Northern Denver Basin and adjacent uplifts*, p. 105-110.

Carlson, M.P., 2003, A basement framework hypothesis for the tectonic architecture and geologic history of the western mid-continent, USA: Paper presented at the AAPG Hedberg Conference on Late Paleozoic Tectonics and Hydrocarbon Systems of Western North America – The Greater Ancestral Rocky Mountains, Vail, Colorado, July 21-26, 2002, AAPG Search and Discovery Article #90012, 4 p.

Clayton, J.L., and Swetland, P.J., 1980, Petroleum generation and migration in the Denver Basin: *AAPG Bulletin*, v. 64, no. 10, p. 1613-1633.

Condon, S.M., 2005, Geologic studies of the Platte River, south-central Nebraska and adjacent areas—geologic maps, subsurface study, and geologic history: U.S. Geological Survey Professional Paper 1706, 55 p., https://doi.org/10.3133/pp1706.

Crone, A.J., and Wheeler, R.L., 2000, Data for Quaternary faults, liquefaction features, and possible tectonic features in the Central and Eastern United States, east of the Rocky Mountain Front: U.S. Geological Survey Open-File Report 00-260, 82 p., https://doi.org/10.3133/ofr00260.

Davidson, J., Siratovich, P., Wallis, I., Gravely, D., and McNamara, D., 2012, Quantifying the stress distribution at the Rotokawa Geothermal Field, New Zealand: Paper presented at the New Zealand Geothermal Workshop 2012, Auckland, New Zealand, November 19-21, 2012, doi: 10.13140/RG.2.1.3565.2088.

Desai, K.P., and Moore, E.J., 1969, Equivalent NaCl determination from ionic concentrations: *The Log Analyst*, v. 10, no. 3, p. 12-21.

Diffendal, R.F. Jr., and Diffendal, A.P., 2005, Review of Lewis and Clark and the Geology of the Great Plains and Lewis and Clark and the Geology of Nebraska and Parts of Adjacent States: Nebraska Geological Survey Report.

Divine, D.P., and Sibray, S.S., 2017, An overview of secondary aquifers in Nebraska: Lincoln, Nebraska, Conservation and Survey Division, 44 p.

Downard, A.D., 2021, Faulting and fracturing across the DJ Basin: Impacts on production from Hereford Field, Northern Colorado: M.S. thesis, Colorado School of Mines, 156 p.

Drake, R.M. II, Brennan, S.T., Covault, J.A., Blondes, M.S., Freeman, P.A., Cahan, S.M., DeVera, C.A., and Lohr, C.D., 2014, Geologic framework for the national assessment of carbon dioxide storage resources: Denver Basin, Colorado, Wyoming, and Nebraska: U.S. Geological Survey, Open-File Report 2012-1024G, https://doi.org/10.3133/ofr20121024G.

Eaton, B.A., 1969, Fracture gradient prediction and its application in oilfield operations: *Journal of Petroleum Technology*, v. 21, no. 10, p. 1353–1360, https://doi.org/10.2118/2163-PA.

Filina, I.Y., Searls, M., and Burberry, C.M., 2018, Seismicity in Nebraska and adjacent states: The historical perspective and current trends: *The Mountain Geologist*, v. 55, p. 217-229, https://doi.org/10.31582/rmag.mg.55.4.217.

Garbarini, G.S., and Veal, H.K., 1968, Potential of the Denver Basin for disposal of liquid wastes: U.S. Geological Survey, United States.

Garrity, C.P., and Soller, D.R., 2009, Database of the geologic map of North America—Adapted from the map by J.C. Reed, Jr., and others (2005): U.S. Geological Survey Data Series 424, accessed August 22, 2024, https://doi.org/10.3133/ds424.

Hagadorn, J.W., Whiteley, K.R., Lahey, B.L., Henderson, C.M., and Holm-Denoma, C.S., 2016, The Permian–Triassic transition in Colorado, in Keller, S.M., and Morgan, M.L., eds., Unfolding the geology of the West: Geological Society of America Field Guide 44, p. 73–92, https://doi.org/10.1130/2016.0044(03).

Heidbach, O., Rajabi, M., Reiter, K., Ziegler, M.O., and the WSM Team, 2016, World Stress Map Database Release 2016: GFZ Data Services, https://doi.org/10.5880/WSM.2016.001.

Higley, D.K., and Cox, D.O., 2007, Oil and gas exploration and development along the front range in the Denver Basin of Colorado, Nebraska, and Wyoming, in Higley, D.K., ed., Petroleum systems and assessment of undiscovered oil and gas in the Denver Basin Province, Colorado, Kansas, Nebraska, South Dakota, and Wyoming—USGS Province 39: U.S. Geological Survey Digital Data Series DDS–69–P, ch. 2, 41 p.

Hobza, C.M., and Sibray, S.S., 2014, Hydrostratigraphic interpretation of test-hole and borehole geophysical data, Kimball, Cheyenne, and Deuel Counties, Nebraska, 2011–12: U.S. Geological Survey Open-File Report 2014–1103, 45 p., https://dx.doi.org/10.3133/ofr20141103.

Hovorka, S.D., Romero, M.L., Warne, A.G., Ambrose, W.A., Tremblay, T.A., Trevino, R.H., and Sasson, D., 2003, Sequestration of greenhouse gases in brine formations: University of Texas, Bureau of Economic Geology.

Kampman, N., Bickle, M., Wigley, M., and Dubacq, B., 2014, Fluid flow and CO2–fluid–mineral interactions during CO2-storage in sedimentary basins: *Chemical Geology*, v. 369, p. 22–50, https://doi.org/10.1016/j.chemgeo.2013.11.012.

Kendigelen, O., 2016, Facies distribution, its implications for climate signals, and hydrocarbon potential of the Permian Lyons Sandstone, Front Range Basin, northern Colorado, USA: M.S. thesis, Colorado School of Mines, Golden, Colorado.

Kendigelen, O., Egenhoff, S., Matthews, W.A., Holm-Denoma, C.S., Whiteley, K.R., Gent, V.A., Longman, M.W., and Hagadorn, J.W., 2023, The edge of a Permian erg: Eolian facies and provenance of the Lyons Sandstone in northern Colorado: *Rocky Mountain Geology*, v. 58, no. 2, p. 57-82, https://doi.org/10.24872/rmgjournal.58.2.57.

Korus, J.T., and Burbach, M.E., 2009, Nebraska Statewide Groundwater-Level Monitoring Report: University of Nebraska-Lincoln, Conservation and Survey Division, School of Natural Resources, Nebraska Water Survey Paper Number 76, 76 p.

Korus, J.T., and Joeckel, R.M., 2011, Generalized geologic and hydrostratigraphic framework of Nebraska, 2011, ver. 2: University of Nebraska-Lincoln, Conservation and Survey Division, School of Natural Resources, Institute of Agriculture and Natural Resources, Geologic Maps and Charts (GMC) 38.

Korus, J.T., and Joeckel, R.M., 2022, Sandstone-body geometry and hydrostratigraphy of the northern High Plains Aquifer system, USA: *Quarterly Journal of Engineering Geology and Hydrogeology*, v. 55, 18 p.

Lee, M.-K., and Bethke, C.M., 1994, Groundwater flow, late cementation, and petroleum accumulation in the Permian Lyons Sandstone, Denver Basin: *AAPG Bulletin*, v. 78, no. 2, p. 217–237.

Levandowski, D., Kaley, M., and Smalley, R., 1973, Cementation in the Lyons Sandstone and its role in oil accumulation, Denver Basin, Colorado: *American Association of Petroleum Geologists Bulletin*, v. 57, no. 11, p. 2217–2244.

Li, S., and Purdy, C., 2010, Maximum horizontal stress and wellbore stability while drilling: modeling and case study: *SPE Paper* 139280, https://doi.org/10.1144/GSL.MEM.1994.015.01.03.

Love, J.D., and Christiansen, A.C., comps., 1985, Geologic map of Wyoming: U.S. Geological Survey, re-released 2014, Wyoming State Geological Survey.

Lowry, M.E., 1966, The White River Formation as an aquifer in southeastern Wyoming and adjacent parts of Nebraska and Colorado: U.S. Geological Survey Professional Paper 550-D, p. 217–222.

Lowry, M.E., Crist, M.A., and Tilstra, J.R., 1967, Geology and ground-water resources of Laramie County, Wyoming; with a section on chemical quality of ground water and of surface water: U.S. Geological Survey Water-Supply Paper 1834.

Lundstern, J.E., and Zoback, M.D., 2020, Multiscale variations of the crustal stress field throughout North America: *Nature Communications*, v. 11, no. 1951, https://doi.org/10.1038/s41467-020-15841-5.

Lundstern, J.E., and Zoback, M.D., 2022, State of stress in areas of active unconventional oil and gas development in North America: *AAPG Bulletin*, v. 106, no. 2, p. 355-385.

Lundstern, J.E., and Zoback, M.D., 2023, Maximum horizontal stress orientation and relative stress magnitude (faulting regime) data throughout North America: U.S. Geological Survey data release, https://doi.org/10.5066/P90LS6QF.

Mallory, W.W., ed., 1972, Geologic atlas of the Rocky Mountain region: Rocky Mountain Association of Geologists, Denver, Colorado, 331 p.

Marshak, S., Karlstrom, K., and Timmons, J.M., 2000, Inversion of Proterozoic extensional faults: An explanation for the pattern of Laramide and Ancestral Rockies intracratonic deformation, United States: *Geology*, v. 28, no. 8, p. 735–738, https://doi.org/10.1130/0091-7613(2000)28<735:IOPEFA>2.0.CO;2.

Miller, J.A., and Appel, C.L., 1997, Ground Water Atlas of the United States: Segment 3, Kansas, Missouri, Nebraska: U.S. Geological Survey Hydrologic Atlas 730-D, 1 sheet, https://doi.org/10.3133/ha730D.

Montgomery, S.L., Goolsby, S., and Pierini, D., 1998, Permian (Wolfcampian) Admire "C": New Exploratory Potential in the Northern Denver Basin: *AAPG Bulletin*, v. 82, no. 12, p. 2173-2191.

NOAA National Centers for Environmental Information, 2023, Monthly Global Climate Report for Annual 2022: published online, https://www.ncei.noaa.gov/access/monitoring/monthly-report/global/202213.

Oldham, D.W., 1996, Permian Salt in the Northern Denver Basin: Controls on Occurrence and Relationship to Oil and Gas Production from Cretaceous Reservoirs, in Longman, M.W., and Sonnenfeld, M.D., eds., Paleozoic systems of the Rocky Mountain region: Society for Sedimentary Geology, Rocky Mountain Section, p. 335-354.

Oldham, D.W., 1997, Influence of Permian salt dissolution on Cretaceous oil and gas entrapment, Denver basin: Graduate Theses, Dissertations, and Problem Reports, West Virginia University, Paper 9535.

Palandri, J.L., and Kharaka, Y.K., 2004, A compilation of rate parameters of water-mineral interaction kinetics for application to geochemical modeling: U.S. Geological Survey Open-File Report 2004-1068, 71 p.

Petersen, M.D., Shumway, A.M., Powers, P.M., Field, E.H., Moschetti, M.P., Jaiswal, K.S., Milner, K.R., Rezaeian, S., Frankel, A.D., Llenos, A.L., Michael, A.J., Altekruse, J.M., Ahdi, S.K., Withers, K.B., Mueller, C.S., Zeng, Y., Chase, R.E., Salditch, L.M., Luco, N., … Witter, R.C., 2023, The 2023 US 50-state national seismic hazard model: Overview and implications: *Earthquake Spectra*, v. 40, no. 1, p. 5–88, https://doi.org/10.1177/87552930231215428.

Pierce, W.G., compiler, 1997, Geologic map of the Cody 1° by 2° Quadrangle, northwestern Wyoming: U.S. Geological Survey, Report No. I-2500, https://doi.org/10.3133/i2500.

Rothe, G.H., and Lui, C.Y., 1983, Possibility of induced seismicity in the vicinity of the Sleepy Hollow oil field, southwestern Nebraska: *Bulletin of the Seismological Society of America*, v. 73, no. 5, p. 1357–1367, https://doi.org/10.1785/BSSA0730051357.

Saadatpoor, E., Bryant, S.L., and Sepehrnoori, K., 2010, New trapping mechanism in carbon sequestration: *Transport in Porous Media*, v. 82, no. 1, p. 3–17, https://doi.org/10.1007/s11242-009-9446-6.

Schlumberger, 2005, Schlumberger Log Interpretation Chart.

Scholle, P.A., 2003, Geologic map of New Mexico (9/7/2022 ed.) [Open-File Geologic Map #304]: New Mexico Bureau of Geology & Mineral Resources.

Sibray, S., Hallum, D.R., Reedy, J., Yuill, J., and Kuntz, T., 2020, Mapping the base of the High Plains Aquifer using borehole geophysical logs and airborne electromagnetic surveys in western Nebraska: University of Nebraska-Lincoln, Conservation and Survey Division, Open File Report 210, 21 p.

Sonnenberg, S.A., and Weimer, R.J., 1981, Tectonics, sedimentation, and petroleum potential, northern Denver Basin, Colorado, Wyoming, and Nebraska: M.S. thesis, Colorado School of Mines, Golden, Colorado, 150 p.

Steele, G.V., Sibray, S.S., and Quandt, K.A., 2007, Evaluation of ground water near Sidney, western Nebraska, 2004-05: U.S. Geological Survey Scientific Investigations Report 2007-5086, 54 p.

Swanson, B.F., 1981, A simple correlation between permeabilities and mercury capillary pressures: *Journal of Petroleum Technology*, v. 33, no. 12, p. 2498-2504, SPE-8234-PA, https://doi.org/10.2118/8234-PA.

Taucher, P., Anderson, R., and Harris, S., 2013, Platte River Basin water plan update, level I (2009–2013), available groundwater determination: Wyoming State Geological Survey Technical Memorandum 5, 584 p., 11 pls.

Terry, D.O. Jr., 1998, Lithostratigraphic revision and correlation of the lower part of the White River Group: South Dakota to Nebraska, in Terry, D.O. Jr., LaGarry, H.E., and Hunt, R.M., eds., Depositional environments, lithostratigraphy, and biostratigraphy of the White River and Arikaree Groups (Late Eocene to Early Miocene, North America): Geological Society of America Special Paper 325, p. 15-38.

Thiercelin, M.J., and Plumb, R.A., 1994, Core-based prediction of lithologic stress contrasts in East Texas formations: *SPE Formation Evaluation*, v. 9, p. 251–258, https://doi.org/10.2118/21847-PA.

Warren, E.A., and Smalley, P.C., 1994, Part 2: SPWLA water resistivity (Rw) atlas: *Geological Society of London Memoir*, v. 15, p. 205-222, https://doi.org/10.1144/GSL.MEM.1994.015.01.03.

Weimer, R.J., and Sonnenberg, S.A., 1996, Guide to the petroleum geology and Laramide Orogeny, Denver Basin and Front Range, Colorado: Colorado Geological Survey Bulletin 51, Colorado Geological Survey, Department of Natural Resources, Denver, Colorado, https://doi.org/10.58783/cgs.b51.bsvl1261.

Wildgust, N., Leroux, K., Botnen, B., Daly, D., Jensen, M., Glazewski, K., Kalenze, N., Burton-Kelly, M., Dalkhaa, C., Torres, J., and Doll, T., 2018, Nebraska Integrated Carbon Capture and Storage Pre-Feasibility Study: University of North Dakota, Energy and Environmental Research Center, Report No. DOE-EERC-0029186, Grand Forks, ND.

Wortmann, C.S., 2021, Irrigation Well Water: Essential Nutrient Contents and Other Properties: *Agrosystems, Geosciences & Environment*, v. 4, e20137, https://doi.org/10.1002/agg2.20137.

Xu, T., Apps, J.A., and Pruess, K., 2001, Analysis of mineral trapping for CO2 disposal in deep aquifers: Report No. LBNL-47471, Lawrence Berkeley National Laboratory, Berkeley, California, https://doi.org/10.2172/789133.

Zhang, J.J., 2019, In situ stress estimate, in Zhang, J.J., ed., *Applied Petroleum Geomechanics*: Gulf Professional Publishing, p. 187-232, https://doi.org/10.1016/B978-0-12-814814-3.00006-X.

Zhang, Y., and Zhang, J., 2017, Lithology-dependent minimum horizontal stress and in-situ stress estimate: *Tectonophysics*, v. 703-704, p. 1-8, http://dx.doi.org/10.1016/j.tecto.2017.03.002.

## 3.0 Area of Review and Corrective Action [40 CFR 146.82(a)(13) and 146.84(b)]

All information satisfying 40 CFR 146.82(a)(13) and 146.84(b-c) is described in **03_AoR_CA_Plan_WNSHub_Conestoga_2024-08-30.pdf**.

## 4.0 Financial Responsibility [40 CFR 146.82(a)(14) and 146.85]

All information satisfying 40 CFR 146.82(a)(14) and 146.85 is described in **04_FR_WNSHub_Conestoga_2024-08-30.pdf**.

## 5.0 Injection Well Construction [40 CFR 146.86]

All information satisfying 40 CFR §146.82(a)(9), (11), and (12) and 40 CFR §146.86 is described in **05_Construction_Details_WNSHub_Conestoga_2024-08-30.pdf**.

## 6.0 Pre-Operational Logging and Testing [40 CFR 146.82(a)(8) and 146.87]

All information satisfying 40 CFR 146.82(a)(8) and 146.87 is described in **06_Pre-Op_Testing_WNSHub_Conestoga_2024-08-30.pdf**.

## 7.0 Injection Well Operation 40 CFR 146.82(7) & (10)

All information satisfying 40 CFR 146.82(a)(7) and (10) is described in **7_Inj_Well_Ops_WNSHub_Conestoga_2024-08-30.pdf**.

## 8.0 Testing and Monitoring [40 CFR 146.82(a)(15) and 146.90]

All information satisfying 40 CFR 146.82(a)(15) and 146.90 is described in **08_ TM_Plan_WNSHub_Conestoga_2024-08-30.pdf**

The associated Quality Assurance and Surveillance Plan (QASP) is provided in **8.11_QASP_WNSHub_Conestoga_2024-08-30.pdf**

## 9.0 Injection Well Plugging [40 CFR 146.82(a)(16) and 146.92(b)]

All information satisfying 40 CFR 146.82(a)(16) and 40 CFR 146.92(b) is described in **09_Plugging_Plan_WNSHub_Conestoga_2024-08-30.pdf**.

## 10.0 Post-Injection Site Care and Site Closure [40 CFR 146.82(a)(17) and 146.93(a)]

All information satisfying 40 CFR 146.82(a)(17) and 146.93(a) is described in **10_PISC_SC_Plan_WNSHub_Conestoga_2024-08-30.pdf.**

## 11.0 EMERGENCY AND REMEDIAL RESPONSE [40 CFR 146.82(A)(19) AND 146.94(A)]

All information satisfying 40 CFR 146.82(a)(19) and 146.94(a)] is described in **11_ERRP_WNSHub_Conestoga_2024-08-30.pdf.**

## 12.0 INJECTION DEPTH WAIVER AND AQUIFER EXEMPTION EXPANSION

Not Applicable—No injection depth waiver nor aquifer exemption expansion is requested or required.

## 13.0 OTHER INFORMATION [40 CFR 146.82(A)(21)]

### 13.1 Environmental Justice [Executive Order 12898]

**13.1_EJ_WNSHub_Conestoga_2024-08-30.pdf** includes a review of High Plains' proposed Western Nebraska Sequestration Hub (WNS Hub) area to determine if any defined populations would be disproportionately affected in compliance with Executive Order 12898.

### 13.2 The National Historic Preservation Act of 1966 [16 U.S. Code 470]

High Plains evaluated the existence of historic places recorded in the National Register of Historic Places[30] within the AoR of Conestoga I-1 (**Figure 13.2.1**). There are no historic places in the Register within the AoR.

[30] https://www.nps.gov/subjects/nationalregister/index.htm

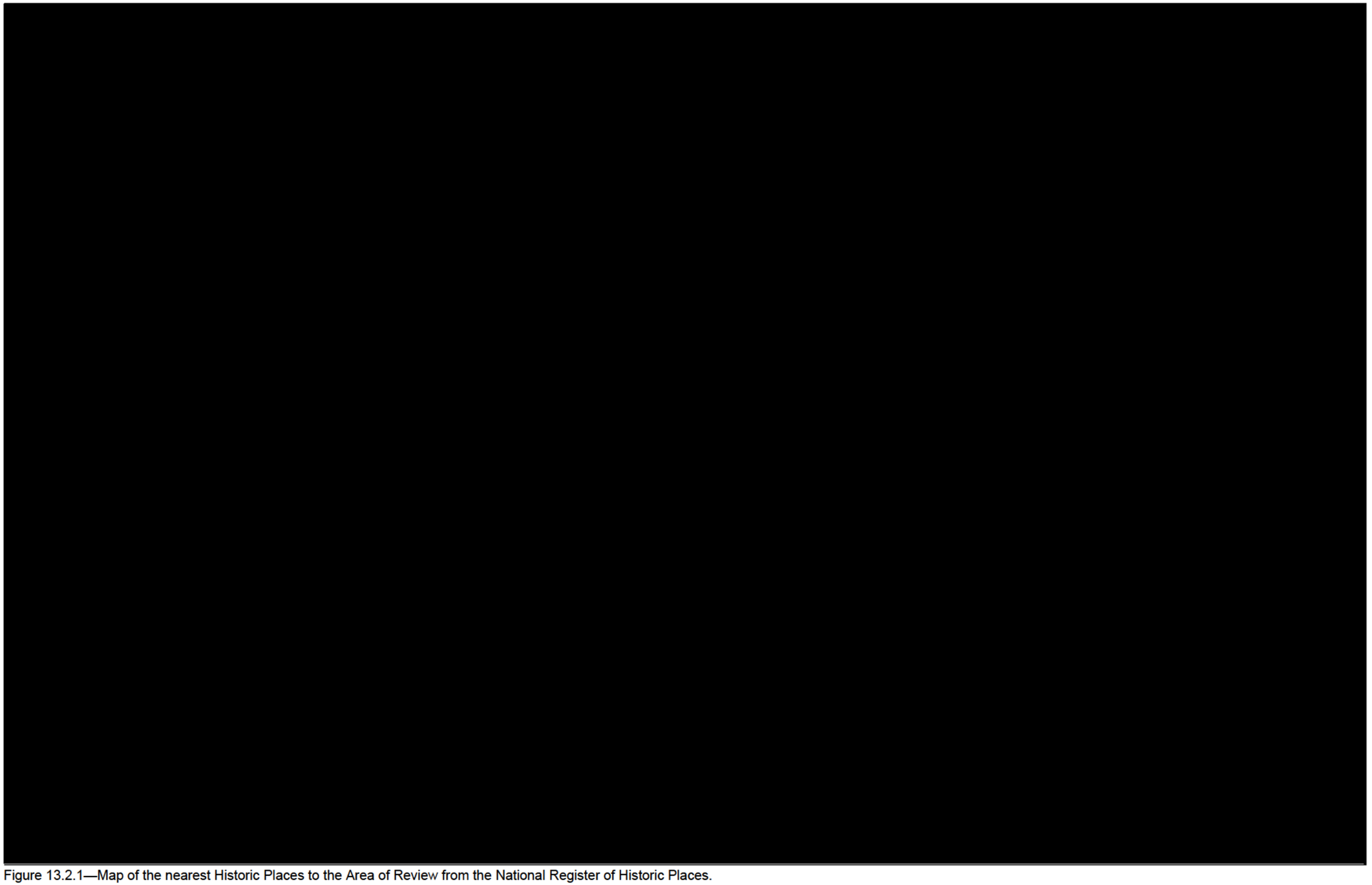

Figure 13.2.1—Map of the nearest Historic Places to the Area of Review from the National Register of Historic Places.

## 13.3 The Endangered Species Act [16 U.S. Code 1531]

High Plains reviewed the U.S. Fish & Wildlife Service's Information for Planning and Consultation tool[31] (IPAC) to evaluate the potential presence of endangered, threatened, and candidate species ranges and critical habitats within the AoR. No critical habitats are present within the AoR. The AoR is within the known or expected ranges of the species listed in **Table 13.3.1** below.

High Plains will comply with all federal and state laws for surface operations, such as drilling permits and seismic surveys, for the planned injection and monitoring well.

Table 13.3.13.1—List of known or expected endangered, threatened, and candidate species ranges within the Project AoR from the USFWS IPAC tool (https://ipac.ecosphere.fws.gov).

[redacted]

### Birds

| NAME | STATUS |
|---|---|
| Piping Plover CH Charadrius melodus | Threatened |
| Whooping Crane CH Grus americana | Endangered |

### Fishes

| NAME | STATUS |
|---|---|
| Pallid Sturgeon<br>Scaphirhynchus albus<br>Wherever found | Endangered |

### Insects

| NAME | STATUS |
|---|---|
| Monarch Butterfly<br>Danaus plexippus<br>Wherever found | Candidate |

### Flowering Plants

| NAME | STATUS |
|---|---|
| Western Prairie Fringed Orchid<br>Platanthera praeclara<br>Wherever found | Threatened |

### Critical habitats

Potential effects to critical habitat(s) in this location must be analyzed along with the endangered species themselves.

[31] https://ipac.ecosphere.fws.gov – accessed 8/22/2024

## APPENDIX 2.1—DAKOTA/MUDDY "J" SANDSTONE OIL AND GAS PRODUCERS WITHIN 10 MILES OF CONESTOGA I-1

| API No. | Well Name | Producing Formation | Oil Cum. (bbl) | Gas Cum. (Mcf) | Distance from Injector (mi) |
|---|---|---|---|---|---|
| 0507509391 | DOUD 23-4 | J SAND | 1 | | 9.0 |
| 2610505531 | LYON 1 | J SAND | 35 | | 0.6 |
| 2610522326 | MOCKETT 1 | J SAND | 75 | | 4.1 |
| 2603322416 | WHITNEY 6 | J SAND | 152 | 68,730 | 8.4 |
| 0507507284 | JENSEN #1 1 | J SAND | 288 | | 9.7 |
| 2610506167 | DIETZ 1 | J SAND | 373 | | 9.6 |
| 0507508652 | ASHBAUGH 1 | J SAND | 473 | 79,766 | 8.4 |
| 2610505170 | SMITH BERT 2 | J SAND | 517 | 4,302 | 5.0 |
| 2603305018 | STATE 915 | J SAND | 544 | | 7.8 |
| 2603321894 | LARSON A 1 | J SAND | 581 | 2,016 | 9.6 |
| 2610506154 | RICHARDSON | D & J SAND | 682 | | 6.8 |
| 2603321497 | STATE 1 | J SAND | 922 | 99,305 | 7.9 |
| 2610506528 | SCHMIDT CLEO -B- | J SAND | 1,117 | 820 | 8.6 |
| 2610506722 | YOUNG 1 | J SAND | 1,259 | | 8.7 |
| 2610521957 | PALMER STATE 2 | J SAND | 1,618 | | 5.0 |
| 2610505057 | PEARL 1 | J SAND | 1,703 | 16,098 | 4.3 |
| 2610505415 | FARRELL M B FARM -C- | J SAND | 1,795 | 18,561 | 1.2 |
| 2610521647 | BAIRD FARMS 1 | J SAND | 1,827 | 3,566 | 1.5 |
| 2603321020 | LARSON | J SAND | 1,883 | | 9.5 |
| 2610521982 | LONG 23 | J SAND | 2,071 | | 4.7 |
| 2610505431 | LUKES | J SAND | 2,113 | | 9.5 |
| 2610505570 | MARCUM S N | J SAND | 2,359 | | 7.0 |
| 2610505107 | BASSETT D F 3 | J SAND | 2,700 | 5,270 | 5.9 |
| 2610505145 | DILLON 1 | J SAND | 2,779 | 1,400 | 9.0 |
| 0507508719 | CLIFF 1 | J SAND | 2,985 | 641,970 | 7.7 |
| 2610506759 | DEDIC 1 | J SAND | 3,155 | 1 | 8.9 |
| 2610522748 | WREDE 1 1 | J SAND | 3,235 | | 6.6 |
| 2603321128 | BEALE 3 | D & J SAND | 3,813 | | 6.2 |
| 0507509313 | CATHERINE 1 | J SAND | 4,471 | 466 | 7.1 |
| 2610505304 | WARREN H L | J SAND | 4,707 | 2,891 | 8.8 |
| 2610521479 | PERKINS 33 | J SAND | 5,020 | 2,350 | 8.8 |
| 2610505946 | LIPKE E | D & J SAND | 5,296 | 2,510 | 6.8 |
| 2610521660 | AYERS 1 | D & J SAND | 5,596 | | 6.4 |
| 2610522108 | GUNDERSON 1 | J SAND | 5,769 | 6,457 | 1.3 |

| API No. | Well Name | Producing Formation | Oil Cum. (bbl) | Gas Cum. (Mcf) | Distance from Injector (mi) |
|---|---|---|---|---|---|
| 2610521048 | CABELA 1 | J SAND | 5,903 | 2,519 | 2.7 |
| 2610508210 | ROSENTHAL 1 | J SAND | 6,176 | 2,225 | 2.8 |
| 2610505196 | POPE 1 | J SAND | 6,347 | 53,933 | 5.3 |
| 2610521421 | HAWTHORNE | J SAND | 6,545 | 2,193 | 5.2 |
| 2610505346 | LYON 1 | J SAND | 6,840 | 32,025 | 2.2 |
| 0512307069 | BUCZKOWSKY J 1X | D & J SAND | 7,019 | 6,806 | 8.0 |
| 2610506268 | ROESSIG H R | J SAND | 7,299 | | 5.5 |
| 2610521535 | NELSON 44 | J SAND | 7,996 | | 8.8 |
| 2610505773 | WREDE | J SAND | 8,314 | 6,177 | 6.6 |
| 2610505590 | KNEIGINGER | D & J SAND | 8,457 | 1,825 | 8.2 |
| 2610505550 | FARRELL FARMS | D & J SAND | 8,471 | 1,535 | 8.2 |
| 2603305237 | HOWARD MADDEN | D & J SAND | 8,650 | 2,181 | 7.6 |
| 2610506047 | BEALE | J SAND | 8,842 | 12,738 | 4.3 |
| 2610521417 | CHRISTENSEN 1 | J SAND | 9,241 | 1,000 | 3.2 |
| 2610505935 | GOODWIN | J SAND | 9,874 | 264 | 3.8 |
| 2603321666 | NELSON 1 | J SAND | 11,000 | 707 | 9.3 |
| 0507508286 | YUNG #1 1 | J SAND | 11,046 | 5,959 | 7.9 |
| 0512309805 | CERVENY #1 1 | J SAND | 11,857 | 67 | 0.0 |
| 2610505295 | OLSEN A | J SAND | 12,914 | 10,431 | 6.1 |
| 0507509430 | STATE BDB 1 | J SAND | 12,914 | 14,070 | 6.6 |
| 2603321110 | BEALE 2 | D & J SAND | 13,113 | | 6.3 |
| 2610506096 | MR PEAK | D & J SAND | 13,714 | | 7.1 |
| 2610505116 | LONG 1 | D & J SAND | 13,768 | 56,753 | 4.1 |
| 2610506215 | MEISSER R C | J SAND | 14,715 | 898 | 7.5 |
| 2610506219 | SHAW LLOYD | J SAND | 15,494 | | 5.3 |
| 0512308108 | BUCZKOWSKYJ 7 | J SAND | 17,163 | 101,726 | 8.8 |
| 2603321731 | MADDEN 1 | J SAND | 17,334 | 75 | 7.7 |
| 2610505267 | ALSEN -B- | J SAND | 17,538 | 8,738 | 6.2 |
| 0507509334 | CATHERINE 3 | J SAND | 18,045 | 138 | 7.0 |
| 2610505583 | FLESNER | J SAND | 18,646 | 2,663 | 3.1 |
| 2610505379 | MINTKEN -B- | J SAND | 20,142 | 100,158 | 0.0 |
| 2610506089 | DIETZ | J SAND | 20,159 | | 7.7 |
| 2603305279 | NELSON 1 | D & J SAND | 20,204 | | 6.3 |
| 2610522283 | LONG 75 | D & J SAND | 20,211 | 99,455 | 7.1 |

| API No. | Well Name | Producing Formation | Oil Cum. (bbl) | Gas Cum. (Mcf) | Distance from Injector (mi) |
|---|---|---|---|---|---|
| 2610505424 | LUKES A | J SAND | 20,935 | 9,450 | 9.9 |
| 2610522231 | AYRES 1 | J SAND | 21,516 | 57,383 | 4.9 |
| 2610505292 | LEONARD A K | J SAND | 23,875 | | 8.7 |
| 2610506057 | ENYEART | D & J SAND | 24,568 | | 8.8 |
| 2610505168 | STATE 1 | J SAND | 26,137 | | 5.9 |
| 2610521603 | LONG 1 | J SAND | 27,211 | 43,232 | 1.7 |
| 2610522540 | SNOWDRIFT 1 | J SAND | 28,249 | 27,594 | 9.9 |
| 2610505498 | FARRELL FARMS B | J SAND | 28,644 | 886 | 8.2 |
| 2610506016 | DALLEGGE M E | J SAND | 29,254 | 8,177 | 4.0 |
| 2610505493 | FUNK 2 | J SAND | 30,713 | 21,514 | 2.5 |
| 2610506155 | NELSON 1 | J SAND | 30,945 | | 5.2 |
| 2603321741 | NELSON -H- 1 | J SAND | 34,580 | 33,554 | 6.7 |
| 2610505653 | KINTON -C- 1 | J SAND | 35,785 | 24,017 | 2.2 |
| 2610521743 | BEALE 1 | J SAND | 36,192 | 206,307 | 5.6 |
| 0507509345 | HIGHBALL 1 | J SAND | 36,433 | 780 | 6.4 |
| 2610522552 | STATE 10 | J SAND | 36,791 | 284 | 7.9 |
| 2610505373 | MINTKEN -A- | J SAND | 37,664 | | 9.8 |
| 2610505450 | FARRELL M F FARM -A- | J SAND | 39,421 | 99,335 | 0.8 |
| 2610505366 | WARREN | J SAND | 42,165 | 4,776 | 9.4 |
| 2610521574 | FRAASS 1 | J SAND | 42,578 | | 4.0 |
| 2610521066 | BERANCK 1 | J SAND | 42,757 | 65,135 | 0.8 |
| 2610505840 | MCNISH C H 1 | J SAND | 43,000 | 620 | 6.4 |
| 2610505394 | HAACK 1 | J SAND | 43,646 | 6,384 | 1.8 |
| 0507508174 | HATCH 1-X 1-X | J SAND | 43,814 | 55,705 | 8.1 |
| 0507508453 | GOVERNMENT X 1 | J SAND | 44,719 | 9,179 | 8.8 |
| 2610506013 | MAAS -A- | J SAND | 45,079 | 53,465 | 4.1 |
| 0507508275 | NELSON #1 1 | J SAND | 45,171 | 69,959 | 7.1 |
| 2610505457 | HAWTHORN | J SAND | 45,446 | 19,599 | 8.2 |
| 2610505028 | BLODGETT | J SAND | 51,564 | 53,474 | 8.6 |
| 0512308036 | BUCZKOWSKY J 1 | J SAND | 52,219 | 135,665 | 9.0 |
| 2610505019 | MINTKEN UNIT NORTH | J SAND | 52,389 | 37,369 | 9.9 |
| 2610505878 | F A HINSHAW 1 | J SAND | 52,405 | 14,934 | 5.0 |
| 2610505818 | EUSTICE 1 | J SAND | 53,247 | 14,938 | 2.5 |
| 2610505402 | HAACK 1 | J SAND | 55,074 | 36,244 | 1.7 |
| 2610505581 | KREIZINGER 1 | J SAND | 55,832 | 6,125 | 8.5 |
| 2610505495 | YUNG 1 | J SAND | 55,921 | 24,619 | 8.4 |
| 2610506056 | MAAS -B- | J SAND | 56,151 | 66,241 | 4.3 |
| 2610506256 | CARL BELGUM 2 | J SAND | 57,107 | 29,525 | 5.5 |

| API No. | Well Name | Producing Formation | Oil Cum. (bbl) | Gas Cum. (Mcf) | Distance from Injector (mi) |
|---|---|---|---|---|---|
| 0507507298 | DURLAND TRUST #1-C 1 | J SAND | 59,317 | 89,364 | 6.1 |
| 2610521109 | MINTKEN 1 | J SAND | 60,146 | 45,305 | 0.0 |
| 2610505496 | HEIDMANN B | J SAND | 61,102 | 29,787 | 9.7 |
| 2610505317 | MOCKETT 2 | J SAND | 61,244 | | 3.9 |
| 2610505650 | JOHNSON NELLE & PHILLIPS | J SAND | 69,409 | 19,687 | 2.5 |
| 2603305319 | NELSON L K | D & J SAND | 70,792 | 38,920 | 6.7 |
| 2610506156 | NELSON-RASMUSSEN | D & J SAND | 75,929 | | 7.4 |
| 0507507427 | J CASEMENT 1 & 2 2 | J SAND | 77,513 | 579,197 | 9.6 |
| 2610521379 | STATE 1 | J SAND | 78,411 | | 8.3 |
| 2610505453 | LUKES | J SAND | 79,358 | 37,451 | 9.9 |
| 0507507297 | DURLAND-PHILLIPS 1 | D & J SAND | 79,465 | 220,204 | 6.2 |
| 2610505045 | BLODGETT | J SAND | 79,899 | 9,287 | 8.8 |
| 2610521741 | KLEINHOLZ 32 | J SAND | 87,491 | | 8.4 |
| 2610505383 | MINTKEN UNIT SOUTH | J SAND | 98,675 | 54,559 | 9.8 |
| 2610506583 | STATE 1 | J SAND | 103,174 | 925 | 7.7 |
| 2610521863 | GOODWIN 1 | J SAND | 103,990 | | 3.8 |
| 2610506192 | FARMER 1 | J SAND | 104,178 | 41,122 | 5.0 |
| 0507507100 | L GRIFFITH #1 1 | J SAND | 107,577 | 154,068 | 0.0 |
| 2610505368 | MINTKEN | J SAND | 109,503 | 147,062 | 9.6 |
| 0507508280 | HATCH 1 | J SAND | 110,443 | 195,967 | 8.1 |
| 2603305318 | NELSON M S -A- | D & J SAND | 121,577 | 41,981 | 6.7 |
| 2610506455 | NELSON V A 1 | J SAND | 124,416 | 10,447 | 8.6 |
| 2610506582 | BEARD 2 | J SAND | 127,738 | 4,159 | 9.1 |
| 2610505150 | CRAIG JOHNSON | D & J SAND | 135,842 | 19,000 | 3.6 |
| 2610521006 | BLODGETT | J SAND | 138,359 | 22,788 | 8.7 |
| 2610505435 | FARRELL | J SAND | 140,140 | 20,015 | 1.0 |
| 2610522061 | SHRIVER 1 | J SAND | 146,459 | 43,762 | 8.4 |
| 2610521788 | MILLARD 1 | J SAND | 164,240 | 231,740 | 1.5 |
| 2610505908 | HINSHAW 1 | J SAND | 165,277 | 116,944 | 5.1 |
| 0507507119 | CASEMENT 1 | D & J SAND | 177,265 | 477,392 | 9.7 |
| 2610506188 | FARMER (B) 1 | J SAND | 185,446 | | 5.0 |
| 2610506855 | TERRACE UNIT | J SAND | 196,253 | 16,973 | 9.5 |
| 2610505172 | WISE 1 | J SAND | 197,196 | 205,448 | 4.6 |
| 0507507283 | C NELSON 3 | J SAND | 198,947 | 333,060 | 6.2 |

| API No. | Well Name | Producing Formation | Oil Cum. (bbl) | Gas Cum. (Mcf) | Distance from Injector (mi) |
|---|---|---|---|---|---|
| 2610505897 | LIPKE E | D & J SAND | 204,538 | 66,526 | 6.4 |
| 2610505302 | SCHRIVER 1 | J SAND | 206,656 | 122,367 | 8.7 |
| 2610505904 | ROBERTS | J SAND | 211,595 | 25,761 | 4.0 |
| 2610521409 | STATE 2 | J SAND | 223,465 | 11,749 | 8.3 |
| 2610505822 | STATE OF NEBRASKA | J SAND | 237,687 | 71,883 | 2.6 |
| 2610505162 | AYRES H S | J SAND | 240,071 | 143,147 | 5.7 |
| 2603305351 | LARSON C L | J SAND | 273,983 | 150 | 7.3 |
| 2610506117 | ALDEN -A- 1 | J SAND | 279,451 | 5,814 | 7.2 |
| 2610505901 | ROBERTS | J SAND | 296,173 | 195,674 | 4.2 |
| 2610505606 | LEONARD 1 | D & J SAND | 300,452 | | 8.7 |
| 2603322100 | HERBOLDSHEIMER | J SAND | 302,311 | 58,614 | 8.3 |
| 2610506091 | ENYEART | J SAND | 309,898 | 22,304 | 8.3 |
| 2610506261 | HILL UNIT 2 | J SAND | 402,216 | 353,827 | 6.2 |
| 2610505907 | VRTATKO UN | J SAND | 402,672 | 76,205 | 3.7 |
| 2610521490 | YOUNG UNIT 1A | J SAND | 404,025 | 68,400 | 8.7 |
| 2610505835 | GOODWIN F L B | J SAND | 448,408 | 88,843 | 2.7 |
| 2610505210 | BUKIN STATE UNIT | J SAND | 512,271 | 415,123 | 5.6 |
| 2610521311 | S HOUTBY UNIT | J SAND | 559,813 | 15,600 | 8.6 |
| 2610506495 | HAFEMAN 1 | J SAND | 645,012 | 22,775 | 8.6 |
| 2610505939 | DIETZ UNIT 3 | J SAND | 664,663 | 218,818 | 6.7 |
| 2610505315 | ALLELY UN 1B | J SAND | 698,318 | 279,762 | 3.6 |
| 2610505193 | PHILLIPS, HARRY 7 | D & J SAND | 745,706 | 893,962 | 3.7 |
| 2610506764 | KENTON UNIT | J SAND | 785,898 | 393,262 | 9.0 |
| 2610506090 | SPATH UNIT | J SAND | 922,131 | 357,124 | 7.5 |
| 2610521138 | SUSAN UNIT | J SAND | 1,174,362 | 180,625 | 7.4 |
| 2603305366 | POTTER SW SU | J SAND | 1,194,924 | 300,826 | 7.2 |
| 2610506634 | SWEARINGEN UNIT, SOUTH | J SAND | 1,514,850 | 340,455 | 10.0 |
| 2610505016 | OSTGREN UNIT | J SAND | 1,980,707 | 320,111 | 7.5 |
| 2610506743 | HOUTBY UNIT | J SAND | 2,739,587 | 217,967 | 8.8 |
| 2610505874 | POTTER UNIT, SW (WESTERN) 1 | D & J SAND | 4,526,759 | 1,145,541 | 5.0 |
| 2610505698 | ENDERS UNIT P-5 | D & J SAND | 9,180,897 | 1,392,728 | 5.8 |
| 2610506227 | SLOSS UNIT | J SAND | 16,287,713 | 4,888,425 | 7.1 |

## APPENDIX 2.2—TOP LYONS FORMATION WELL CONTROL

| API No. | Well Name | Formation Top | TVDSS (ft) | MD (ft) |
|---|---|---|---|---|
| 0500105215 | RKY MTN ARSENAL 1 | LYONS | -4,396 | 9,599 |
| 0500507210 | TEBO 4 1H | LYONS | -3,594 | 9,513 |
| 0501306011 | YOUNG 1 | LYONS | -912 | 6,068 |
| 0501706096 | BERNAL WALLACE ETAL 20-1 | LYONS | 1,336 | 2,708 |
| 0501706181 | WILKERSON A 1 | LYONS | 1,467 | 3,019 |
| 0501706243 | CHAMPLIN-PETERSON 1 | LYONS | 1,426 | 3,065 |
| 0501706265 | MCCORMICK-C 1 | LYONS | 1,453 | 3,020 |
| 0501706372 | S-S-M FICK 1-2 | LYONS | 1,411 | 2,894 |
| 0501706427 | CHAMPLIN 124 AMOCO-F 1 | LYONS | 1,272 | 2,920 |
| 0501706575 | MITCHEK 1 | LYONS | 1,506 | 2,819 |
| 0501706650 | ISLEY 1 | LYONS | 1,380 | 2,957 |
| 0501706669 | UPRC-ACKERMAN 1 | LYONS | 1,289 | 2,749 |
| 0501707666 | ROTHER SHIRLEY 1 | LYONS | 1,268 | 2,681 |
| 0501707674 | HULL W W 1 | LYONS | 1,270 | 2,742 |
| 0501707708 | APC SCHEIMER 1-21 | LYONS | 1,647 | 2,512 |
| 0501707727 | PRONGHORN STATE 16-15-48 1P | LYONS | 1,696 | 2,586 |
| 0503906208 | PACKARD-STATE 1 | LYONS | -1,232 | 6,998 |
| 0504105023 | FIELD BOHART 1 | LYONS | -760 | 6,451 |
| 0504106082 | GRAHAM 1-13 | LYONS | -748 | 6,872 |
| 0506106136 | PLUNKETT 1 | LYONS | 1,754 | 2,209 |
| 0506106406 | REIHARDT-MICHEL 1-5 | LYONS | 1,864 | 2,144 |
| 0506106778 | TEMPEL A 1-6 | LYONS | 1,847 | 2,282 |
| 0506305002 | LOWE 1 | LYONS | 1,003 | 3,478 |
| 0506305091 | GERING 1 | LYONS | 163 | 4,515 |
| 0506306031 | STATE-A 1-36 | LYONS | 989 | 4,124 |
| 0506306351 | GRAMM 1-26 | LYONS | 495 | 3,612 |
| 0506906054 | BERTHOUD-STATE 3 | LYONS | 169 | 4,962 |
| 0506906247 | REDWIN 22-64 | LYONS | -2,156 | 7,456 |
| 0507305055 | ELLISTON J F 1 | LYONS | -258 | 5,184 |
| 0507306052 | STATE 1 | LYONS | 557 | 4,487 |
| 0507306178 | STATE-V 1 | LYONS | 1,249 | 3,515 |
| 0507306283 | SMITH CATTLE 1-19 | LYONS | 419 | 4,994 |
| 0507306438 | MAHALO 1 | LYONS | -86 | 5,310 |
| 0507306477 | CRAIG JOHN 6-2 | LYONS | -262 | 5,546 |
| 0507306497 | FORRISTALL STATE 36-11S-56W-02 | LYONS | 43 | 5,356 |
| 0507306617 | WAR EAGLE 16 | LYONS | -256 | 5,535 |
| 0507306664 | PICK SIX 2 | LYONS | -95 | 5,418 |
| 0507508840 | HOUSTON 20-1 | LYONS | -1,663 | 5,653 |

| API No. | Well Name | Formation Top | TVDSS (ft) | MD (ft) |
|---|---|---|---|---|
| 0507509022 | CASEMENT TRUST 1-7 | LYONS | -2,120 | 6,511 |
| 0507509050 | SEGELKE M 1 | LYONS | -1,863 | 6,477 |
| 0507509063 | ROELLE F 1 | LYONS | -1,763 | 6,301 |
| 0507509115 | ARCO-SINDT 6-15 | LYONS | -1,730 | 5,770 |
| 0507509240 | LEBLANC 1 | LYONS | -1,761 | 6,243 |
| 0507509382 | STATE 1-36 | LYONS | -1,631 | 6,082 |
| 0511505118 | COZAD 1 | LYONS | -843 | 4,816 |
| 0511506040 | STATE 1 | LYONS | -876 | 4,838 |
| 0511506041 | STATE 1-36 | LYONS | -678 | 4,602 |
| 0511506042 | NORTH MARKS BUTTE-STATE 2 | LYONS | -896 | 4,851 |
| 0511506043 | STATE 3 | LYONS | -865 | 4,812 |
| 0511506044 | STATE 1 | LYONS | -927 | 4,816 |
| 0511506045 | STATE 4 | LYONS | -875 | 4,850 |
| 0511506048 | HIATT FARMS 1 | LYONS | -459 | 4,097 |
| 0511506051 | MUNSON 4-1 | LYONS | -826 | 4,808 |
| 0511506052 | EAGLE VIEW STATE 1-B | LYONS | -879 | 4,850 |
| 0511506055 | MCCORMICK 1 | LYONS | -729 | 4,388 |
| 0512105256 | GALBREATH 1 | LYONS | -205 | 4,750 |
| 0512109845 | BRUNKHARDT D 1-33 | LYONS | -1,808 | 6,079 |
| 0512110006 | SCHMIDT D 1-28 | LYONS | -1,616 | 6,179 |
| 0512110166 | STATE 16 1 | LYONS | -1,521 | 6,225 |
| 0512305100 | WILLIAM KATCHEN 1 | LYONS | -3,978 | 8,819 |
| 0512306129 | GRAEFE 1 | LYONS | -3,645 | 8,662 |
| 0512306129 | GRAEFE 1R | LYONS | -3,643 | 8,660 |
| 0512307196 | STATE 1-16 | LYONS | -3,294 | 8,338 |
| 0512307198 | STRASSER 1-27 | LYONS | -3,212 | 8,208 |
| 0512309953 | UPRR-DEVRIES 1-29 | LYONS | -4,077 | 9,336 |
| 0512310072 | UPRR-TURNER 1-7 | LYONS | -3,967 | 9,313 |
| 0512310091 | FRANKS 2 | LYONS | -3,439 | 8,419 |
| 0512310135 | GRACE-WISE 19-1 | LYONS | -3,552 | 8,568 |
| 0512310188 | SUPRON-UPRR 27-1 | LYONS | -4,217 | 9,158 |
| 0512310384 | DIXON 1-28 | LYONS | -2,772 | 7,550 |
| 0512310675 | DOME-HILL 1-6 | LYONS | -3,225 | 8,166 |
| 0512310677 | MARATHON-AVALO 1-32 | LYONS | -2,473 | 7,017 |
| 0512310694 | AMOCO-UPRR 1 | LYONS | -4,488 | 9,736 |
| 0512310939 | CENSOR 13-28 | LYONS | -3,434 | 8,476 |
| 0512311469 | COLORADO STATE-A 1 | LYONS | -4,183 | 9,496 |
| 0512311559 | STATE 1-16 | LYONS | -4,252 | 9,256 |
| 0512311747 | SHARK FEDERAL 1 | LYONS | -3,818 | 8,801 |

| API No. | Well Name | Formation Top | TVDSS (ft) | MD (ft) |
|---|---|---|---|---|
| 0512312660 | STECKEL 1-14 | LYONS | -4,367 | 9,456 |
| 0512313451 | FORSYTHE 31-24 | LYONS | -4,388 | 9,589 |
| 0512313645 | PIERCE 4 | LYONS | -4,169 | 9,234 |
| 0512313885 | WECO STATE 2B-28 1 | LYONS | -4,305 | 9,908 |
| 0512314167 | COAL CREEK FEDERAL 6-32 1 | LYONS | -3,834 | 8,764 |
| 0512314188 | CLARK 1-3 | LYONS | -3,738 | 8,744 |
| 0512314635 | LUCKY LADY 16-4 | LYONS | -3,336 | 8,847 |
| 0512314652 | SHAPLEY 1-25 | LYONS | -2,566 | 7,270 |
| 0512315385 | TOEDTLI 1-10 | LYONS | -2,618 | 7,409 |
| 0512315685 | FOSSTON/STATE 10-16 | LYONS | -3,787 | 8,630 |
| 0512316802 | FOSSTON/STATE 8-16 | LYONS | -3,780 | 8,658 |
| 0512319199 | STATE 1 | LYONS | -3,405 | 8,402 |
| 0512319199 | MCGAHEY OIL LLC STATE 1A | LYONS | -3,414 | 8,400 |
| 0512319694 | PAWNEE FEDERAL 1-28 | LYONS | -2,491 | 7,413 |
| 0512321426 | CROISSANT 1 | LYONS | -3,650 | 8,666 |
| 0512321651 | CROISSANT 4 | LYONS | -3,641 | 8,663 |
| 0512323778 | DUNBAR 2 | LYONS | -3,482 | 8,529 |
| 0512323849 | DUNBAR 3 | LYONS | -3,489 | 8,545 |
| 0512325585 | WEST 11-24 | LYONS | -3,562 | 8,590 |
| 0512326086 | SHABLE - USX AB 11-6 | LYONS | -4,012 | 8,874 |
| 0512326155 | WALCKER USX AB 1-13 | LYONS | -3,920 | 8,767 |
| 0512326947 | SHABLE USX AB 11-3 | LYONS | -3,936 | 8,823 |
| 0512326968 | DILLARD USX AB 03-16 | LYONS | -3,957 | 8,822 |
| 0512328014 | SHABLE 14-22 | LYONS | -4,007 | 8,834 |
| 0512330025 | DF RANCH 1161-21-42 | LYONS | -3,596 | 8,850 |
| 0512330267 | MCKAY AB 02-13 | LYONS | -3,972 | 8,866 |
| 0512330293 | DILLARD AB 10-01 | LYONS | -3,965 | 8,812 |
| 0512330616 | SHABLE E USX AB 11-02 | LYONS | -4,006 | 8,900 |
| 0512330633 | SHABLE USX AB 11-04P | LYONS | -3,919 | 8,790 |
| 0512331035 | SIMBA 1-06 SWD | LYONS | -3,937 | 9,312 |
| 0512331035 | SIMBA 1-06 SWD | LYONS | -3,934 | 9,308 |
| 0512331069 | DILLARD AB 10-07 | LYONS | -3,942 | 8,787 |
| 0512331225 | WALCKER USX AB 01-07P | LYONS | -3,930 | 8,829 |
| 0512331301 | WALCKER USX AB01-08P | LYONS | -3,898 | 8,803 |
| 0512331319 | SHABLE USX AB 11-09P | LYONS | -3,981 | 8,818 |
| 0512331464 | DILLARD AB 10-06 | LYONS | -3,945 | 8,797 |
| 0512331470 | DILLARD USX AB 03-15P | LYONS | -3,951 | 8,810 |
| 0512331473 | DILLARD AB 10-02 | LYONS | -3,982 | 8,831 |
| 0512331488 | DILLARD AB 10-11 | LYONS | -2,990 | 7,848 |

| API No. | Well Name | Formation Top | TVDSS (ft) | MD (ft) |
|---|---|---|---|---|
| 0512331495 | MCKAY AB 02-14 | LYONS | -3,949 | 8,854 |
| 0512331496 | STATE PC AB 16-09 | LYONS | -3,968 | 8,863 |
| 0512331540 | FURROW USX AB 15-05P | LYONS | -3,984 | 8,852 |
| 0512331744 | HILLMAN 9-1 | LYONS | -3,079 | 8,196 |
| 0512331745 | ENDERSON 31-14 | LYONS | -3,274 | 8,710 |
| 0512332207 | SWD C7A | LYONS | -3,780 | 8,508 |
| 0512332935 | DYER 15-8 | LYONS | -4,047 | 9,012 |
| 0512334185 | MCKAY FEDERAL AB02-15 | LYONS | -3,905 | 8,801 |
| 0512334431 | NIELSEN 4-23 | LYONS | -3,351 | 8,338 |
| 0512334520 | NGL C7B | LYONS | -3,790 | 8,810 |
| 0512334890 | BALL RANCH AC15-04 | LYONS | -3,776 | 8,661 |
| 0512335471 | FORD 29-21-7-59 | LYONS | -2,978 | 7,883 |
| 0512335654 | CON GQ 07-01 | LYONS | -3,638 | 8,729 |
| 0512335817 | LONGS AC 02-15 | LYONS | -3,762 | 8,612 |
| 0512335855 | BETHYL GW30-16 | LYONS | -3,831 | 8,827 |
| 0512335868 | BETHYL GW29-13 | LYONS | -3,827 | 8,810 |
| 0512336262 | JEANIE AB10-01R | LYONS | -3,927 | 8,772 |
| 0512336782 | BETHYL GW 29-12 | LYONS | -3,825 | 8,783 |
| 0512337246 | VIGILANT STATE AC16-01 | LYONS | -3,782 | 8,661 |
| 0512337248 | VIGILANT STATE AC16-07 | LYONS | -3,798 | 8,661 |
| 0512337249 | VIGILANT STATE AC16-08 | LYONS | -3,792 | 8,679 |
| 0512337374 | WILDHORSE 16-13L | LYONS | -3,056 | 8,134 |
| 0512337495 | RAZOR 26J-2633L | LYONS | -2,864 | 7,609 |
| 0512339484 | WEITZEL 1 | LYONS | -3,196 | 8,110 |
| 0512339770 | EWS 1 | LYONS | -3,160 | 8,087 |
| 0512339885 | HORSETAIL 19N-1924M | LYONS | -2,694 | 7,460 |
| 0512339891 | EWS 1A | LYONS | -3,174 | 8,460 |
| 0512340194 | NGL C9 | LYONS | -3,445 | 8,518 |
| 0512340630 | HORSETAIL 19N-1924M-R | LYONS | -2,677 | 7,463 |
| 0512340770 | NGL C9B | LYONS | -3,420 | 8,504 |
| 0512340771 | NGL C9C | LYONS | -3,464 | 8,554 |
| 0512340775 | TIGERTAIL FEDERAL 2-3 | LYONS | -4,005 | 8,907 |
| 0512340777 | RAZOR 21 SWD 1 | LYONS | -2,867 | 7,709 |
| 0512505019 | WARNER 1 | LYONS | 246 | 3,529 |
| 0512506924 | MENTER 1 | LYONS | -160 | 3,789 |
| 0512506932 | FRANSON 1 | LYONS | -637 | 4,591 |
| 2600721735 | OLSEN ILER 1 | LYONS | -2,485 | 6,728 |
| 2600721997 | OPIS 1P | LYONS | -2,182 | 6,675 |
| 2603321941 | MCMILLAN RANCH 1 | LYONS | -1,828 | 6,387 |

| API No. | Well Name | Formation Top | TVDSS (ft) | MD (ft) |
|---|---|---|---|---|
| 2603321958 | ACKERMAN 1 | LYONS | -1,447 | 5,854 |
| 2603321959 | MAHR 1 | LYONS | -1,395 | 5,733 |
| 2603321977 | D CHRISTENSON 34-21 | LYONS | -1,836 | 6,395 |
| 2603321978 | DEAVER 12-27 | LYONS | -1,844 | 6,399 |
| 2603322025 | MATHEWSON-FEE 13-15 | LYONS | -1,698 | 6,074 |
| 2603322117 | LYNGHOLM 1-23 | LYONS | -1,683 | 6,096 |
| 2603322130 | TOOF 1 | LYONS | -1,166 | 5,306 |
| 2603322136 | SCHOU 1A | LYONS | -1,083 | 5,150 |
| 2603322137 | OLSON 1-25 | LYONS | -1,670 | 6,055 |
| 2603322199 | HAUPT 3-27 | LYONS | -1,548 | 5,702 |
| 2603322241 | LIVINGSTON 1-33 | LYONS | -1,708 | 6,055 |
| 2603322248 | BIRD 4-1 | LYONS | -1,721 | 6,050 |
| 2603322262 | R F ANDERSON 1 | LYONS | -1,723 | 6,000 |
| 2603322263 | WALKER 2 | LYONS | -1,857 | 6,402 |
| 2603322268 | MATHEWSON 20-1 | LYONS | -1,735 | 6,190 |
| 2603322272 | DRENGUIS 2-4 | LYONS | -1,717 | 6,019 |
| 2603322276 | M MICHAELS 1 | LYONS | -1,804 | 6,345 |
| 2603322289 | MCMILLEN 3-1 | LYONS | -1,651 | 5,970 |
| 2603322290 | LIVINGSTON 33-2 | LYONS | -1,744 | 6,093 |
| 2603322299 | CLIFF FARMS 1-13A | LYONS | -1,796 | 6,280 |
| 2603322302 | RGM CORP 44-27 | LYONS | -1,896 | 6,349 |
| 2603322307 | BIRD 4-2 | LYONS | -1,671 | 5,979 |
| 2603322308 | TERMAN 14-34 | LYONS | -1,901 | 6,330 |
| 2603322309 | BEYER 1 | LYONS | -1,561 | 5,965 |
| 2603322310 | KURZ 2 | LYONS | -1,554 | 5,933 |
| 2603322311 | MOLLY 1 | LYONS | -1,609 | 5,851 |
| 2603322312 | F J F 1 | LYONS | -1,347 | 5,602 |
| 2603322316 | CLIFF FARMS 1 | LYONS | -1,954 | 6,448 |
| 2603322317 | MC MILLEN 34-2 | LYONS | -1,652 | 6,148 |
| 2603322322 | AF HOLT 1 | LYONS | -1,638 | 6,040 |
| 2603322324 | BRAUER 6-13 | LYONS | -1,764 | 6,272 |
| 2603322327 | CLARA STATE 1 | LYONS | -1,697 | 6,097 |
| 2603322329 | BRAUER L E 14-1 | LYONS | -1,604 | 5,922 |
| 2603322331 | GUINOUARD 1 | LYONS | -1,302 | 5,465 |
| 2603322332 | ERNEST 10-33 | LYONS | -1,332 | 5,557 |
| 2603322333 | MC MILLEN 35-1 | LYONS | -1,747 | 6,100 |
| 2603322336 | RAPP-WOOD 1 | LYONS | -1,511 | 5,809 |
| 2603322339 | MOLLY 2 | LYONS | -1,704 | 5,960 |
| 2603322340 | C BALL 7-1 | LYONS | -1,462 | 5,858 |

| API No. | Well Name | Formation Top | TVDSS (ft) | MD (ft) |
|---|---|---|---|---|
| 2603322341 | RGM 13-28 | LYONS | -1,874 | 6,430 |
| 2603322343 | PREBLE 25-5 | LYONS | -1,308 | 5,494 |
| 2603322344 | OLSEN 1 | LYONS | -1,662 | 6,063 |
| 2603322345 | SCHAF 10-2 | LYONS | -1,616 | 5,970 |
| 2603322347 | BORCHERT 1 | LYONS | -1,702 | 6,048 |
| 2603322351 | CLIFF FARMS 41-13 | LYONS | -1,814 | 6,241 |
| 2603322352 | TERMAN 11-34 | LYONS | -1,897 | 6,443 |
| 2603322353 | RUSH CREEK 31-17 | LYONS | -1,006 | 4,889 |
| 2603322362 | CIZEK 1 | LYONS | -2,021 | 6,682 |
| 2603322364 | MC-MILLEN 1 | LYONS | -1,668 | 6,132 |
| 2603322368 | BORCHERT 2 | LYONS | -1,715 | 6,087 |
| 2603322375 | WALTERS 35-13 | LYONS | -1,872 | 6,258 |
| 2603322377 | GEORGE 1 | LYONS | -1,802 | 6,092 |
| 2603322391 | REZANINA 1-M21 | LYONS | -1,461 | 5,756 |
| 2603322393 | CLIFF FARMS 1-X | LYONS | -1,752 | 6,160 |
| 2603322396 | MCMILLEN 1 | LYONS | -1,691 | 6,188 |
| 2603322409 | CHURCH 1 | LYONS | -1,721 | 6,090 |
| 2603322496 | PHYLLIS BAIRD 93-1 | LYONS | -1,648 | 5,899 |
| 2603322547 | FREI-OBRIEN 1 | LYONS | -1,927 | 6,508 |
| 2603322580 | LORENZO FLATS 1 | LYONS | -1,791 | 6,291 |
| 2603322616 | FEDERAL 1-28 | LYONS | -1,547 | 5,954 |
| 2603322619 | POTTER 1 | LYONS | -1,855 | 6,349 |
| 2603322679 | LUDEMAN 1 | LYONS | -1,156 | 5,106 |
| 2603322684 | STAGECOACH 16-14 | LYONS | -1,209 | 5,224 |
| 2603322703 | POROS 1P | LYONS | -1,929 | 6,461 |
| 2603322704 | ZEUS 1H | LYONS | -1,849 | 6,284 |
| 2603322708 | SCHMALE 34-20 | LYONS | -1,181 | 5,223 |
| 2604921098 | CERNY 1 | LYONS | -757 | 4,657 |
| 2604921099 | LINDSEY 1-24 | LYONS | -809 | 4,766 |
| 2606905065 | RUSH CREEK 1 | LYONS | -396 | 4,160 |
| 2606905073 | GILBAUGH 1 | LYONS | -362 | 4,162 |
| 2606921079 | 12-16 STATE 1 | LYONS | -829 | 4,353 |
| 2606921080 | RUSH CREEK LAND 1 | LYONS | -953 | 4,498 |
| 2606921085 | WITHERS 1 | LYONS | -884 | 4,326 |
| 2606921096 | RUSH CREEK 24-10 | LYONS | -1,060 | 4,765 |
| 2606921099 | SUGARLOAF HILL 1 | LYONS | -679 | 4,376 |
| 2610121020 | WILLIAMS 1 | LYONS | -449 | 3,979 |
| 2610121021 | HOLSHER 1 | LYONS | -333 | 3,715 |
| 2610521766 | CHEVRON-DUNCAN-COMPTON 1 | LYONS | -3,310 | 8,470 |

| API No. | Well Name | Formation Top | TVDSS (ft) | MD (ft) |
|---|---|---|---|---|
| 2610522298 | KOENIG JAMES 1 | LYONS | -2,786 | 7,763 |
| 2610522339 | PRAIRIE STATE 1 | LYONS | -2,745 | 7,776 |
| 2610522343 | HAUG 3 | LYONS | -2,883 | 8,037 |
| 2610522344 | JAMES KOENIG 2 | LYONS | -2,744 | 7,717 |
| 2610522346 | GUNDERSON 2-11 | LYONS | -2,213 | 6,969 |
| 2610522356 | EVERTSON 1 | LYONS | -2,612 | 7,557 |
| 2610522362 | PRAIRIE STATE A 2 | LYONS | -2,786 | 7,834 |
| 2610522369 | HEIDEMAN 41-23 | LYONS | -2,689 | 7,711 |
| 2610522371 | GUNDERSON 14-26 | LYONS | -2,264 | 6,801 |
| 2610522372 | MATHEWSON 1 | LYONS | -2,189 | 6,957 |
| 2610522373 | PALMER STATE 1 | LYONS | -2,391 | 7,294 |
| 2610522376 | GIBBS 24-1 | LYONS | -2,656 | 7,580 |
| 2610522378 | L D YOUNG 1 | LYONS | -2,626 | 7,564 |
| 2610522385 | UPRC-DJP 1 | LYONS | -3,170 | 8,382 |
| 2610522386 | GIESEKING 1 | LYONS | -2,552 | 7,408 |
| 2610522389 | DAVID P HAGSTROM 1 | LYONS | -2,757 | 7,710 |
| 2610522390 | FORSLING-VAVRA 1 | LYONS | -2,830 | 7,856 |
| 2610522394 | NEBRASKA STATE B 1 | LYONS | -2,739 | 7,704 |
| 2610522395 | JOSEPH L VOLKMER 1 | LYONS | -2,763 | 7,732 |
| 2610522398 | LORALEE PAULINE MILLER 1 | LYONS | -2,764 | 7,736 |
| 2610522399 | TERRESTRIAL 1 | LYONS | -2,732 | 7,678 |
| 2610522402 | LUKASSEN 1 | LYONS | -2,819 | 7,800 |
| 2610522403 | HAGSTROM B 1 | LYONS | -2,761 | 7,742 |
| 2610522407 | MARY L QUINN 1 | LYONS | -2,745 | 7,697 |
| 2610522408 | LINN-TERRESTRIAL 1 | LYONS | -2,820 | 7,676 |
| 2610522419 | LINN-TERRESTRIAL 2 | LYONS | -2,820 | 7,652 |
| 2610522420 | MAST-SAUNDERS 1 | LYONS | -2,830 | 7,773 |
| 2610522426 | SCHWINDT 1 | LYONS | -2,802 | 7,620 |
| 2610522429 | GROSS BROTHERS 1 | LYONS | -2,734 | 7,700 |
| 2610522431 | LYDIA STAHLA 1 | LYONS | -2,726 | 7,614 |
| 2610522432 | HOTTELL 1-14HW | LYONS | -3,164 | 8,166 |
| 2610522433 | LYDIA STAHLA 1 | LYONS | -2,726 | 7,600 |
| 2610522434 | READ-VOLKMER 1 | LYONS | -2,747 | 7,740 |
| 2610522435 | GROSS BROTHERS B-1 | LYONS | -2,750 | 7,685 |
| 2610522436 | MARY L QUINN 2 | LYONS | -2,773 | 7,610 |
| 2610522437 | JAMES KOENIG 2X | LYONS | -2,769 | 7,725 |
| 2610522439 | GROSS BROTHERS-STAHLA D-1 | LYONS | -2,747 | 7,550 |
| 2610522440 | CAMPBELL 2 | LYONS | -2,821 | 7,613 |
| 2610522442 | GROSS BROTHERS 2 | LYONS | -2,721 | 7,660 |

| API No. | Well Name | Formation Top | TVDSS (ft) | MD (ft) |
|---|---|---|---|---|
| 2610522443 | GROSS BROTHERS C-1 | LYONS | -2,711 | 7,645 |
| 2610522444 | GROSS BROTHERS C-2 | LYONS | -2,733 | 7,610 |
| 2610522445 | GROSS BROTHERS C-3 | LYONS | -2,717 | 7,507 |
| 2610522448 | JAMES KOENIG 3 | LYONS | -2,800 | 7,775 |
| 2610522450 | ND CEDERBURG 8-28 | LYONS | -2,812 | 7,810 |
| 2610522453 | LODGEPOLE STATE 1 | LYONS | -2,906 | 7,735 |
| 2610522455 | TRAVELERS 1 | LYONS | -2,804 | 7,665 |
| 2610522458 | FREDRICK L J 1 | LYONS | -2,678 | 7,642 |
| 2610522459 | NEBRASKA STATE B 3 | LYONS | -2,732 | 7,690 |
| 2610522460 | KATHLEEN CAMIN 1 | LYONS | -2,753 | 7,533 |
| 2610522465 | LUKASSEN 1-17 | LYONS | -2,835 | 7,766 |
| 2610522469 | FERGUSON 1 | LYONS | -2,765 | 7,514 |
| 2610522470 | FERGUSON 2-34 | LYONS | -2,770 | 7,504 |
| 2610522471 | FERGUSON 1-G-82 | LYONS | -2,740 | 7,500 |
| 2610522473 | ELLIAS HAGSTROM 8-27ND | LYONS | -2,734 | 7,719 |
| 2610522476 | TRAVELERS 2-21 | LYONS | -2,778 | 7,689 |
| 2610522477 | FLYING EAGLE 1 | LYONS | -2,669 | 7,635 |
| 2610522479 | FLYING EAGLE 2 | LYONS | -2,705 | 7,636 |
| 2610522480 | SWANSON 11X-21 | LYONS | -2,769 | 7,818 |
| 2610522482 | TREVETHAN 1-17 | LYONS | -2,792 | 7,874 |
| 2610522482 | TREVETHAN 1-17 | LYONS | -2,779 | 7,861 |
| 2610522485 | CAMPBELL 3-20 | LYONS | -2,826 | 7,680 |
| 2610522486 | JAMES KOENIG 4 | LYONS | -2,806 | 7,747 |
| 2610522487 | TORGESON 1 | LYONS | -2,695 | 7,560 |
| 2610522488 | JANICEK 1-31 | LYONS | -2,648 | 7,506 |
| 2610522489 | EDNA SCHRACK 1-6 | LYONS | -2,862 | 7,849 |
| 2610522496 | F E FARMER 1 | LYONS | -2,771 | 7,734 |
| 2610522497 | DONALD LONG DEEP TEST 11-10 | LYONS | -2,400 | 7,318 |
| 2610522498 | CAMPBELL 4-20 | LYONS | -2,819 | 7,670 |
| 2610522499 | LUKASSEN 1-7 | LYONS | -2,835 | 7,840 |
| 2610522500 | LUKASSEN 3-17 | LYONS | -2,839 | 7,740 |
| 2610522503 | BERNICE ZWIENER 16-20 | LYONS | -2,540 | 7,478 |
| 2610522504 | NEBRASKA STATE 7-36 | LYONS | -2,675 | 7,625 |
| 2610522505 | BERRY 1-32 | LYONS | -3,220 | 8,448 |
| 2610522506 | LUKASSEN 2-17 | LYONS | -2,823 | 7,726 |
| 2610522507 | MOCKETT 1 | LYONS | -2,843 | 7,819 |
| 2610522508 | GIESEKING ESTATE 41X-9 | LYONS | -2,532 | 7,412 |
| 2610522509 | PLATTE 1 | LYONS | -2,849 | 7,705 |
| 2610522510 | CULEK 15-19 | LYONS | -2,575 | 7,531 |

| API No. | Well Name | Formation Top | TVDSS (ft) | MD (ft) |
|---|---|---|---|---|
| 2610522513 | CAMBELL 5-20 | LYONS | -2,820 | 7,635 |
| 2610522514 | TRAVELERS 3-21 | LYONS | -2,804 | 7,624 |
| 2610522521 | STATE 44X-16 | LYONS | -2,764 | 7,779 |
| 2610522524 | FLYING EAGLE 3 | LYONS | -2,687 | 7,636 |
| 2610522526 | PETERSON 7-2 | LYONS | -2,408 | 7,132 |
| 2610522531 | RUTH A CROMIE 1-19 | LYONS | -3,025 | 8,157 |
| 2610522532 | EVERTSON QUINN 3 | LYONS | -2,770 | 7,630 |
| 2610522533 | STANDER 1 | LYONS | -2,494 | 7,384 |
| 2610522535 | EVERTSON QUINN 4 | LYONS | -2,778 | 7,610 |
| 2610522536 | TERRESTRIAL 1-32 | LYONS | -2,775 | 7,554 |
| 2610522543 | KENNEDY 6-21 | LYONS | -2,555 | 7,480 |
| 2610522545 | ENDERS UNIT DEEP-WREDE 7-15 | LYONS | -2,470 | 7,369 |
| 2610522559 | VRTATKO 1 | LYONS | -2,337 | 7,142 |
| 2610522560 | STATE 36-1 | LYONS | -2,483 | 7,140 |
| 2610522561 | HEIDEMANN 1 | LYONS | -2,671 | 7,624 |
| 2610522571 | MILLER 1-10 | LYONS | -2,546 | 7,410 |
| 2610522574 | SWANSON 16-28 | LYONS | -2,719 | 7,757 |
| 2610522576 | DOE STATE 13-36 | LYONS | -2,610 | 7,615 |
| 2610522577 | YUNG-SEVERSON 1-29 | LYONS | -2,583 | 7,541 |
| 2610522579 | CAMIN 2 | LYONS | -2,798 | 7,551 |
| 2610522580 | NEBRASKA STATE 4 | LYONS | -2,768 | 7,734 |
| 2610522582 | WILSON-SCHRACK 13-34 | LYONS | -2,759 | 7,700 |
| 2610522589 | LUKASSEN 2-8 | LYONS | -2,837 | 7,823 |
| 2610522590 | LINN-TERRESTRIAL 3-29 | LYONS | -2,816 | 7,670 |
| 2610522591 | TERRESTRIAL 2-32 | LYONS | -2,839 | 7,648 |
| 2610522592 | WILKE PAULA 12-5 | LYONS | -2,829 | 7,808 |
| 2610522614 | WILSON SUE ANN 15-34 | LYONS | -2,757 | 7,690 |
| 2610522615 | HEIDEMANN FARMS INC 1-13 | LYONS | -2,712 | 7,564 |
| 2610522617 | HEIDEMANN FARMS 7-11 | LYONS | -2,737 | 7,725 |
| 2610522618 | YUNG ED 5-7 | LYONS | -2,691 | 7,588 |
| 2610522636 | ART PIRNIE 6-3 | LYONS | -2,751 | 7,716 |
| 2610522637 | HEIDEMANN FARMS ET AL 1-14 | LYONS | -2,709 | 7,685 |
| 2610522642 | NOVOTNY 22-2 | LYONS | -3,018 | 8,284 |
| 2610522653 | LUKASSEN ET AL 10-18 | LYONS | -2,592 | 7,528 |
| 2610522654 | ELROD ET AL 4-2 | LYONS | -2,721 | 7,646 |
| 2610522719 | LUKASSEN 44-7 | LYONS | -2,864 | 7,861 |
| 2612321365 | LAPASEOTES 1 | LYONS | -1,215 | 4,893 |
| 2612321404 | CRANMORE 1 | LYONS | -1,192 | 5,084 |
| 2612321411 | JESSEN 1 | LYONS | -994 | 4,527 |

| API No. | Well Name | Formation Top | TVDSS (ft) | MD (ft) |
|---|---|---|---|---|
| 2612321412 | STEVENS 1 | LYONS | -813 | 4,914 |
| 2612321413 | PETERSEN 2-24 | LYONS | -1,237 | 5,364 |
| 2612321483 | STATE OF NEBRASKA 1 | LYONS | -1,328 | 5,451 |
| 2612321485 | GREENWOOD RANCH 15-1 | LYONS | -1,486 | 5,696 |
| 2612321487 | COOPS-LINBERG 1 | LYONS | -1,667 | 6,133 |
| 2612321501 | HART 1 | LYONS | -1,149 | 4,957 |
| 2612321502 | AURICH 1 | LYONS | -1,283 | 5,375 |
| 2612321518 | LINDBERG RANCH 42X-6 | LYONS | -1,646 | 6,106 |
| 2612321523 | LESSMAN 1 | LYONS | -1,255 | 5,281 |
| 2615721110 | J C GOODELL 1 | LYONS | -3,201 | 7,481 |
| 2615721295 | NORMAN E JOHNS 3-12 | LYONS | -2,007 | 5,961 |
| 2616521108 | BIRDSALL ANNA 1-6 | LYONS | -2,445 | 6,955 |
| 2616521124 | DOWNER 18-8 | LYONS | -2,517 | 6,947 |
| 2616521135 | BIRD CORMAN 11-16-2X | LYONS | -2,188 | 6,895 |
| 2616521139 | HUGHSON 22-14 | LYONS | -2,243 | 6,737 |
| 4901505089 | SEIMSEN 1-2 | LYONS | 804 | 4,041 |
| 4901520088 | FEDERAL 1-19 | LYONS | -1,841 | 6,273 |
| 4901520157 | ELLIS 3 1 | LYONS | -5,181 | 10,634 |
| 4901520172 | BADGER RANCH 9-1 | LYONS | 2,348 | 2,374 |
| 4902105033 | FRITZ 1 | LYONS | -3,498 | 8,706 |
| 4902120159 | BERRY 1 | LYONS | -4,845 | 10,933 |
| 4902120231 | CHAMPLIN 318 1 | LYONS | -3,732 | 9,234 |
| 4902120234 | HANSON 28-2 | LYONS | -3,552 | 8,940 |
| 4902120252 | MILLER 1-18 | LYONS | -4,103 | 9,764 |
| 4902120254 | UPRR-PALM 1-21 | LYONS | -3,872 | 9,302 |
| 4902120259 | LOUTH GEORGE 1 | LYONS | -3,707 | 9,131 |
| 4902120391 | HORSE CREEK UNIT T84X-31G | LYONS | 132 | 6,535 |
| 4902120391 | HORSE CREEK UNIT T84X-31G | LYONS | 152 | 6,515 |
| 4902120398 | BASTIAN 1-21 | LYONS | -3,778 | 9,267 |
| 4902120399 | HUTCH HIEBER 44-20 1 | LYONS | -3,725 | 9,177 |
| 4902120402 | CHILDERS 13-7 1 | LYONS | -4,800 | 10,932 |
| 4902120588 | BOLTON 36-22D | LYONS | -3,455 | 8,783 |
| 4902120910 | COONEY 13-33 | LYONS | -3,422 | 8,720 |
| 4902121011 | BIG SANDY 132-33M | LYONS | -4,610 | 10,529 |
| 4902121517 | JUBILEE 700-22M | LYONS | -4,560 | 10,491 |
| 4902129393 | LASSO SWD 17-4S | LYONS | -4,582 | 10,740 |
| 4902129548 | JUNIPER M-1 | LYONS | -3,746 | 9,125 |
| 4902129598 | CYPRESS M-2 | LYONS | -3,572 | 8,821 |

# APPENDIX 2.3—GEOCHEMICAL MODELING REPORT

## Introduction

The mineral-brine-$CO_2$ interactions that occur during $CO_2$ sequestration lead to the alteration of host rock and eventual equilibrium in the mineral-brine-$CO_2$ system. Chemical modeling and laboratory experiments show that these reactions and eventual equilibria are driven by the specific mineralogy of the target formation, the composition of the brine, the acidity of the $CO_2$-brine mixture and the pressure and temperature in the subsurface. This chapter covers the modeling of the mineral-brine-$CO_2$ system across the mineralogical facies associations present for the subject site.

## Methods

Simplified, batch kinetic simulation experiments (models) were created for each facies present at the subject location. The models use phase thermodynamic data in the PHREEQC Lawrence Livermore National Laboratory Database and reaction kinetics from Palandri and Kharaka (2004) to model the $CO_2$-brine-rock interactions. Each simulation experiment is isothermal, with the temperature set to match the subject location and depth. The pressure for each simulation experiment is also static and set to match the subject location and depth. The thermodynamic model is based on local equilibrium for the minerals and ions in an aqueous phase. The kinetic calculations assume that abundant $CO_2$ is supplied to the system during the simulation and that any consumed molecule of $CO_2$ is replaced. These simplifying assumptions align with the reality of the physical system in that continuous injection allows for abundant gas supply to the system.

## Brine Geochemistry

The brine composition used for the simulations is derived from three flash water samples acquired during the Juniper M-1 testing program. In the testing process, the well was perforated from 9,165 ft to 9,171 ft, within the Lyons Formation interval. The water sampling tool was then placed at three depths while the well was pumped resulting in three samples from the injection target interval. The anion composition of each sample was analyzed using ion chromatography while cation compositions were analyzed using inductively coupled plasma optical emission spectrometry. The pH and alkalinity were measured using ASTM D1293 and ASTM D1125 respectively. A subset of anions and cations relevant to mineral-brine-$CO_2$ interactions are summarized for each sample in **Table A2.3-1**. The available analytical values were averaged for each mineral facies to create a composite brine composition that was used in each model (**Table A2.3-2**).

Table A2.3-1—Composition of water samples.

| Formation | Depth | pH | TDS | $HCO_3$ | $SO_4$ | Cl | I | Ca | Fe | K | Mg | Na |
|---|---|---|---|---|---|---|---|---|---|---|---|---|
| Lyons | 9,081.92 | 6.36 | 216,280 | 134 | 3,515 | 128,666 | 126 | 495 | 18 | 2,529 | 904 | 82,175 |
| Lyons | 9,096.26 | 6.43 | 216,280 | 160 | 3,610 | 128,581 | 0 | 508 | 18 | 2,426 | 874 | 80,734 |
| Lyons | 9,066.67 | 6.45 | 216,280 | 130 | 3,607 | 128,976 | 127 | 500 | 18 | 2,564 | 948 | 79,384 |

Table A2.3-2—Average brine composition by mineral facies.

| Mineral Facies | Facies Name | Modeled Depth | Stratigraphic Interval | pH | TDS | $HCO_3$ | $SO_4$ | Cl | I | Ca | Fe | K | Mg | Na |
|---|---|---|---|---|---|---|---|---|---|---|---|---|---|---|
| Facies 0 | Sandstone | 9,153 | Lyons | 6.40 | 216,280 | 147 | 3,577 | 128,741 | 84 | 501 | 18 | 2,506 | 909 | 80,764 |
| Facies 1 | Mudstone | 8,727 | Chugwater | 6.40 | 216,280 | 147 | 3,577 | 128,741 | 84 | 501 | 18 | 2,506 | 909 | 80,764 |
| Facies 1 | Mudstone | 9,187 | Satanka | 6.40 | 216,280 | 147 | 3,577 | 128,741 | 84 | 501 | 18 | 2,506 | 909 | 80,764 |
| Facies 2 | Carbonate and Dolostone | 9,119 | Goose Egg | 6.40 | 216,280 | 147 | 3,577 | 128,741 | 84 | 501 | 18 | 2,506 | 909 | 80,764 |

## Mineral Geochemistry

Despite the well understood nature of the stratigraphy in the vicinity of the subject site, published X-Ray Diffraction (XRD) data across the study formations are scarce. There is, however, good well-log control including numerous log suites that enabled the creation of a multi-mineral petrophysical model. The values from this model were analyzed using K-nearest neighbor (KNN) clustering in order to determine the number of mineralogical facies present.

An elbow plot and a silhouette plot, as shown in Figure 1, are used to select the number of clusters to be used in the KNN process. In the Elbow Plot, the number of clusters present is indicated by a flattening in the distortion value (y-axis). In the silhouette plot, the number of clusters present is indicated by a maximum in the average value (y-axis). In the case of this dataset, the number of clusters indicated by both methods is three. The mineralogical facies clusters can be plotted against a matrix of the mineralogical volume curves, this is called a small multiples plot and shows the veracity of the clustering. This plot can be viewed in **Figure A2.3-1**.

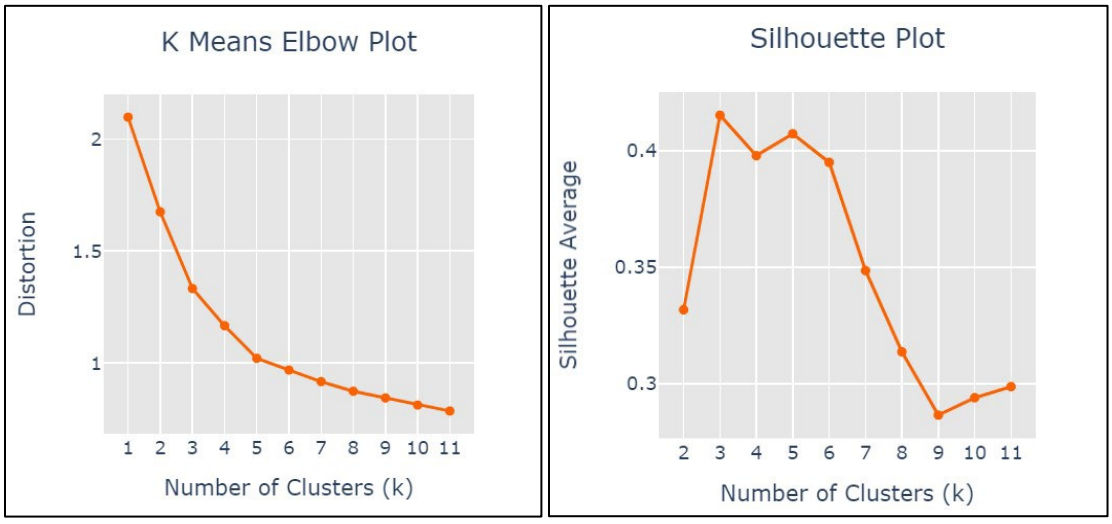


Figure A2.3-1—Elbow and silhouette plots for the multi-mineral model dataset in the Juniper M-1 well are shown.

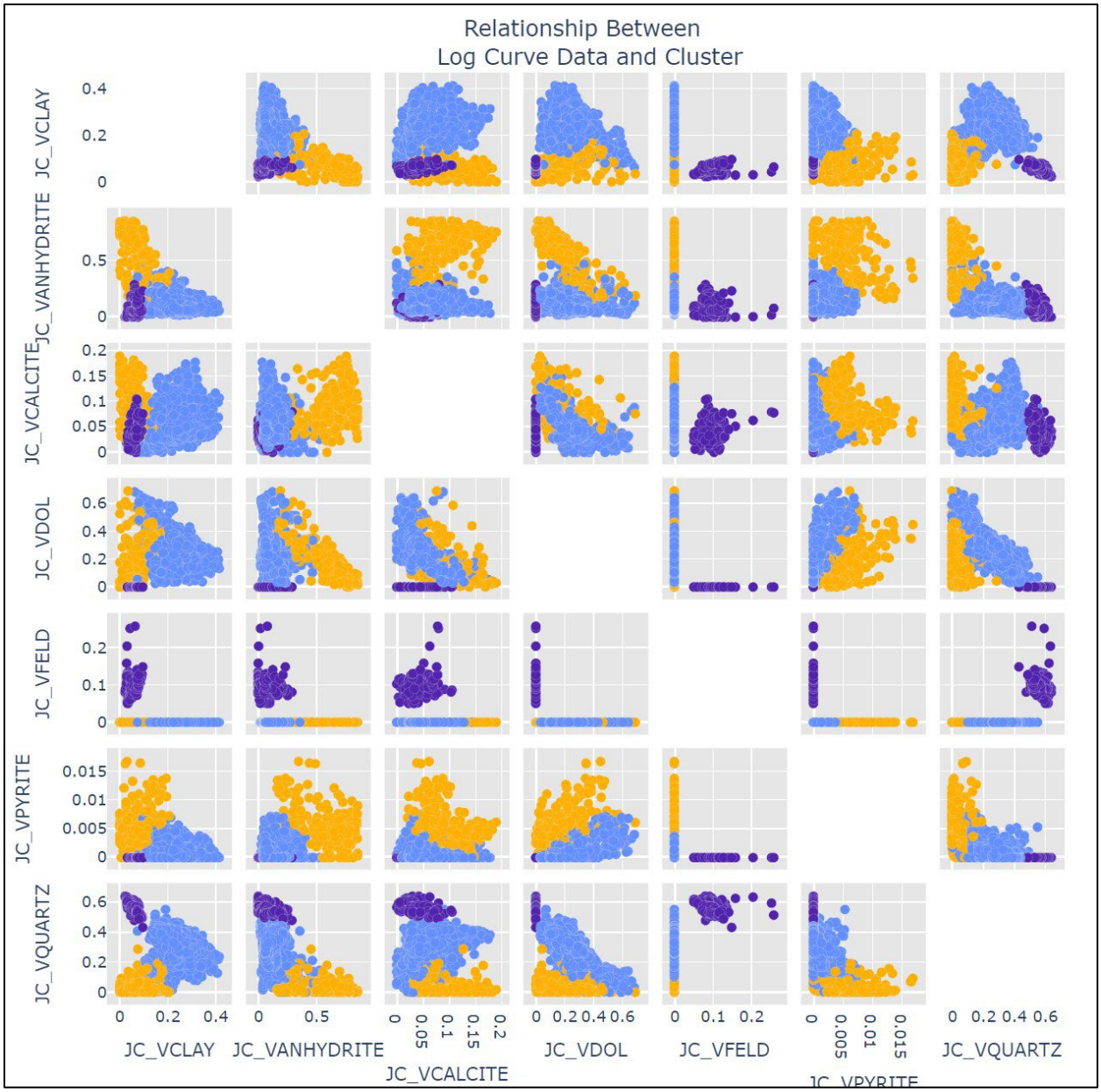


Figure A2.3-2—Relationship between mineral facies (KNN clusters) and the multi-mineral petrophysical model compositions in the Juniper M-1.

Data from 24 core plug samples obtained during the Juniper M-1 testing program across the injection and seal intervals were used in this analysis. Those samples were used in conjunction with XRF data to calibrate the multi-mineral model for the Juniper M-1 well and to create an LAS file. This LAS file was analyzed and broken into four mineral facies specified by the KNN analysis. Average mineralogic compositions were calculated for each of the four mineral facies and used to represent the injection and seal zone mineralogy for batch modeling.

Mineral compositions used in the models are shown in **Table A2.3-3**. Facies 1, a silica-rich mudstone, has two end-member compositions, one for the Chugwater Formation and a second for the Satanka Formation. The Lyons Formation injection zone endmember (Facies 0) is a quartz-

rich facies with feldspar, clay, and anhydrite. The Chugwater endmember, Facies 1, is a mudstone made up of near equal parts clay, quartz, and carbonate. The Satanka end member of Facies 1 is a quartz-rich mudstone with carbonate and clay. The Goose Egg end member (Facies 2) is an anhydrite-rich, carbonate mudstone with quartz and clay.

Table A2.3-3—Mineral composition of facies clusters.

| Mineral Facies | Facies Name | Modeled Depth | Stratigraphic Interval | Quartz | Calcite | Plag. (albite) | K-spar | Smectite | Illite | Anhydrite |
|---|---|---|---|---|---|---|---|---|---|---|
| Facies 0 | Sandstone | 9,153 | Lyons | 76.6 | 0 | 4 | 6.3 | 0 | 1.9 | 9.6 |
| Facies 1 | Mudstone | 8,727 | Chugwater | 34 | 30 | 0 | 0 | 3.2 | 28.8 | 0 |
| Facies 1 | Mudstone | 9,187 | Satanka | 42 | 25 | 0 | 0 | 2.7 | 24.3 | 0 |
| Facies 2 | Carbonate | 9,119 | Goose Egg | 13 | 46 | 0 | 0 | 1.2 | 10.8 | 27 |

The depth plot of the mineralogical facies assemblages for the Juniper M-1 well is shown in **Figure A2.3-3**. The eighth track shows the results of the KNN clustering with each 0.5-foot interval colored to match the cluster to which it is assigned.

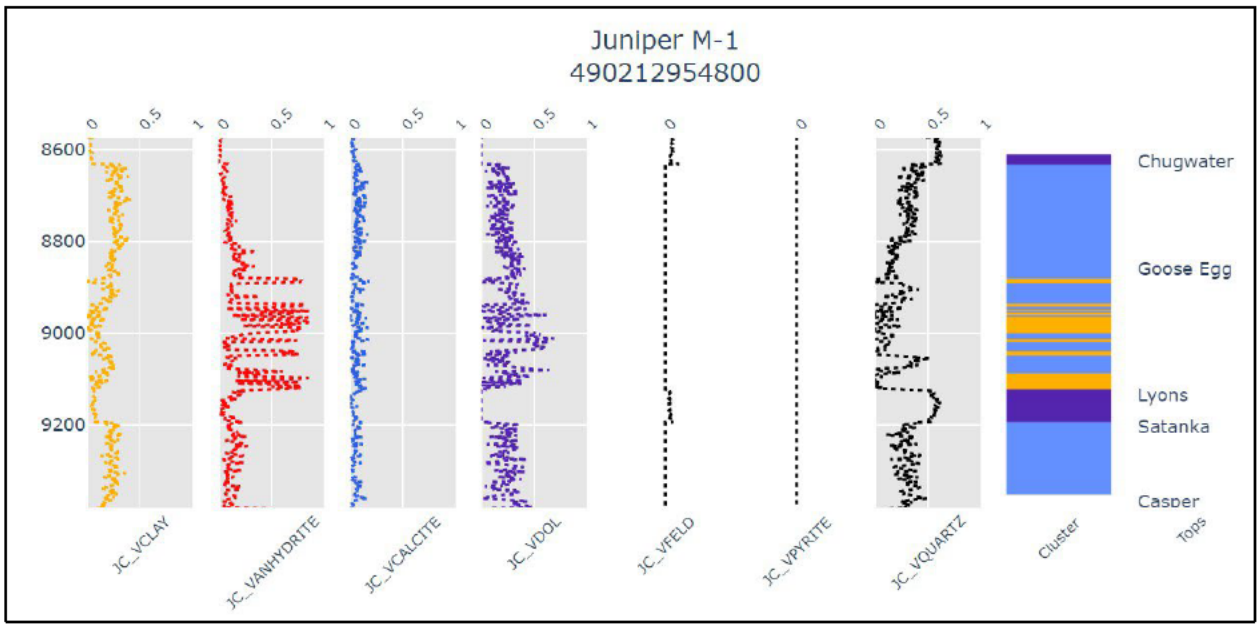


Figure A2.3-3—Depth plot of the mineralogical facies assemblages for the Juniper M-1 well. Track eight shows the mineralogical facies to which each depth interval is assigned.

## Models

A total of four geochemical models were created using the three mineral facies associations calculated from the well log analysis. The Chugwater and Lyons formation models were evaluated

at their average depth. The Goose Egg model was evaluated at the Goose Egg-Lyons interface. The Satanka model was evaluated at the Lyons-Satanka interface.

The processes expected in the subsurface were modeled as a product of thermodynamic equilibrium and kinetic reactions using PHREEQC. The models were created as simplified, 1-D batch models that occur at pressure and temperatures dictated by their stratigraphic position. The models assume a pressure gradient of 0.30 psi/ft and a thermal gradient of 1.34°F/100 ft with a mean annual surface temperature of 75°F. The injected volume of $CO_2$ was assumed to fill the pore spaces.

## Results

Across all the models, the results show that quartz and dolomite precipitate while other species have complex reactions dependent on the initial composition. Reactions begin to occur after a few seconds of contact and accelerate through the first several hundred years. From 1,000 to 10,000 years the reactions reach equilibrium (**Figure A2.3-4**).

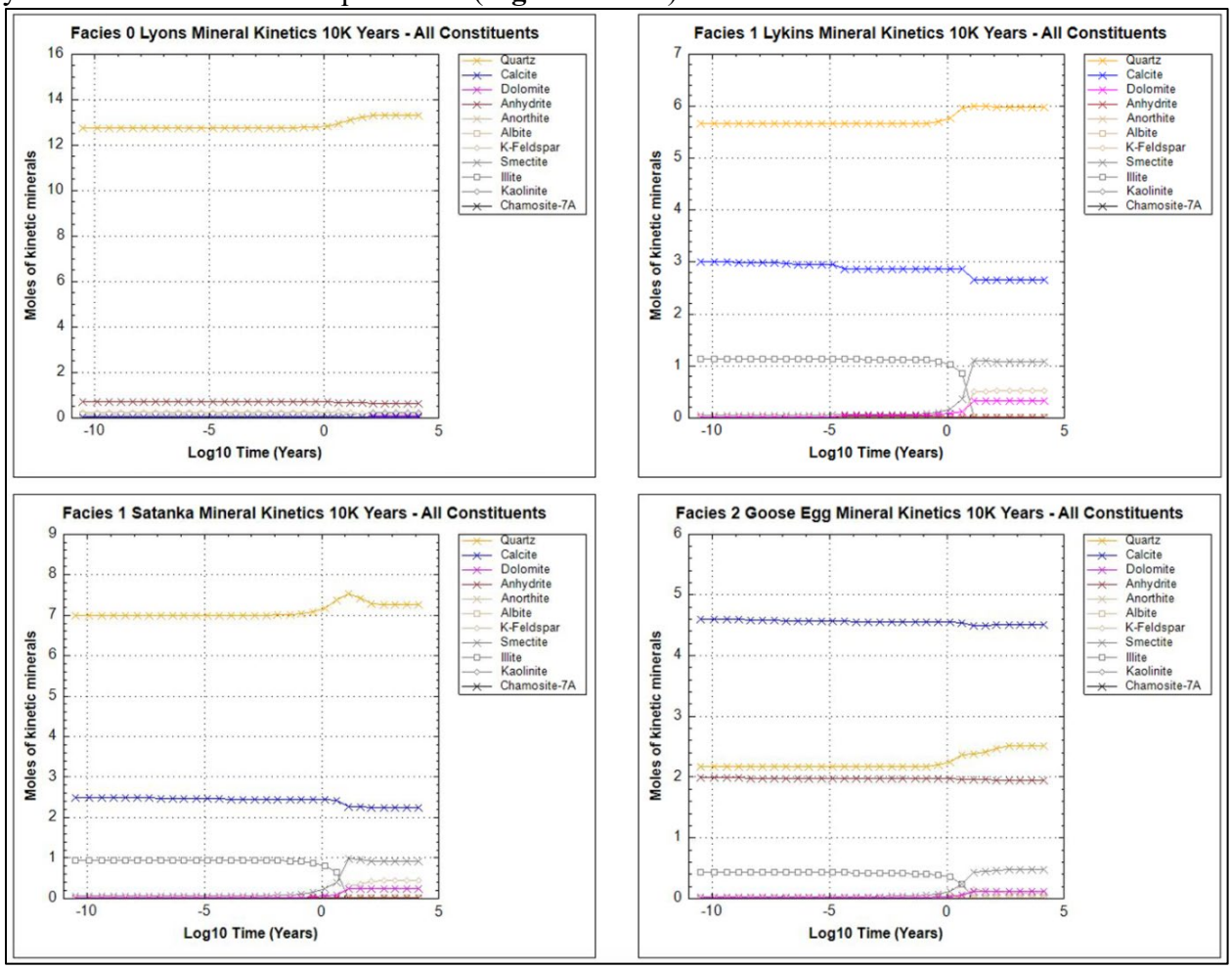


Figure A2.3-4—Batch model results by facies. The x-axis is log 10 time in seconds. The reaction time spans from 0.001 seconds to 10,000 years.

The Chugwater and Satanka mudstone confining intervals show precipitation of quartz and dissolution of calcite (the principal mineral constituents) along with dissolution of illite and

precipitation of smectite and feldspar in the minor constituents. The Goose Egg confining interval shows precipitation quartz and mild dissolution of anhydrite (the principal components) along with dissolution of illite and precipitation of smectite in the minor components. In the Lyons injection interval the largest constituent (quartz) shows net precipitation while in the minor constituents anhydrite, k-feldspar, plagioclase (albite), and illite dissolve while kaolinite and calcite precipitate.

Across all the models, the simulations show a net mineral change of less than 8%.

Mild net precipitation in the injection facies will lead to a small amount of porosity reduction over time especially at the upper confining zone-injection zone interface. Net precipitation and alteration of illite to smectite at the Goose Egg-Lyons interface should support seal capacity over the course of injection. Net precipitation and conversion of illite to smectite should support seal capacity over time in the Chugwater and Satanka confining intervals.